Inducible lysosome renitence in macrophages

by

Michael J. Davis

A dissertation submitted in partial fulfillment
of the requirements for the degree of
Doctor of Philosophy
(Immunology)
In The University of Michigan
2011

Doctoral Committee:

Professor Joel A. Swanson, Chair
Professor Cheong-Hee Chang
Professor Victor J. DiRita
Professor Kyung-Dall Lee
Professor Nicholas W. Lukacs

For all the fantastic teachers I've had though the years; my mother and father foremost among them.

Acknowledgements

First, and foremost, I would like to thank Joel Swanson for his patience and his scientific and mentoring endeavor. My time in lab has been an honor and a pleasure.

Special thanks also to all the members of the Swanson lab, past and present. It has been a privilege, and a lot of fun, to work near such excellent scientists.

I would like to thank all the members of my thesis committee for all the valuable advice.

I need to thank the Center for Live Cell Imaging, who picked me up when my scope was down. Sam Straight has been extremely helpful in fixing problems both in the Swanson Lab and the CLCI.

Kyung-Dall Lee and his lab gave generous support and technical expertise to early projects. Special thanks to Chasity Andrews, who was especially generous with time and reagents.

Jason Gestwicki and his group have also been great collaborators and generous with support and reagents.

I would like to express my gratitude to Brian Gregorka an excellent undergraduate student whom I had the pleasure of working with during the later part of my time here.

Table of Contents

List of figures

Abstract

Lysosomes are membrane-bounded intracellular compartments responsible for degradation of macromolecules and destruction of engulfed microbes. Extracellular molecules are taken up by pinocytosis in the case of soluble molecules and by phagocytosis in the case of particulates while cytoplasmic molecules are isolated by the process of autophagy. All of these pathways converge on delivery of contents to lysosomes where lysosomal acid-hydrolases degrade macromolecules to basic subunits for recycling. Damage to the lysosomal membrane spills acid-hydrolases and lysosome contents into the cytosol, which can lead to inflammasome activation and cell death. While lysosome damage has been studied for decades, previous assays for measuring lysosome damage were non-quantitative or insufficiently sensitive to detect small levels of damage. In this thesis I describe a novel, ratiometric, live-cell, fluorescence imaging method for measuring lysosome damage which allowed us to study mechanisms of damage and repair. Murine bone marrow-derived macrophage lysosomes were loaded with fluorescein-dextran and release from acidic lysosomes into the neutral cytosol was measured using the pH-sensitive fluorescence of fluorescein. Using this assay, we showed that lysosome damage following phagocytosis depends on the physical properties of the phagocytosed particle. Inflammasome assembly and IL-1β secretion correlated

with the extent of lysosome damage. Importantly, pre-stimulation of macrophages with lipopolysaccharide resulted in reduced lysosome damage following silica particle phagocytosis. Peptidoglycan, interferon-γ, and tumor necrosis factor-α were observed to induce similar lysosome protection. Macrophage lysosomes were protected from different kinds of damage, implying that this induced effect is a general lysosome resistance to physical damage, which we call lysosome renitence. Lysosome renitence inhibited *Listeria monocytogenes* vacuolar escape in macrophages and lysosome damage resulting from *Listeria* infection, indicating that induced lysosome renitence is a novel activity which activated macrophages use to combat infection. The mechanisms responsible for lysosome renitence were examined. Luminal calcium and autophagy may be part of the lysosome repair mechanism. Lysosome renitence is a potentially important therapeutic target, as pharmacological induction of renitence without inflammation could bolster defenses against intracellular pathogens and irritant particulates.

Chapter 1
Introduction

1.1 Macrophages and relevance to immunology

Macrophages are immune cells derived from myeloid bone marrow progenitors. Circulating monocytes enter tissues and differentiate into macrophages which function in tissue maintenance by engulfing particulate debris by a process called phagocytosis. Macrophages and other tissue resident immune cells monitor tissues for infection and damage. Upon sensing pathogens or tissue damage, macrophages secrete soluble factors which initiate an innate immune response by drawing an influx of immune cells including other macrophages. Following this influx of immune cells, macrophages and other immune cells can present processed foreign antigens to T-lymphocytes, contributing to the adaptive immune response. Macrophages sense the local environment of infected or damaged tissues and become activated, contributing to the clearance of microbes.

In addition to immune signaling, macrophages contribute to the immune response by ingesting and killing invading pathogens. Activation of macrophages up-regulates several microbicidal activities such as the phagosomal oxidase, which catalyzes the generation of reactive oxygen species (ROS) in microbe-containing phagosomes. Trafficking of microbes into lysosomes is also toxic to pathogens.

While there are many cellular interactions involved in the induction of an immune response, macrophage signals resulting from microbial or cellular damage detection are important early events in immune and disease responses. Recently, damage to lysosomes was shown to trigger potent immune responses in several diseases (Duewell et al., 2010; Halle et al., 2008; Hornung et al., 2008). Lysosomes and damage to these compartments will be reviewed below. Lysosome damage responses are relevant to early surveillance activities of macrophages, to hyper-inflammatory conditions, and to anti-microbial responses against phagocytosed pathogens.

1.2 Cell structure

The focus of this thesis is on issues surrounding damage to the lysosome, an intracellular organelle of macrophages. This should begin with a description of the intact cell. Cells compartmentalize distinct biochemical functions into separate volumes by the use of phospholipid membranes. All cells differentiate internal from external space by a bounding lipid bilayer, the plasma membrane. Eukaryotic cells define sub-regions of their internal space using internal membranes. These membrane delineated spaces are termed organelles and are distinguished based on function; Figure 1.1 shows a schematic of relevant compartments. The nucleus contains cellular DNA and contains enzymes for DNA synthesis, transcription and mRNA splicing. While the free cytosolic space, outside of organelles, contains enzymes for protein translation and most metabolic and catabolic functions, several organelles assist with specialized forms of these processes. Trans-membrane, organelle luminal, and secreted proteins are synthesized into the rough-endoplasmic reticulum. From there, molecules move into the Golgi apparatus, which sorts molecules bound for the plasma membrane from those destined for other organelles.

Mitochondria contain enzymes which catalyze an electron transport chain which converts electrochemical potential energy into ATP. Lysosomes contain many hydrolases which degrade macromolecules into subunits for recycling. Most of these hydrolases have broad specificities and can degrade molecules from a variety of sources, including foreign material brought into the cells through endocytosis. Solid particles are wrapped in membranes and internalized by a process called phagocytosis. These newly formed membrane compartments containing particles or microbes are termed phagosomes. Extracellular soluble material and very small particles are bound into membranes in a process called pinocytosis, or macropinocytosis in the case of very large inclusions, which produces organelles called pinosomes, or macropinosomes. Phagosomes and pinosomes are collectively termed endosomes. Molecules in endosomes are sorted; some recycle back to the plasma membrane while most are delivered into lysosomes for degradation. Lysosomes will be discussed in greater detail below.

Compartmentalization of functions into discrete organelles allows cells to express enzymes which could not function in the cytosol of healthy cells. Some organelles have a specialized environment which sequesters chemical reactions that would be toxic in the cytosol. The low pH of lysosomes allows distinct degradation reactions which could not occur in the neutral pH of cytoplasm. Compartmentalization also allows cells to use enzymes which would otherwise be harmful for the cell. For example, many of the lysosomal hydrolases could degrade cellular contents if expressed in the cytosol. Hence, damage to organelles can be dangerous for cells.

1.3 Lysosomes

Lysosomes are single membrane-bounded intracellular organelles containing various acid hydrolyases in their acidic lumen. They serve as the end degradative compartment of the endocytic and autophagic processes (reviewed in (de Duve, 1983; de Duve, 2005)). The term lysosome was originally coined by De Duve in 1955 to denote the compartments his lab isolated by centrifugation of mouse hepatocyte homogenates. They were distinguished as sub-cellular bodies containing a cellular acid phosphatase (De Duve et al., 1955). Lysosomes were eventually found to contain acid hydrolases for macromolecules and lipids, often with overlapping specificities, indicating the role of lysosomes and their enzymes in degrading a wide variety of molecular targets from a variety of sources (Luzio et al., 2007).

1.3.1 Trafficking to lysosomes

Containment of most of the cellular hydrolyases in membrane-bounded compartments shields cellular components from degradation but implies that molecules destined for degradation in lysosomes must be trafficked through either the plasma membrane, in the case of extracellular molecules, or the lysosomal membrane, in the case of cytosolic molecules. Extracellular particles greater than 0.5 μm are internalized by phagocytosis while smaller particles and soluble molecules may enter cells by pinocytosis (Conner and Schmid, 2003; Swanson, 2008). Recently endocytosed cargo is trafficked into early endosomes, which are typically identified by the localization of Rab5 (Kinchen and Ravichandran, 2008). Early endosomes contain some sorting capabilities, as some molecules delivered to endosomes are recycled to the cell surface while others are trafficked into late endosomes. Late endosomes are typically more acidic and are

characterized by the localization of Rab7. Late endosomes eventually deliver their cargo to acidic lysosomes, which contain hydrolases and the trans-membrane proteins LAMP-1 or LAMP-2 (Kinchen and Ravichandran, 2008; Luzio et al., 2007). Cytosolic molecules can be sequestered into double membrane-bounded compartments called autophagosomes, which are often identified using the protein Lc3 (Tooze et al., 2010). These pathways of endocytosis and autophagy converge by delivering their cargo to lysosomes for degradation (Scott et al., 2003) (Kinchen and Ravichandran, 2008).

Acid hydrolases and membrane proteins destined for lysosomes are synthesized in the rough endoplasmic reticulum using N-terminal signal sequences, similar to secreted proteins. In the lumen of the endoplasmic reticulum, lysosomal proteins are given a characteristic mannose 6-phosphate glycosylation, their N-terminal signal sequence is removed and they become otherwise glycosylated. Glycosylation protects lysosomal proteins from the harsh environment of the lysosomes and, in the case of trans-membrane proteins, protects lysosomal membrane from the lysosomal lipases. The mannose 6-phosphate glycosylation is important for proper trafficking of lysosomal proteins and requires the action of a phosphotransferase (Reitman and Kornfeld, 1981; Waheed et al., 1981) and a diesterase (Varki and Kornfeld, 1981; Waheed et al., 1981). This mannose 6-phosphate group is recognized by a Golgi receptor which sorts lysosome-bound proteins from those destined for secretion. These mannose 6-phosphate-labeled proteins are bound into vesicles and trafficked into late-endosomes; from there the lysosomal proteins are delivered into lysosomes and the mannose 6-phosphate receptors are recycled to the trans-Golgi network (Gonzalez-Noriega et al., 1980). It should be noted that this sorting process is not perfectly efficient as a small fraction of lysosomal proteins

are secreted. These proteins can be scavenged by mannose 6-phosphate receptors on cell surfaces and trafficked into lysosomes. This second pathway forms the basis for enzyme replacement therapy used to treat individuals with genetic deficiencies for certain lysosomal hydrolases; this topic will be discussed in more detail below. Throughout the trafficking process, lysosomal acid hydrolases remain inactive by their non-catalytic conformation and by the neutral pH of these compartments. Full activation occurs in the lysosomes, where the binding partners and acidic pH lead to activation of hydrolase function.

1.3.2 Labeling and identifying lysosomes

In De Duve's original cell fractionation studies, lysosomal fractions were identified by the presence of acid phosphatase activity and the absence of cytochrome oxidase and glucose 6-phosphatase, which marked the mitochondrial and endoplasmic reticulum fractions, respectively (De Duve et al., 1955). Eventually acid phosphatase was localized to lysosomes by cytochemical methods. Later, weak bases were found to accumulate in the acidic lumen of lysosomes. The modern widely used "Lysotracker" reagents sold by Invitrogen (Carlsbad, CA, USA) are fluorescent dye molecules with weakly basic functional groups which causes them to accumulate in lysosomes. Alternatively, endocytosis can be used to label lysosomes. In this technique, cells are allowed to pinocytose membrane-impermeant tracer molecules, which are then allowed to reach lysosomes by incubating cells for several hours in medium without the tracer. Membrane trafficking moves internalized contents from early to late endocytic compartments (examples (Davis and Swanson, 2010; Ohkuma and Poole, 1978). Finally, characteristic membrane-associated proteins localize to different compartments of

endocytic trafficking. LAMP-1 and LAMP-2 are the most commonly labeled proteins for identifying lysosomes; they can be localized using antibodies or fluorescent protein chimeras such as green fluorescent protein, for example GFP-LAMP-1. Thus, a variety of techniques are available for labeling lysosomes.

1.3.3 Lysosomal pH

The lysosomal lumen is maintained at pH 4-5. Lysosomal pH was originally measured in living cells using fluorescein-dextran by Ohkuma (Ohkuma and Poole, 1978) and confirmed by others (Christensen et al., 2002). The acid hydrolyses responsible for the degradative function of lysosomes all have optimum activity at around pH 4.75. Many of these enzymes are most active on acid-denatured substrates, further underlining the optimization of these enzymes to the lysosome (Coffey and De Duve, 1968). The pH gradient across membranes of lysosomes and late endosomes is maintained by the vacuolar ATPase, a trans-membrane protein complex which uses the energy of ATP to pump protons from the cytosol into the lysosomal lumen, reviewed in (Nakanishi-Matsui et al., 2010).

1.4 Diseases from deficiencies in lysosomes

There was a significant breakthrough in the understanding of lysosomes as degradative compartments upon the identification of the first lysosomal storage disorder by Hers (Hers, 1963). The study of lysosomal storage disorders led to many of the discoveries which underlie current knowledge of the physiologic functions as well as the pathologic disfunctions of lysosomes. Lysosomal storage disorders are rare genetic diseases caused by a biochemical deficit in the degradation or trafficking of some metabolite or group of metabolites. As their name would suggest, these disorders are

characterized by the aberrant accumulation of cargo molecules in lysosomal compartments, which often leads to the swelling of lysosomes observed by microscopy. The topic of lysosomal storage disorders has been extensively reviewed (Ballabio and Gieselmann, 2009; Futerman and van Meer, 2004; Parkinson-Lawrence et al., 2010; Vellodi, 2005).

All lysosomal storage disorders are single gene disorders and the vast majority are autosomal recessive mutations. The genetic lesions themselves can be mis-sense or non-sense mutations, leading to varying residual activity in the resulting mutant proteins. The simplest lysosomal storage disorders, conceptually, are those caused by mutations conferring deficiencies in lysosomal hydrolases which lead to an accumulation of the substrate. These include deficiencies which result in accumulation of sphingolipids, mucopolysaccharides and oligosaccarides. Deficiencies in activators of pathways can also cause disease. For example acid sphingomyelinases require activators and saposins to function properly, so genetic deficiencies in these activators (Conzelmann and Sandhoff, 1978) or saposins (Bradova et al., 1993; Christomanou et al., 1989; Wenger et al., 1989) lead to accumulation of sphingomyelins. Another example of co-factor deficiency leading to lysosomal storage disease involves the lysosomal sulfatases. This group of acid hydrolases requires a cysteine reaction in their active site to become catalytic. Deficiency in the enzyme responsible results in severe disease resulting from the loss of activity of the entire group of enzymes (Dierks et al., 2003).

More complicated and often more severe lysosomal storage disorders are caused by deficiencies in trafficking of enzymes or substrates. Deficiencies in the mannose 6-phosphate phosphotransferase results in inefficient sorting of lysosomal hydrolases such

that these enzymes are secreted instead of trafficked into lysosomes. This leads to high levels of extracellular hydrolase, accumulation of a wide variety of undegraded metabolites and the severe lysosomal storage disorder called I-cell disease (Hasilik et al., 1981; Hickman and Neufeld, 1972). Although lysosomal storage disorders are single gene deficiencies, many are characterized by secondary accumulations. Secondary accumulations are especially prevalent in lipid lysosomal storage disorders as endosomal trafficking of different lipid species are often interconnected. One example is Niemann-Pick disease type C, which is primarily a deficiency in NPC1, a trans-membrane protein involved in cholesterol processing. As cholesterol and sphingolipid comprise lipid rafts, which are sub-regions of membranes of decreased fluidity rich in cholesterol and sphingolipids, this disease is characterized by accumulation of sphingolipids along with cholesterol (Neufeld et al., 1999). Another important secondary accumulation which occurs in a variety of lysosomal storage disorders is the accumulation of autophagic cargo, whereby inefficient lysosome-autophagosome fusion results in the accumulation of ubiquinated proteins and dysfunctional mitochondria (Settembre et al., 2008).

1.4.1 Pathology of lysosome storage diseases

The pathogenic consequences of lysosomal storage disorders depend on which gene is mutated, but in general lysosomal storage disorders are characterized by the buildup of undegraded material within lysosomes and sometimes other endosomes. This accumulated material is observable by light and electron microscopy and was the initial phenotype by which these diseases were identified. This build-up of material often leads to macro-scale swelling of the affected organs. On the cellular level, lysosomal storage of material can interfere with cellular function, especially in neuronal and renal cells,

leading to tissue disfunction. Certain lysosomal storage disorders have also been linked to perturbations in macrophage activation and aberrant inflammatory cytokine secretion (Allen et al., 1997; Hollak et al., 1997; Wu and Proia, 2004). This activation can result in damage to the blood-brain barrier and neuronal death from activated microglia.

Many substrates, intermediates and products of lysosomal enzymes mutated in lysosome storage diseases are potent signaling molecules or important second messengers. Accumulation of these molecules can lead to signaling perturbations within cells. One example is a group of lysosomal storage disorders characterized by deficiency in the degradation of glycosaminoglycans. This deficiency results in the accumulation of undigested polysaccharides which can function as TLR4 agonists (Johnson et al., 2002). This TLR4 activation contributes to significant pathology of this group of lysosomal storage diseases (Simonaro et al., 2005). Another example is acid sphingomylinase deficiencies in which sphingomyelin cannot be hydrolysed to ceramide. Ceramide is an important second messenger compound much like another membrane lipid diacylglycerol (Hannun and Obeid, 2002). In mice lacking acid sphingomylinase, a mouse model of Niemann-Pick, perturbation of this pathway can result in altered sensitivity to apoptosis (Lozano et al., 2001).

Perturbations in lysosome function can perturb cellular signaling in other ways. The release of calcium from intracellular stores in response to signaling is perturbed in some lysosomal storage disorders (Pelled et al., 2003). Mitochondrial disfunction has also been reported for some lysosomal storage disorders. Disorders which perturb lipid metabolism can also disrupt the formation of lipid rafts, which may disrupt the signals from receptors which normally localize to these micro-domains (Futerman and van Meer,

2004) These changes in cell signaling can also induce changes in gene expression which may, in turn, alter other biochemical pathways. For many individual lysosomal storage disorders it remains difficult to determine the primary effects of stored material and the many secondary effects induced by long term tissue disfunction. In some cases, even effective treatment of the mutated gene is insufficient to reverse all of the secondary pathological changes (Futerman and van Meer, 2004).

1.4.2 Lysosome storage and lysosome stability

There has been long term interest in the role of lysosome damage and weakened lysosomal membranes in lysosomal storage disorder pathologies. Overall, there is little evidence of lysosome integrity problems in lysosomal storage disorders (Futerman and van Meer, 2004). However in fibroblasts from patients suffering from Niemann-Pick type A, acid sphingomyelinase mutations result in lysosomal membranes with increased susceptibility to damage. Interestingly, this increased susceptibility could be reversed by endocytosis of exogenously administered, heat shock protein-70 (HSP-70) (Kirkegaard et al., 2010).

In summary, the study of lysosomal storage disorders has led to a greater understanding of the role of lysosomal degradation in healthy tissue function. The loss of one of many lysosomal degradative functions compromises the function of a wide variety of tissues leading to potentially devastating pathologies. The existence and severity of lysosomal storage disorders confirms the importance of lysosomes in a wide variety of tissues and cell types. Also of note is that lysosomes of macrophages/monocytes are especially important, in that repair or restoration of lysosome function in this one cell type can reverse much of the disease. While the etiologies of lysosomal storage disorders

remind us that the primary function of lysosomes is homeostatic degradation and recycling of materials, there are other important functions of lysosomes in microbe killing and cell signaling.

1.5 Lysosome damage and cell death

Soon after the initial discovery of lysosomes, De Duve proposed that lysosomes may be involved in cell death, calling lysosomes suicide bags (Turk and Turk, 2009). This early idea was based on the hypothesis that lysosomal hydrolases, especially cathepsins, released into the cytosol would digest the cytosolic contents and kill the damaged cell. This prediction was that programmed cell death would result in large scale disruptions of lysosomes followed by degradation of cellular contents, mostly by lysosomal enzymes. Later it was found that most lysosomal hydrolases have very little activity in the cytosol due to the sub-optimal pH for the hydolases as well as the presence of cytosolic inhibitors of lysosomal hydrolases (Turk and Turk, 2009). Additionally, caspases, which are cysteine-aspartate-specific proteases distinct from cathepsins, were identified as the major degradative proteases in programmed cell death. More recent studies have found that lysosomes have subtle but important roles in cell death pathways.

Mitochondria are another example of membrane-bounded intracellular organelles with a distinct function. Damage to mitochondria, induced by various stimuli, releases cytochrome C. Cytosolic cytochrome C is sensed by a protein called Apaf-1, which nucleates the formation of a signaling complex which activates a cascade of caspases. These caspases trigger apoptotic cell death. This pathway is often termed the intrinsic pathway or mitochondrial pathway of apoptosis. Damage to lysosomes may occur

before, after or in the absence of mitochondrial disruption and affect cell death (Boya and Kroemer, 2008).

In some stressed cells, lysosome damage may occur subsequent to mitochondrial damage in the apoptosis pathway. In this model, lysosome damage is induced by apoptosis products subsequent to cytochrome C release from mitochondria and may function in a positive feedback loop leading to cell death. Several candidate molecules link mitochondrial release to lysosome damage. One is activated caspase-9-induced lysosomal content release and cell death, which is independent of the mitochondrial apoptosis pathway (Gyrd-Hansen et al., 2006). Damaged mitochondria, which cause apoptosis, release reactive oxygen species (ROS) which can trigger lysosome damage (discussed in more detail below). Also, several proteins which induce mitochondrial damage can in some situations induce lysosomal damage and may induce cell death via one or both pathways in cells.

Other work has found that lysosome damage can precede and in some cases induce mitochondrial cell death. Damage to lysosomes releases the lysosome's luminal contents into the cell cytosol, including cathepsins. While cathepsins are probably not responsible for large scale proteolysis in the cytosol following lysosomal release, many groups have studied the effects of cathepsin release from lysosomes into the cytosol. Cathepsin D released into the cell cytosol by ROS-mediated lysosome damage caused mitochondrial damage, caspase activation and cell death (Zang et al., 2001). Multiple cathepsins are capable of cleaving purified pro-apoptotic protein Bid. This cathepsin-cleaved Bid induced mitochondrial outer membrane destabilization in purified mitochondria (Cirman et al., 2004). Lysosomal release of cathepsins and subsequent Bid

cleavage, mitochondrial destabilization and apoptotic cell death have been observed in several cell types (Cirman et al., 2004; Garnett et al., 2007; Heinrich et al., 2004; Lamparska-Przybysz et al., 2006; Nagaraj et al., 2006; Sandes et al., 2007; Yacoub et al., 2008). Inhibition of cathepsin activity also decreased Bid cleavage and cell death (Caruso et al., 2006) reinforcing the conclusion that cathepsin release by lysosome damage can cleave Bid and trigger cell death.

In some cases, cytosolic cathepsins can directly activate caspases by proteolytic cleavage. Cathepsin B cleaves caspase-2, which in turn mediated mitochondrial destabilization and subsequent cell death (Guicciardi et al., 2005). Cathepsin L activates caspase-3 (Hishita et al., 2001; Ishisaka et al., 1999). Thus Bid and initiator caspases represent two targets which cathepsins released from lysosomes into cytosol can activate to initiate classical mitochondrial apoptosis.

Lysosome damage can also mediate caspase-independent cell death. Cells can sometimes proceed from lysosome damage to cell death in the presence of caspase inhibitors (Broker et al., 2004; Garnett et al., 2007). Some forms of apoptosis augment caspase pathways with caspase-independent pathways such as the release of a protein called apoptosis-inducing factor (AIF) from the mitochondrial lumen. AIF has been shown to be important for cell death following lysosome damage in some cells, probably through mitochondrial release (Bidere et al., 2003; Chen et al., 2005).

The pathways activated in response to death signals vary by cell type and stimulus, so the contribution of mitochondria-independent cell death similarly varies. Some immune cells with lysosome damage undergo an apoptotic caspase-independent inflammatory cell death termed pyroptosis. Pyroptosis is an immune cell death pathway

activated following the assembly of a signaling complex termed the inflammasome. Inflammasomes are caspase-1-activating complexes assembled upon cytosolic recognition of a variety of microbial or tissue damage stimuli (Schroder and Tschopp, 2010). Activated caspase-1 cleaves and activates the proinflammatory cytokines IL-1β and IL-18. Inflammasomes can be activated by many inflammatory stimuli such as the detection of microbial DNA, lipopeptides and flagellin in host cell cytoplasm. The consequences of cell and tissue damage, such as plasma membrane damage, phagocytosis of urate crystals and lysosome damage can also induce inflammasome assembly (Schroder and Tschopp, 2010). Lysosome damage-mediated by a variety of stimuli induces inflammasome activation and IL-1β secretion (Halle et al., 2008; Hornung et al., 2008). These pathways may link lysosome damage to pyroptotic cell death by macrophages. Pyroptosis depends on the inflammasome-associated caspase-1, but not on the apoptosome-associated caspases, caspase-3 or caspase-8 (Bergsbaken et al., 2009). Pyroptosis results in cell swelling, lysis and release of pro-inflammatory molecules (Fink and Cookson, 2006). It remains unclear whether the lysosome damage-dependent cell death pathways previously described as necrosis are in fact pyroptosis.

As mitochondria-induced cell death can induce lysosome damage and lysosome damage can trigger mitochondrial and other cell death mechanisms, lysosome and mitochondrial damage may contribute to positive feedback loops which further commit a cell to programmed cell death after damage to one of the two types of organelles (Boya and Kroemer, 2008; Terman et al., 2006). The level of lysosomal content release may also be important in determining which type of cell death pathway becomes activated. Low levels of damage may lead to slower types of cell death such as apoptosis. Massive

lysosome damage has been suggested to lead to faster cell death by necrosis or, in activated macrophages, pyroptosis. The threshold level of lysosome damage necessary for commitment to any type of cell death has not yet been determined.

1.6 Inducers of lysosome damage

A wide variety of conditions can induce lysosome damage. This section will explore the various molecules and categories of molecules which are capable of damaging lysosomes as well as the mechanisms by which these conditions cause lysosome damage. While some conditions are interrelated, no one mechanism can account for all lysosome damage.

1.6.1 An expanded role for the Bcl-2 family; Bax and p53 in lysosome damage

Further evidence that lysosome and mitochondrial damage may be related is that some of the proteins implicated in pore formation in the outer mitochondrial membrane can also induce damage to lysosomes. Mitochondrial outer membrane permeabilization in apoptosis is regulated by the binding interactions of several Bcl-2 family proteins. Pro-apoptotic conditions result in the liberation of Bax which can act on the mitochondrial outer membrane to induce permeabilization (Giam et al., 2008). In some circumstances, activated Bax can also act on the lysosomal membrane, releasing lysosome contents. Bax was observed to localize to mitochondrial and lysosomal membranes during cell death (Feldstein et al., 2004; Kagedal et al., 2005). Inhibition of Bax using siRNA, over-expression of Bcl-X_L, or pharmacologically reduced lysosome damage and subsequent cell death (Feldstein et al., 2006). In a death receptor ligation model, Bim, another pro-apoptotic Bcl-2 family member, localized with Bax to lysosomes and mediated lysosome damage preceding mitochondrial damage (Werneburg

et al., 2007). It is unclear if Bcl-2 family members mediate lysosome localization and damage is regulated differently than mitochondrial localization and damage, or if instead Bax and Bim localize to both organelles whenever they are released by signaling. Lysosome damage does not always occur when mitochondria are permeabilized, which indicates some additional levels of regulation exist. Another hypothesis is that low level lysosome damage always accompanies mitochondrial-damage-dependent apoptosis, but that such damage has been undetectable by current methods.

The tumor suppresser protein p53 is an important regulator of cell fate in apoptosis and seems to have an important role in the consequences of lysosome damage. Activated p53 has many roles in apoptosis. It can bind to anti-apoptotic Bcl-2 family members, leading to mitochondrial outer membrane perforation and commitment to apoptosis (Mihara et al., 2003). p53 was also shown to activate Bax independent of other proteins (Chipuk et al., 2004). In other systems, p53 accumulation and activation led to lysosome damage before mitochondrial membrane permeabilization (Yuan et al., 2002). Lysosome-associated protein containing PH and FYVE domains (LAPF) also localizes to lysosomes early in apoptosis and participates in p53-mediated lysosomal membrane damage (Chen et al., 2005; Li et al., 2007). Thus, p53 plays an important role in lysosome-mediated cell death, consistent with p53's role as a cell fate determinant in many systems.

1.6.2 The role of cathepsin proteases in lysosome damage

Cathepsins also facilitate lysosome damage. Cells lacking the gene for cathepsin B were less sensitive to TNF-α-stimulation. Lysosomes purified from cathepsin B-deficient cells were less sensitive to sphingosine, another mediator of lysosome damage,

suggesting that cathepsin B was important for promoting lysosome damage (Werneburg et al., 2002). In other systems, pharmacological inhibition of cathepsins reduced lysosome damage upon subsequent challenge (Feldstein et al., 2004; Michallet et al., 2004). The cathepsins may act on lysosomes directly following initial lysosome damage or they may activate other cell death pathways such as Bcl-2 family proteins which feed back to increase lysosome damage. This second explanation cannot be ruled out in the above studies, as current methods cannot detect low levels of lysosome content release.

1.6.3 Lysosomotropic agents which damage lysosomes

At neutral pH, small weakly basic molecules can readily cross cell membranes. In acidic compartments, these molecules become charged and membrane-impermeant. Different molecules with these properties and certain functional groups are used for labeling, neutralizing or destabilizing lysosomes. Damaging lysosomotropic agents are weakly basic surfactants which accumulate in lysosomes and act as detergents to perforate lysosomes once they rise above a threshold concentration (Firestone et al., 1982; Miller et al., 1983).

Some endogenous molecules, such as amine-functionalized lipids, can induce lysosome damage in a similar manner. Sphingosine is a weak base sphingolipid and component of ceramide and sphingomyelin. At moderate doses, sphingosine induces lysosome damage, followed by apoptosis. At higher doses, sphingosine causes high lysosome damage and necrosis (Kagedal et al., 2001a; Kagedal et al., 2001b). Sphingosine-dependent lysosome toxicity is important for cell death subsequent to TNF-α administration to cultured hepatocytes (Werneburg et al., 2002). Ceramide, which is sphingosine covalently bound to a fatty acid, and sphingomyelin, ceramide bound to

phosphorylcholine, remain lipophilic but are not lysosomotropic, as they lack the weak base functional group necessary for lysosomal accumulation. Other endogenous molecules such as bile salts and fatty acids can also rupture lysosomes (Feldstein et al., 2004; Feldstein et al., 2006; Roberts et al., 1997).

Leu-Leu-OMe is another amphipathic molecule which disrupts lysosomes. This experimental drug is endocytosed and trafficked through endosomes into lysosomes. There the drug is polymerized into leucine polymers by the action of lysosomal acyl-transferase activity. These polymers are lipiphilic and damage only the lysosomes of cells which can polymerize Leu-Leu-OMe, mainly myeloid lymphocytes (Hornung et al., 2008; Thiele and Lipsky, 1985; Thiele and Lipsky, 1990).

1.6.4 The Role of reactive oxygen species in lysosome damage

Much lysosome damage involves ROS. In the cytosol, ROS are generated mainly in the form of hydrogen peroxide (H_2O_2). This peroxide can be generated from several sources; mitochondria, especially damaged mitochondria, cytosolic oxidases, peroxidases and P450 system of the endoplasmic reticulum (Terman et al., 2006). As ROS typically does not diffuse long distances in cytoplasm before being converted to water by cytosolic catalase, it has been hypothesized that lysosomes juxtaposed to damaged mitochondria may be at highest risk of damage from H_2O_2 (Boya and Kroemer, 2008; Terman et al., 2006). ROS can also be generated directly into the endosomal lumen by the phagosomal oxidase system, which catalyses the formation of luminal superoxide using the reducing potential of NADPH (Minakami and Sumimotoa, 2006). This superoxide can be converted into hydrogen peroxide as well as other ROS.

While ROS can damage many cellular components and organelles, it is especially effective against lysosome membranes. Lysosomes lack many of the anti-oxidants found in cytosol. Perhaps to make up for this, lysosomal membranes have high concentrations of vitamin E (Wang and Quinn, 1999) a membrane lipid antioxidant (Traber and Atkinson, 2007). If ROS are not neutralized by antioxidants, they can lead to radical chemistries which can disrupt disulfide and peptide bonds in proteins and peroxidate membrane phospholipids. These peroxidated lipids are also highly reactive. In addition to taking part in other chemistries, accumulation of modified lipids can destabilize lipid bi-layers and damage lysosomes (Zdolsek and Svensson, 1993).

The presence of redox-active, unchelated iron can potentiate ROS toxicity in lysosomes. Ferrous iron (Fe^{2+}) in lysosomes can react with hydrogen peroxide to form hydroxyl radical and Fe^{3+}. Lysosomal redox potential typically returns this ferric iron to the 2+ oxidation state, making this reaction effectively catalytic. Lysosomal reduction of Fe^{3+} to Fe^{2+} also generates reactive oxygen radicals; thus lysosomal iron is extremely toxic to lysosomes. These reactions, collectively termed Fenton reactions, as well as the role of iron in lysosomes, are reviewed in (Terman et al., 2006). The role of iron in lysosome damage has been demonstrated in several systems. Administration of an iron chelator protects cells from lysosome damage and cell death while addition of exogenous iron increases lysosome damage and cell death (Doulias et al., 2003; Kurz et al., 2006; Yu et al., 2003). Iron can accumulate in lysosomes from several sources. Autophagic recycling can result in the lysosomal destruction of many mitochondrial and cytosolic enzymes containing iron co-factors, consequently releasing iron into lysosomes upon

proteolysis of the enzymes. Lysosomes can also accumulate iron by autophagy and by recycling of intracellular ferritin (Terman et al., 2006).

1.6.5 TNF-α-induced cell death can involve lysosome damage

TNF-α is a cytokine secreted by a variety of immune cells. It can stimulate inflammatory pathways in certain cell types and cell death in others. In hepatocytes (Werneburg et al., 2002) and fibroblasts (Heinrich et al., 2004) treated with TNF-α, lysosome damage preceded cell death and was associated with sphingosine, cathepsin and activation of proapoptotic Bcl-2 family members. Lysosome damage in cholangiocarcinoma cells following exposure to another TNF family ligand, TRAIL, depended on cathepsins and Bcl-2 family members (Werneburg et al., 2007). Thus lysosome damage may be involved in exogenous cell death signaling.

1.6.6 Silica particle-induced phagolysosome damage

The phagocytosis of some particles damages lysosomes. The most studied phagolysosome-damaging particle is silica ground into micro-or nanometer-sized particles. These particles are medically relevant as they are the causative agents of silicosis, which results in progressive fibrosis of the lungs (Mossman and Churg, 1998). Silica crystals in the lungs are phagocytosed by resident macrophages (Huaux, 2007). The silica-containing phagosomes fuse with lysosomes to become phagolysosomes. Some of these phagolysosomes then release their contents, triggering inflammation and, in some cases, cell death (Hornung et al., 2008; Persson, 2005; Thibodeau et al., 2004). The mechanism by which silica induces lysosomal damage remains somewhat controversial. Some groups claim ROS are unimportant for silica-mediated lysosome damage (Hornung et al., 2008; Thibodeau et al., 2004). Other groups reported that ROS

contribute to lysosome damage (Dostert et al., 2008; Persson, 2005). Pre-treatment of silica particles with iron-chelators reduced subsequent lysosome damage, suggesting that silica surface iron content may be important for lysosome damage by this pathway (Persson, 2005). One interpretation of these data is that different preparations of ground silica may contain different amounts of iron and thus the ROS-mediated damage by these particles would depend on the iron content. Silica-mediated, ROS-independent lysosome damage mechanisms remain uncharacterized. Asbestos particles may also induce lysosome damage by a similar mechanism, as they induce similar inflammatory profiles to silica particles in tissue culture models (Dostert et al., 2008).

1.6.7 Lysosome damage by cholesterol crystals contributes to arteriosclerosis

While lipid overload is known to induce lysosome damage, crystallized cholesterol particles damage lysosomes similarly to ground silica. Cholesterol, probably originating from oxidized LDL particles, crystallizes in arteriosclerotic plaques early in plaque formation (Duewell et al., 2010). In vitro experiments using human and mouse macrophages showed that cholesterol crystals damage phagolysosomes after phagocytosis (Duewell et al., 2010; Rajamaki et al., 2010; Yuan et al., 2000). The inflammatory mediators released after this lysosome damage were critical to the progression of arteriosclerosis (Duewell et al., 2010). Iron-mediated ROS contributed to this lysosomal damage, as chelation of iron reduced lysosome damage (Yuan et al., 2000). Thus lysosomal damage contributes to the pathology of an important disease.

1.6.8 Other particles capable of inducing phagolysosome damage

While silica and cholesterol are well characterized phagolysosome-damaging particles, others can mediate these effects. β-amyloid, which condenses into insoluble

material in neural plaques in Alzheimer's disease, is phagocytosed and damages lysosomes in microglial cells (Halle et al., 2008), suggesting a role for lysosome damage in that disease.

Aluminum salts (alum) are commonly used adjuvants in human and animal vaccine formulations. Phagolysosomes containing alum particles are perforated similarly to those containing silica (Hornung et al., 2008). These data suggest a mechanism by which antigens administered along with alum adjuvants may gain access to the cytosol of antigen-presenting cells. However, the significance of damage-mediated inflammation to the adjuvant activity of alum is controversial (Eisenbarth et al., 2008; Franchi and Nunez, 2008; Kool et al., 2008; McKee et al., 2009). Prior to this work, it was unknown whether lysosome damage was a common outcome of particle phagocytosis or if certain particles damage lysosomes more than others.

1.6.9 Infectious particles and lysosome damage

Another major category of particles capable of damaging lysosomes are intracellular pathogens, which must access the host cell cytosol as a replicative niche or which must damage intracellular membranes to transmit to the next cell. Many pathogenic bacteria escape the microbicidal activities of lysosomes and utilize the cytosol as a replicative niche. Some bacteria escape from intracellular compartments to gain access to the cytosol. For example, *Listeria monocytogenes* (*L.m.*) is a facultative intracellular bacterium which utilizes a pore-forming toxin to perforate endosomes and escape into the host cell cytosol. *L.m.* usually escapes from endocytic compartments before they fuse with lysosomes. *L.m.* escape from lysosomes is inefficient (Henry et al., 2006). Nonetheless, lysosome damage may still occur in the course of *L.m.* infection,

either as an infrequent event or as the result of non-productive *L.m.* activity. Some other bacterial pathogens which replicate in the host cell cytosol, such as various *Francisella, Salmonella* and *Legionella* species, may also damage lysosomes as they escape. Other bacteria, including *Mycobacterium tuberculosis*, *Brucella* and *Chlamydia* replicate inside of host cell vacuoles which in some ways resemble lysosomes. While these bacteria do not need to rupture this compartment to replicate, substantial evidence of bacterial communication with host cell cytosol suggests that minor or transient damage occurs (Kumar and Valdivia, 2009; van der Wel et al., 2007).

Viruses may also damage lysosomes, as they must gain access to the cytosol to replicate. HIV-infected T cells undergo apoptosis after lysosome damage and cathepsin D release into the cytoplasm. Transfection of T cells with the cDNA for the viral protein NEF was sufficient to induce lysosome damage (Laforge et al., 2007), which suggests that viral gene expression leads to this lysosome damage. Lysosome damage has also been reported following infection with human papilloma virus (Kaznelson et al., 2004), parvovirus (Di Piazza et al., 2007) and HSV-1 (Peri et al., 2011). While lysosome damage may occur during viral invasion, it appears that late stage lysosome damage-mediated cell death is a common result of viral infection.

The mechanisms by which most of these infectious and non-infectious particles damage lysosomes are unknown and sometimes controversial, in the case of silica particles. It is unknown if ROS, Bcl-2 family proteins and sphingosine, which are common mediators of lysosome damage leading to cell death, are also important for lysosome damage by particles. Virulence factors of microbes may damage lysosomes.

Alternatively, ROS produced in microbe-containing endosomes by the phagosomal NADPH oxidase may lead to some infection-associated lysosome damage.

1.7 Protection of lysosomes from damage

In contrast to the many conditions recognized as lysosome-damaging, there are relatively few conditions known to reduce lysosome damage. Administration of antioxidants or the chelation of iron reduces lysosome damage in some systems (Bivik et al., 2007; De Milito et al., 2007; Kurz et al., 2006; Persson, 2005; Roussi et al., 2007). In mitochondrial damage-induced cell death, pro-apoptotic Bcl-2 family proteins are regulated by the anti-apoptotic Bcl-2 family members. Bcl-2 function prevents high levels of lysosome damage in an ROS system (Zhao et al., 2001), suggesting that anti-apoptotic Bcl-2 family members prevent the cathepsin-activated Bax and or Bid from initiating a positive feedback loop which would otherwise increase lysosome damage.

Pre-exposure of cells to the chaperone protein HSP70 reduces lysosome sensitivity to damaging agents (Daugaard et al., 2007a; Daugaard et al., 2007b; Dudeja et al., 2009; Gyrd-Hansen et al., 2004; Kirkegaard et al., 2010; Nylandsted et al., 2004). The mechanism by which a chaperone protein induces protection of lysosomes has been incompletely elucidated. Endocytosed HSP70 activates the lysosomal acid sphingomyelinase in fibroblasts leading to damage-resistance. Inhibition of lysosomal acid sphingomyelinase reversed the HSP70-mediated protection (Kirkegaard et al., 2010). Sphingomyelinase converts sphingomyelin into ceramide and phosphocholine. It remains unclear how this chemistry protects lysosomes, although sphingosine may be involved.

1.8 Existing methods for measuring lysosome damage

One of the earliest reports of damaged lysosomes was based on electron microscopy, in which lysosomes were observed with visibly perforated membranes. However, this technique was insensitive (Terman et al., 2006). More modern methods for measuring lysosome damage detect lysosome contents in the cytosol, either by using probes for endogenous lysosomal enzymes, such as antibodies or reporter substrates, or by pre-loading lysosomes with reporter molecules and measuring their release into cytoplasm. One technique is to fractionate cells using ultracentrifugation into lysosomal fractions and cytosolic fractions. Lysosomal contents can then be detected in the cytosolic fractions by western blotting (Michallet et al., 2004) or by detecting specific enzyme activities (Groth-Pedersen et al., 2007). Another technique for the detection of native lysosomal proteins released into the cell cytosol is immuno-fluorescence, in which cells are fixed, stained and scored, using a fluorescence microscope. For example, diffuse cathepsin distributions which do not resemble control cells indicates lysosomal damage (Werneburg et al., 2002; Werneburg et al., 2007).

To measure lysosome damage in live cells, lysosomes are loaded with fluorescent molecules and the redistribution of these molecules is measured. There are three main methods for labeling lysosomes. The first method is to express fluorescent protein-cathepsin chimeras in cells. When properly constructed, these molecules are trafficked into lysosomes and their release is typically measured by microscopy of live or fixed cells (Werneburg et al., 2002; Werneburg et al., 2007). Another method for labeling lysosomes uses the endocytic process to deliver membrane-impermeant molecules into lysosomes. Dye-containing medium which is taken up by endocytosis and endocytic

trafficking delivers these molecules to lysosomes. A chase step in unlabeled medium is usually included to ensure that all endocytosed molecules reach the lysosomes. Dextrans are mostly inert bacterial polysaccharides which can be covalently labeled with fluorophores. Lysosomes are typically loaded with these fluorescent dextrans. Detection of lysosome damage is typically monitored by microscopy looking for diffuse cytoplasmic signals. Interestingly, lysosomes loaded with different sizes of fluorescent dextrans show different amounts of lysosome release following the same stimulus, indicating that lysosome damage in these systems is incomplete and that smaller molecules diffuse out of lysosomes more easily than large molecules (Bidere et al., 2003; Laforge et al., 2007).

The last method for labeling lysosomes is by using fluorophores with weakly basic groups which accumulate in lysosomes, so-called lysosomotropic dyes. The accumulation of these dyes into lysosomes requires maintenance of lysosomal pH. Dye amounts are limited, as excessive dye accumulation can inhibit acidification. One commonly used technique labels lysosomes with a weakly basic fluorophore called 'Lysotracker'. Lysosome damage is measured as a loss of fluorescence intensity, detectable by microscopy or by flow cytometry (Hornung et al., 2008). Another commonly used lysosomotropic dye is acridine orange, whose fluorescence exhibits concentration-dependent spectral shift. Concentrated, lysosomal acridine orange fluoresces red, while dilute, cytoplasmic acridine orange fluoresces green. Some released acridine orange binds cytosolic molecules and is retained in cells, resulting in a dim green fluorescence in cells with damaged lysosomes. A significant advantage of acridine orange is that lower levels of release can be detected by measuring a rise in green

fluorescence upon lysosome damage (Antunes et al., 2001; Hornung et al., 2008; Kirkegaard et al., 2010).

1.9 Disadvantages associated with current measures of lysosome damage

Current methods for analyzing lysosome damage have significant drawbacks. Detection of reduced native cathepsin, either by immunostaining or cell fractionization, is complicated by the fact that cathepsin is quickly degraded in cytosol (Turk and Turk, 2009). Thus, methods which monitor cathepsin release directly may show the amount of protein in the cytosol at the time of fixation or harvest but may not show the total amount of lysosome damage that has occurred. Cells may also express low levels of these enzymes, making their detection difficult.

In these assays which measure release of fluorescent molecules from lysosomes, one cannot determine what percentage of the fluorescence is associated with intact lysosomes versus fluorescence from released molecules. Thus, while lysosome damage can be detected based on an altered pattern of fluorescence, it is difficult to quantify the damage. Low levels of damage may also be difficult to differentiate from background signals. Another drawback to these types of techniques is that fluorescence from out-of-focus, intact lysosomes can appear as diffuse staining and be mistaken for lysosome damage. This problem is diminished but not eliminated by using confocal microscopy.

Measuring the loss of lysosomotropic dyes can also be problematic. Loading efficiency of cells with these dyes depends on pH and lysosome size. Normalizing experimental fluorescence to the fluorescence from the same cell before treatment is not always possible. Loss of a pH gradient across the lysosome membrane is sufficient to deplete lysosomotropic dyes from lysosomes, but that does not necessarily indicate

damage or release of other lysosomal contents. Like the previous methods, this method is also insensitive to small releases of lysosomal contents, as small losses in fluorescence could indicate damage, a minor change in pH or even a decreased lysosome size. Acridine orange can detect minor damage; and although an increase of released green fluorescence does indicate damage, this too is difficult to quantitate as a fraction of lysosomes damaged or percentage of lysosomal contents released. As a weakly basic dye, acridine orange becomes deprotonated in the neutral cytosol, which should decrease its retention in cells. Also, the fluorescence of acridine orange is non-linear due to the spectral emission shift. Thus even though detection of released acridine orange in the cytosol is an improvement over lysotracker dyes, quantitation of lysosomal release remains difficult to measure. While present methods of measuring lysosome damage are an improvement over those that preceded them, there remains a need for a quantitative and sensitive method for measuring lysosome damage. The development of such a method is a significant portion of the work described in this thesis.

1.10 Organization of the thesis

This thesis begins with the development of a novel method for measuring lysosome damage in macrophages (Chapter 2). Release of fluorescein-dextran from macrophage lysosomes was measured by pH-dependent, ratiometric microscopic imaging. This novel method demonstrated that different types of phagocytosed particles induce different levels of lysosome damage and that damage correlates with inflammasome assembly. Chapter 2 also presents our discovery that stimulation of macrophages with lipopolysaccharide reduces subsequent lysosome damage. In chapter 3, this observation is extended to several other macrophage activators. In a *Listeria*

monocytogenes infection model, activated macrophages were protected from endosomal escape and lysosome damage. These data imply that induced lysosome renitence (resistance to damage or force) is a novel activity of activated macrophages which opposes infection by cytosolic pathogens. Studies described in chapter 4 examine potential mechanisms of lysosomal renitence. Evidence is presented consistent with lysosomal calcium and autophagy playing a role in lysosome renitence, possibly through a lysosomal repair mechanism. In chapter 5, the implications of this work are discussed; including the relative merits of this novel lysosome damage assay, the potential mechanisms of lysosomal damage induction and repair, and finally the types of potential therapeutics suggested by the data in this thesis.

Figure 1.1

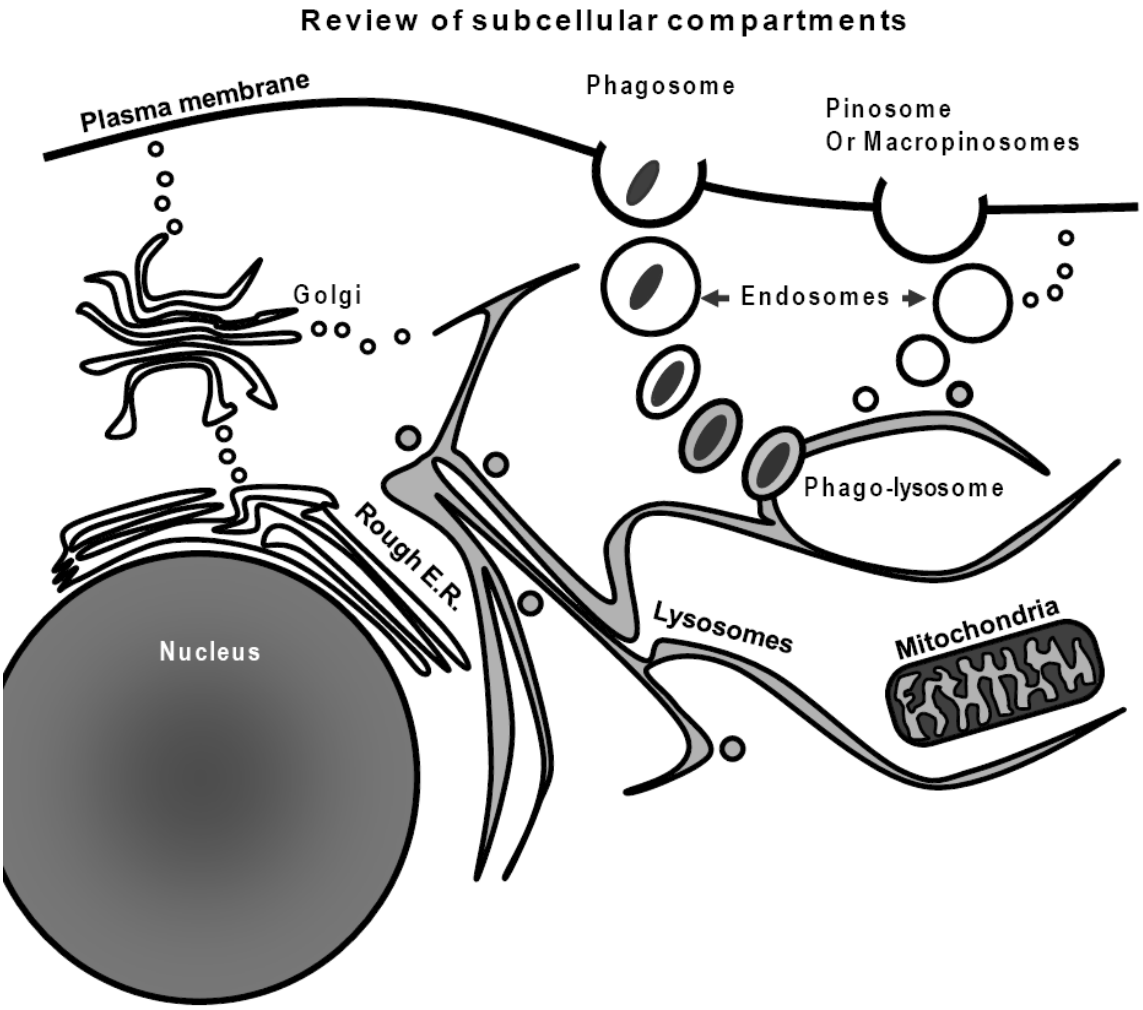

Figure 1.1 Review cartoon depicting structure of subcellular organelles. Eukaryotic cells sub-divide their internal space into functionally distinct compartments termed organelles. Each organelle is bound by lipid-bilayer membranes which prevent passive diffusion of macromolecules between the cytosol and organelles. This organization protects cellular components from potentially destructive enzymes, such as those in lysosomes.

Chapter 2
Caspase-1 activation and IL-1β release correlate with the degree of lysosome damage as illustrated by novel imaging method to quantify phagolysosome damage.

2.1 Abstract

In addition to the lysosome's important roles in digestion, antigen processing and microbial destruction, lysosome damage in macrophages can trigger cell death and release of the inflammatory cytokine IL-1β. To examine the relationship between endocytosis, lysosome damage and subsequent events such as caspase-1 activation and IL-1β secretion, we developed a method for measuring lysosome disruption inside individual living cells which quantifies release of fluorescein dextran from lysosomes. Unperturbed, cultured, murine bone marrow-derived macrophages exhibited low levels of lysosome damage, which were not increased by stimulation of macropinocytosis. Lysosome damage following phagocytosis differed with different types of ingested particles, with negligible damage after ingestion of sheep red blood cell ghosts, intermediate damage by polystyrene beads, and high levels of damage by ground silica. Pretreatment with LPS decreased the amount of lysosome damage following phagocytosis of polystyrene beads, silica microspheres or ground silica. Activation of caspase-1 and subsequent release of IL-1β was proportional to lysosome damage following phagocytosis. The low level of damage following polystyrene bead phagocytosis was insufficient to activate caspase-1 in LPS-activated macrophages. These

studies indicate that lysosome damage following phagocytosis is dependent on particle composition and dose and that caspase-1 activation and IL-1β secretion correlate with the extent of lysosome damage.

2.2 Introduction

Lysosomes are membrane-bounded, hydrolase-rich organelles capable of degrading a variety of macromolecules (Kinchen and Ravichandran, 2008; Scott et al., 2003) and microbial molecules acquired by fusion with phagosomes, endosomes or autophagosomes (Kinchen and Ravichandran, 2008; Scott et al., 2003). In macrophages, most phagocytosed microbes are trafficked into lysosomes, killed, and degraded. The luminal space of lysosomes is maintained at pH 4-5 (Christensen et al., 2002), considerably more acidic than the pH neutral cytoplasm that surrounds them. Antigens from exogenous sources are degraded and loaded onto MHC class II molecules in late endosomes and lysosomes (Burgdorf and Kurts, 2008). Thus, lysosomes function as the end point for the endocytic pathway and the major cellular recycling compartment for internalized macromolecules.

Some pathogenic microorganisms evade trafficking into lysosomes through various mechanisms (Ray et al., 2009), including escape from the endocytic pathway into the host cell cytoplasm. These can be detected by cytosolic recognition systems, such as the NOD-like receptor (NLR) family. Upon recognition of microbial molecules, NLR proteins self-associate into oligomeric structures which can further multimerize with adaptor proteins. These inflammasomes (Martinon et al., 2002) activate inflammatory caspases, mainly caspase-1, which catalyze the proteolytic activation of pro-interleukin (IL)-1β and pro-IL-18 (Martinon et al., 2009). Although the mechanism of IL-1β

secretion is incompletely understood (Eder, 2009), IL-1β maturation is critical for proper cytokine function (Dinarello, 2009; Thornberry et al., 1992).

Inflammasomes containing NLRP3, also known as NALP-3, can be activated by conditions which damage cells, so called "danger signals". Three naturally occurring danger signals monosodium-urate crystals (Martinon et al., 2006), extracellular ATP (Mariathasan et al., 2006; Perregaux and Gabel, 1994) and plasma membrane perforation (Mariathasan et al., 2006; Perregaux and Gabel, 1994) activate the NLRP3 inflammasome. This pathway is also induced following phagocytosis of certain particulates: asbestos (Dostert et al., 2008), β-amyloids (Halle et al., 2008), silica (Cassel et al., 2008; Dostert et al., 2008; Hornung et al., 2008) and alum (Eisenbarth et al., 2008; Hornung et al., 2008). The NLRP3 inflammasome activity is also triggered by dilution of intracellular potassium which is a consequence of damage to plasma membranes (Petrilli et al., 2007).

Phagolysosome disruption was shown to be important for caspase-1 activation following phagocytosis of silica, alum (Hornung et al., 2008) and β-amyloid (Halle et al., 2008). Hornung et al (Hornung et al., 2008) showed that silica-induced inflammasome activation required phagocytosis. Fluorescent molecules pre-loaded into lysosomes were released into the cytosol following exposure to silica crystals. An inhibitor of the lysosomal protease cathepsin B significantly reduced the amount of IL-1β secretion following silica exposure, suggesting that cathepsin B released from lysosomes into cytoplasm is important for inflammasome activation. However, the role of cathepsin B is still unclear, as two groups have reported no difference in NLRP3 inflammasome activation following lysosome disruption in mouse cells lacking the cathepsin B gene

(Dostert et al., 2009; Newman et al., 2009). The lysotropic drug Leu-Leu-OMe (LLME) also strongly activated the NLRP3 inflammasome, demonstrating that lysosome damage in the absence of particle phagocytosis can also trigger inflammasome assembly.

Although these studies showed that lysosome damage after phagocytosis of silica or alum can trigger inflammasome assembly, it remains to be determined if these particles are distinct in their ability to damage lysosomes. Quantifying the extent and frequency of lysosome damage following phagocytosis would allow lysosome damage levels induced by silica to be placed into the context of phagosome maturation in general. Once the extent and frequency of lysosome damage following silica exposure is quantified, a correlation between that and downstream inflammasome signals can be explored. Moreover, inflammasome activation and activity typically follows priming of the cell with lipopolysaccharide (LPS) or other TLR agonists. The effects of such priming on damage responses have not been examined.

Lysosome damage could release exogenous molecules into the macrophage cytosol which could lead to the cross-presentation of exogenous antigens on the MHC class I antigen presentation system. Macropinocytosis (Norbury et al., 1995; Rock et al., 1992) as well as phagocytosis of certain particles (Harding and Song, 1994; Kovacsovics-Bankowski et al., 1993; Oh et al., 1997; Reis e Sousa and Germain, 1995) increase this cross-presentation and thus we hypothesize that macropinocytosis and phagocytosis may involve some degree of lysosome damage.

Here we introduce a method for analyzing lysosome integrity and demonstrate that only particles which damage lysosomes activate inflammasomes. Using a novel fluoresence microscopic technique to quantify lysosome damage in live cells, we

determined that silica particles induced more lysosome damage than did other particles. Not all kinds of phagolysosome became permeable, as macrophages fed sheep red blood cell ghosts or polystyrene (PS) beads induced less lysosome damage than did silica. Pre-treatment of macrophages with LPS reduced the lysosome damage following phagocytosis of PS beads, silica microspheres (SMS) and ground silica. Caspase-1 activation and IL-1β release correlated with the extent of phagolysosome damage. This therefore indicates LPS pretreatment, which is a prerequisite for inflammasome activation, also lessons the damage caused by particles inside phagolysosomes.

2.3 Materials and Methods

2.3.1 Materials

Fluorescein dextran average molecular weight 3000 dalton (Fdx), Texas-red dextran average molecular weight 10,000 dalton, phosphate-buffered saline (PBS), Dulbecco's modified essential medium (DMEM) low glucose, RPMI 1640, fetal bovine serum (FBS), and sheep red blood cells were purchased from Invitrogen (Carlsbad, California). Purified rabbit IgG was purchased from Sigma Scientific (St. Louis, Missouri). Lipopolysaccharide was LPS #225 Salmonella Typhurium, purchased from List Biological Laboratories, Inc. (Campbell, California). Caspase-1 FLICA reagent was purchased from Immunochemistry Technologies LLC (Bloomington, Minnesota). IL-1β ELISA was purchased from BD biosciences (BD OptEIA, San Jose, California). 3 μm diameter polystyrene beads were purchased from Polysciences, Inc. (Warrington, Pennsylvania). Uncoated 3 μm silica oxide microspheres were purchased from Microspheres-Nanospheres (Cold Spring, NY). Recombinant murine macrophage/monocyte-colony-stimulating factor (M-CSF) was purchased from R&D

Systems (Minneapolis, Minnesota). 35 mm dishes with 14 mm diameter cover glass were purchased from MatTek Corporation (Ashland, Massachusetts). Fisherbrand select #1.5 cover glass was purchased from Fisher Scientific (Hampton New Hampshire). Silica crystals (MIN-U-SIL-15) were a generous gift of US Silica (Berkeley Springs, West Virginia).

2.3.2 Bone marrow differentiation of macrophages

C57BL/6J mice were purchased from Jackson Laboratories (Bar Harbor, Maine; stock number 000664). Macrophages were cultured as in (Swanson, 1989). Briefly, marrow was obtained from mouse femurs. Macrophages were then differentiated in DMEM with 20% FBS and 30% L-cell-conditioned medium. Bone marrow cultures were differentiated for one week with additions of fresh differentiation medium at days 3 and 6.

2.3.3 Loading of lysosomes with Fluorescein-dextran

Labeling lysosomes by endocytosis of Fdx has been described previously (Christensen et al., 2002; Shaughnessy et al., 2006). Macrophages were resuspended from dishes after incubation in cold PBS for 10 min. Cells were then counted, diluted in RPMI with 10% FBS, added to coverslips or Mat-tek dishes, and allowed to attach to the glass surface for at least 4 hours. Plating medium was replaced with RPMI with 10% FBS containing Fdx at 150 μg/mL, and cultures were incubated overnight. Dishes or coverslips were then rinsed extensively with Ringer's buffer (RB; 155 mM NaCl, 5 mM KCl, 2 mM $CaCl_2$, 1 mM $MgCl_2$, 2 mM NaH_2PO_4, 10 mM Hepes and 10 mM glucose, pH 7.2) at 37 C. The Fdx was chased into the lysosomes for at least 4 hours using fresh RMPI with 10% FBS without Fdx.

2.3.4 Opsonization of particles

Sheep red blood cell (sRBC) ghosts were prepared as described previously (Oh et al., 1997). Briefly, sRBC were osmotically lysed in water and the released contents rinsed away by centrifugation and resuspension. Texas-red dextran was then mixed with sRBC membranes, which were then re-sealed in osmotically balanced PBS. These sRBC ghosts were then opsonized using anti-sRBC antibody, rinsed, and counted using a hemocytometer on a fluorescence microscope. Polystyrene beads were opsonized by absorption with rabbit IgG for 30 minutes at 37 C, followed by rinsing in PBS.

Silica microspheres (SMS) were acid-washed overnight in 1 M HCl then rinsed three times in PBS. SMS were then coated with 0.1 mg/mL Poly-L-Lysine (PLL) in PBS for 30 minutes followed by another round of three PBS washes. PLL-coated SMS were then coated in 5 mg/mL BSA for an hour and then rinsed three times in PBS. SMS were then opsonized with anti-BSA IgG for an hour then rinsed in PBS. Samples were reserved following each step for experimentation.

2.3.5 Microscopes and imaging

Ratiometric imaging was performed on two different instruments. The first was an Olympus IX70 (Olympus; Center Valley PA) inverted epi-fluorescence microscope using a 100X oil UPlan Fl objective (NA=1.30). Fluorescence images were acquired using an X-Cite 120 metal halide light source (EXFO; Mississauga, ON, Canada) and a CoolSNAP HQ2 monochrome camera (cooled CCD, 1392x1040, 14 bit). The second instrument was an inverted Nikon TE300 microscope equipped for multicolor fluorescence imaging using a mercury arc lamp. Cells were examined using a 60x, numerical aperture 1.4 plan-apochromat objective and images were recorded using a

cooled digital charge-coupled device camera (Quantix; photometrics). Both microscopes used temperature-controlled stages for live cell imaging and were equipped with CFP/YFP/DsRed dichroic mirrors (Chroma Techonology Corp cat # 86006), with filter wheels and shutters controlled by lambda 10-2 filter wheel controllers (Sutter Instruments).

Images were acquired and analyzed using Metamorph software (Molecular Devices, Downingtown, PA), following a one-hour incubation with phagocytic targets. Cells were rinsed and mounted onto the microscope stage in warm RB. For each field of cells, three images were collected; using a 436/10 nm excitation, a 492/18 nm excitation, and a phase-contrast image. A 535/30 nm emission filter was used for both fluorescence images. An additional image using red excitation and emission filters was acquired for cells fed sRBC ghosts containing Texas-red dextran.

2.3.6 Image analysis

Epi-fluorescence images contain contaminating signals from both camera background noise and uneven illumination. The level of background signal was determined by capturing images without a coverslip mounted on the stage. These values were subtracted from all experimental and calibration images. Illumination correction was performed by collecting images of fluorescein-containing solution sandwiched between two coverslips in order to generate an even layer of fluorophore (Hoppe et al., 2002). Experimental and calibration images were normalized for illumination levels. Incubation of coverglasses or Mat-tek dishes in Fdx medium, even when followed by rinsing, created residual background fluorescence. This background was subtracted from

all experimental images using regions selected from non-cellular portions of the experimental and calibration images (Hoppe et al., 2002; Shaughnessy et al., 2006).

The pH of intracellular compartments was determined as described previously (Christensen et al., 2002; Shaughnessy et al., 2006). The microscope was calibrated by imaging intracellular organelles held at a series of fixed pHs. Macrophages were loaded with Fdx by endocytosis and the pH of intracellular compartments was clamped using calibration buffer (10 μM nigericin, 10 μM valinomycin, 130 mM KCl, 1 mM $MgCl_2$, 15 mM Hepes, 15 mM MES) at pH 7.5. Several sets of epi-fluorescence images using both the 435 nm and 492 nm excitation filter settings were acquired, the calibration buffer was exchanged for buffer at another pH and another set of images were acquired from other cells. This process was repeated using buffers at pH 9.0, 7.5, 7.0, 6.5, 6.0, 5.5, 5.0, 4.5, and 4.0. Subsequent image processing determined the average ratio of the 492 nm image divided by the 435 nm image for each pH. The data were fit to a four parameter sigmoid model and this model was used to convert every Fdx-labeled pixel in the 492 nm/435 nm ratio images into values representing pH (Fig. 2.1C).

In processed images of unperturbed macrophages, most pixels indicated pH less than 5.5. This was determined empirically by examination of many Fdx-loaded but otherwise unperturbed cells on many different days and was true for both microscopes. Thus, cellular areas in pH maps with a pH below 5.5 were considered to represent intact lysosomes, while areas with a pH above 5.5 indicated Fdx in pH neutral cytosol.

Using cellular pH maps and image processing software, masks were created which contained only pixels indicating a pH above 5.5. These masks were applied to the otherwise unmasked 435 nm excitation images. As the fluorescence of fluorescein

excited at 435 nm is relatively insensitive to pH, pixel fluorescence values in 435 nm excitation images were considered to be proportional to the amount of Fdx in each pixel. Thus the total cellular fluorescence in the 435nm excitation image was proportional to the total Fdx in the cell and the total cellular fluorescence in the masked 435nm excitation image approximated the total amount of Fdx released from the lysosomes. The values of total Fdx content and total Fdx released were recorded for each cell and the ratio of Fdx released was divided by total Fdx to obtain the fraction of Fdx released. Since the fluorescence images are only masked based on pH and never masked based on fluorescence intensity, this technique does not rely on any subjective masking to define the presence or absence of lysosome damage.

It should be noted that in figures 2.1, 2.2 and 2.3 the brightness of the 492 nm ex. and 435 nm ex. grayscale image samples are identically scaled to illustrate the differences in intensity ratios. In cells with low levels of lysosome damage the 435 nm ex. and the 492 nm ex. image were similarly bright, however in cases of very high levels of lysosome damage the 492 nm ex image was much brighter than the 435 nm ex image; thus, identical brightness scaling can result in 435 nm ex. images which appear dim in cases of high lysosome damage.

2.3.7 Caspase-1 activation levels

Levels of active caspase-1 in live cells were determined using the caspase-1 FLICA probe, which irreversibly labels the active site of cleaved (activated) caspase-1 with fluorophore. Macrophages were stimulated overnight in 100 ng/mL LPS. Cells were fed particles in fresh medium and incubated for 1 hour. Particle medium was then replaced with the diluted FLICA reagent as per the manufacturer's recommendations and

incubated for 1 hour. Propidium iodide was added to the staining solution for the last 10 minutes of the incubation. Cells were then rinsed to remove the unbound dye and imaged using the 492/18 nm excitation, 535/30 nm emission filters for the active caspase-1 signal and 580/20 nm excitation, 630/60 nm emission filters for propidium iodide staining. Images were corrected for background and illumination, as described above. Regions of interest were then drawn around each cell and the total 492/18 nm excitation 535/30 nm emission fluorescence was calculated as the total active caspase-1 signal. The propidium iodide staining and nuclear phase-contrast status were also noted for each cell.

2.3.8 Statistical tests

Lysosome damage levels were compared between groups using Student's T-test, with p-values calculated in Microsoft excel. Error bars displayed in the figures were all standard error of the mean (SEM).

2.4 Results and Discussion

2.4.1 Release of fluorescein dextran from lysosomes into cytoplasm

To measure lysosome damage, lysosomes were first labeled by endocytosis of fluorescein dextran (Fdx). RAW 264.7 (RAW) macrophages were incubated overnight in Fdx-containing medium, then incubated in fresh medium to allow the Fdx to reach the lysosomes by vesicular trafficking. Ratiometric imaging with a calibrated microscope was then used to measure the pH of cytoplasmic and lysosomal Fdx (Fig. 2.1C is a sample calibration curve). Fdx fluorescence (514 nm) was imaged at two different excitation wavelengths. Excitation at 435 nm produced fluorescence that was relatively unaffected by pH, which was used to approximate the amount of Fdx in a pixel, whereas excitation at 492 nm produced a pH-dependent fluorescence. Release of Fdx from

lysosomes into cytosol was detected by both the physical redistribution of the dye in the images and by the increase in Fdx signal at 492 nm excitation. pH maps of cells provided a clear distinction between Fdx trapped in acidic, undamaged lysosomes and Fdx which had been released into the pH-neutral cytosol. Fdx in unperturbed macrophages was contained in acidic lysosomes (Fig. 2.1A). In similarly loaded macrophages exposed to the lysotropic drug Leu-Leu-OMe (LLME), Fdx was released into the cytosol (Fig. 2.1B & D). LLME disrupted all of the lysosomes in RAW macrophages, as the pH map of these cells appeared uniform and neutral (Fig. 2.1B & D). To quantify lower levels of Fdx release from lysosomes, image analysis algorithms were developed to measure the percentage of total cellular Fdx in the cytoplasm (Fig. 2.1D).

2.4.2 Undisturbed murine BMM show little lysosome damage

Murine bone marrow-derived macrophages (BMM) contained spherical and elongated tubular lysosomes. The areas of highest lysosome density were near the nuclei, with tubular structures extending into the periphery (Fig. 2.1Ei), consistent with previous observations (Knapp and Swanson, 1990). Lysosomal pH was 4.0 to 5.0, as reported previously (Christensen et al., 2002; Tsang et al., 2000). Unperturbed macrophages showed little evidence of lysosome damage (Figs. 2.1Ei and F). Most pixels in the pH maps of intact cells represented acidic environments. A few cells displayed higher levels of lysosome damage (Figs. 2.1E ii & iii).

Rare cells exhibited low levels of lysosome damage in otherwise unperturbed cells. While many of the pH neutral pixels were dim, their intensity in the 435 nm images was several times greater than the noise level. Nuclear regions were the best cellular locations to detect low levels of released Fdx, as those regions contained no

fluorescence from lysosomes. The low levels of Fdx in the cytosol of these cells produced undetectable signals in the periphery.

2.4.3 Increasing the rate of macropinocytosis does not increase lysosome damage

The low level of damage in unperturbed macrophages suggested that some basic cellular process can damage lysosomes. Macropinocytosis is the process by which macrophages and other cells take up extracellular solute into large endocytic vacuoles. Solutes taken into macropinosomes traffic through the endocytic pathway, eventually entering lysosomes (Tsang et al., 2000). M-CSF increases the rate of macropinocytosis in macrophages (Racoosin and Swanson, 1989). Induction of macropinocytois in macrophages increases cross-presentation of soluble exogenous antigens on MHC class I molecules (Norbury et al., 1995; Rock et al., 1992).

To measure effects of macropinocytosis on lysosome damage, macrophage lysosomes were loaded with Fdx in cells deprived of M-CSF, chased in Fdx-free medium and incubated 1 hour in medium containing M-CSF or control medium before imaging. Cells incubated in M-CSF displayed prominent macropinosomes (Fig. 2.1G phase-contrast). Lysosome damage in cells exposed to M-CSF was no greater than in control cells (Fig. 2.1H). These data suggest that macropinocytosis-mediated increases in soluble antigen cross-presentation in macrophages (Norbury et al., 1995) are not due to increased lysosome damage following macropinocytosis.

2.4.4 Lysosome damage following phagocytosis

To examine whether lysosome damage is a general outcome of phagocytosis, macrophages with Fdx-labeled lysosomes were fed Texas-red-dextran-labeled sheep red blood cell (sRBC) ghosts. Fluorescent sRBC ghosts were imaged an hour after

phagocytosis and levels of Fdx release from lysosomes were quantified (Fig. 2.2). Phagocytosis of sRBC ghosts induced a redistribution of macrophage lysosomes to phagosomes (Fig. 2.2B), consistent with previous observations (Knapp and Swanson, 1990). In cells containing several sRBC ghosts, nearly all of the phagolysosomes coalesced into large round structures containing the sRBC ghosts and most of the cellular Fdx. Despite this dramatic redistribution, no additional lysosome damage followed phagocytosis of sRBC ghosts (Fig. 2.2E).

The Fdx-release assay was used to measure phagolysosome damage by various particles. Macrophages fed ground silica showed extensive phagolysosome damage (Fig. 2.2D). In some ground silica-containing cells, lysosome damage was evident without the aid of the pH map, while in other cells no damage was detected. Most silica-fed macrophages showed intermediate levels of lysosome damage, with Fdx in both cytosol and intact lysosomes.

The highly variable lysosome damage in cells containing ground silica contrasts with Leu-Leu-OME-treated cells, which exhibited complete lysosome release in all cells. The lack of uniformity in cells fed silica could be due to some non-uniform aspect of these particles, such that only some of them were disruptive. Perhaps not all particles possess sharp edges that cause damage. Alternatively, resistance to lysosome perforation may be regulated and the non-uniformity in lysosome release could be the result of subtly different gene expression patterns in different cells of the examined populations.

Fdx-loaded macrophages were also fed 3 μm PS beads, which are widely used as inert phagocytic targets. PS beads were shown earlier to facilitate the delivery of exogenous antigens into the MHC class I antigen processing and presentation pathways

(Oh et al., 1997), suggesting that they induce damage at some stage of their endocytic trafficking. Other types of microspheres have also been shown to facilitate exogenous antigen presentation on MHC class I molecules (Harding and Song, 1994; Kovacsovics-Bankowski et al., 1993; Reis e Sousa and Germain, 1995). The amount of Fdx released into the cytosol of PS bead-containing macrophages was significantly greater than in unfed cells or cells fed sRBC ghosts, but less than that released in cells fed ground silica (Figs. 2.2E & F). Thus, phagocytosis of particles yields a range of lysosome damage dependent on dosage and the type of particle phagocytosed.

The heterogeneity among cells showing lysosome damage may have implications for cross-presentation of exogenous antigens on MHC class I molecules. The sub-population of cells showing lysosome release in unperturbed cultures could represent those which have released exogenous antigens into the cytosol, which would then be accessible to the MHC class I antigen presentation pathway. This could underlie the low but detectable level of cross presentation of soluble antigens observed in macrophages (Kovacsovics-Bankowski et al., 1993; Norbury et al., 1995; Reis e Sousa and Germain, 1995; Rock et al., 1993). While macropinocytosis did not increase lysosome damage in macrophages, increased uptake of soluble antigen into cells could nonetheless mediate increased cross-presentation of soluble antigens in the small fraction of cells that undergo lysosome damage. PS beads fed to unactivated macrophages induced low but detectable levels of damage, which may explain the reported cross-presentation of antigens loaded onto PS beads (Oh et al., 1997). The release of lysosomal contents after PS bead phagocytosis supports a direct mechanical route for antigen delivery into cytosol for MHC class I antigen presentation.

2.4.5 LPS reduces the phagolysosome damage

Recent studies have shown that lysosome damage can induce maturation and secretion of the pro-inflammatory cytokine IL-1β (Halle et al., 2008; Hornung et al., 2008). IL-1β secretion from murine macrophages requires pre-stimulation with a Toll-like receptor ligand such as LPS. LPS pre-stimulation is required for transcription and translation of pro-IL-1β (Mariathasan et al., 2006) and NLRP3 (Sutterwala et al., 2006) as well as many other changes in gene expression.

To investigate whether these physiologic changes modulate lysosome damage, the damage induced by various particles was compared in LPS-activated and untreated control macrophages. Macrophage lysosomes were loaded with Fdx in medium with or without LPS, and the cells were fed particulate targets. LPS treatment did not alter lysosomal pH. Fdx release after phagocytosis of ground silica was less in LPS-stimulated macrophages than in unstimulated macrophages (Fig. 2.3A). LPS treatment also decreased lysosome damage following phagocytosis of PS beads to levels which were significantly lower than in untreated cells fed similar doses of beads (Fig. 2.3B, 1.5 PS beads/cell). This relationship was also evident in macrophages fed higher doses of PS beads (Fig. 2.3B, 18.3 PS beads/cell). These data indicate that lysosome damage may be modulated by the activation state of the macrophages.

To confirm that LPS pre-stimulation reduces lysosome damage, silica microspheres (SMS) were employed. SMS are uniform 3 μm spheres which are chemically similar to the ground silica. This uniformity of size and shape allowed for particle dose to be determined independently for each cell. Acid-washed SMS were coated with various materials then fed to Fdx-loaded macrophages which had or had not

been pre-stimulated with LPS. The number of SMS internalized by each cell was counted and populations of cells which had phagocytosed the same dose of particles were compared. Macrophages fed acid-washed SMS showed moderate levels of lysosome damage (Fig. 2.3C). Phagocytosis of poly-L-lysine-coated SMS induced high levels of lysosome damage, while SMS coated with BSA or BSA and anti-BSA IgG induced lower levels of lysosome damage (Fig. 2.3C). Lysosome damage was dose-dependent. LPS pre-stimulation reduced lysosome damage for all SMS coatings and all dose levels (Fig. 2.3C). These data confirmed that LPS-prestimulation reduces lysosome damage following particle phagocytosis. Experiments with SMS suggested that particle surface chemistry may play an important role in inducing lysosome damage, as the SMS with different surface treatments damaged lysosomes to different extents. Coating of SMS did not change the particles apparent size or appearance by phase contrast microscopy. The effects of particle size on phagolysosome damage remain unknown. Thus lysosome damage was not intrinsic to phagocytosis but rather was due to surface features of the ingested particles.

2.4.6 Lysosome damage correlates with caspase-1 activation.

To determine if inflammasome activation was proportional to lysosome damage, caspase-1 activation was measured in macrophages fed various particles. Cells were stained with the fluorescent caspase-1 reporter FLICA, which labels the active site of cleaved caspase-1 in live cells (Fig. 2.4A). The percent of cells positive for caspase-1 activation increased with increasing doses of silica (Fig. 2.4B & Table). Most caspase-1-positive cells were also positive for propidium iodide (90-96%; Table, Fig. 2.4A), indicating plasma membrane permeabilization. This FLICA-positive, propidium iodide-

positive population also exhibited phase-dark nuclear morphologies indicative of cell death (Fig. 2.4A & Table). Caspase-1 activation was LPS dependent, as even high doses of silica failed to induce FLICA staining in unstimulated cells (Fig. 2.4B bottom panel). The percent of cells positive for lysosome damage also increased with increasing doses of silica (Fig. 2.4C). While LPS stimulation reduced subsequent lysosome damage, some level of damage was still evident in cells fed highly damaging particles (Fig. 2.3). This effect is also evident in Figure 2.4C which compares cells fed 170 μg/mL ground silica with or without LPS stimulation (Fig. 2.4C middle and bottom histograms). The average level of lysosome release observed at 500 μg/mL silica was not greater than that observed at 170 μg/mL. However, macrophages fed the higher doses of silica contained many more cells with phase-dark nuclei than did those fed intermediate doses (Table I) and cells with phase-dark nuclei did not retain sufficient Fdx to allow the lysosome release analysis. Measurements of IL-1β release indicated a correlation between IL-1β secretion and the amount of silica provided to cells (Fig. 2.5A). Overall, lysosome damage, caspase-1 activation and IL-1β secretion all showed large increases between 57 and 170 μg/mL silica and leveled off between 170 and 500 μg/mL.

Thus, in activated macrophages, various doses of silica showed corresponding percentages of lysosome damage, caspase-1 activation and secretion of IL-1β, suggesting a pattern of progression to inflammasome activation following silica phagocytosis. In silica-fed macrophages, inflammasome activation was accompanied by loss of plasma membrane integrity and nuclear condensation. These data suggest a role for cell death in the silica-induced lysosome damage response, possibly through pyroptosis (Ting et al., 2008). LPS pre-stimulation was critical for cell death, as unstimulated cells fed

lysosome-damaging doses of silica failed to activate caspase-1 or to lose plasma membrane integrity. The staining protocols precluded measurement of the relative timing of caspase-1 activation, membrane permeabilization and nuclear condensation.

2.4.7 The lysosome damage induced by polystyrene beads did not induce IL-1β release

The lack of lysosome damage in LPS-stimulated cells fed PS beads suggested that caspase-1 activation and IL-1β secretion in such cells should also be low. Macrophages fed PS beads or sRBC ghosts showed low levels of caspase-1 activation (Fig. 2.4D). In contrast, macrophages fed silica exhibited high levels of caspase-1 activation. These data correlated with the IL-1β secretion data, in that LPS-activated macrophages fed PS beads failed to secrete IL-1β (Figs. 2.5A and B). Thus, IL-1β secretion and caspase-1 activation in LPS-activated macrophages fed PS beads correlated with the low levels of lysosome damage in such cells. Similar relationships were observed in cells fed higher doses of beads: LPS-activated macrophages that ingested an average of 18.3 PS beads per cell displayed very little lysosome damage (Fig. 2.3B) and secreted little IL-1β (Fig. 2.5B). These data indicate that LPS stimulation interferes with or counteracts lysosome damage after phagocytosis of PS beads.

Previous work showed that silica, alum (Hornung et al., 2008), and β-amyloid (Halle et al., 2008) damage lysosomes. In contrast, this study found that macrophages fed sheep red blood cell ghosts showed lysosome release levels no higher than control cells (Fig. 2.2). Cells fed PS beads, another classic phagocytic target, showed low levels of lysosome damage which were higher than control cells or cells fed sRBC ghosts but lower than cells fed silica. Although SMS phagocytosis seemed to damage lysosomes to

a lesser extent than did ground silica, direct comparisons were difficult due to irregularities of the ground silica particle shape and size.

Some bacterial pathogens escape from macrophage vacuoles to propagate in the host cell cytosol. The macrophage IL-1β response to *Listeria monocytogenes* is partially dependent on NLRP3 and bacterial escape (Warren et al., 2008) suggesting that the escape process damages lysosomes. On the other hand, *Francisella tularensis* escapes from vacuoles but does not activate the NLRP3 inflammasome (Fernandes-Alnemri et al.). These data may reflect differences in the vacuolar compartments from which these bacteria escape or the severity of lysosome damage induced during escape.

LPS-stimulated cells fed ground silica, PS beads or SMS showed less lysosome damage than un-stimulated cells (Fig. 2.4), suggesting either that LPS-activated cells are refractory to damage induced by particles or that there exists a mechanism for lysosomal repair which is increased by LPS prestimulation. The LPS-dependent phagolysosome damage resistance activity is limited as particles which cause high amounts of lysosome damage, such as ground silica and poly-L-lysine-coated SMS, still induce significant levels of phagolysosome damage in LPS-stimulated cells. As pre-stimulation with LPS or other TLR ligands is critical for inflammasome activation following lysosome damage, due to the dependence of NLRP3 expression on pre-stimulation (Sutterwala et al., 2006), the dampening effect of LPS on phagolysosome damage seems to counteract inflammasome activation after phagocytosis. Thus LPS stimulation sets the stage for lysosome damage-mediated inflammasome activation but also raises the threshold amount of lysosome damaging chemistry required to damage lysosomes. Thus it may be that activated macrophages are prepared to resist infection or damage but have a fail-safe

system, the inflammasome, in place for cases where the lysosome damaging chemistries are too powerfull to contain. It remains to be seen whether the inflammasome gene expression effects can be separated from the lysosome-stabilizing effects of LPS signaling. While inflammasome induction by LPS requires gene expression, it is unknown whether the phagolysosome-protecting activities also require induced gene expression. Perhaps the inflammasome gene expression signals can be separated from the phagolysosome protective signals. As other solid particles are known to mediate the cross-presentation of antigens (Harding and Song, 1994; Kovacsovics-Bankowski et al., 1993; Reis e Sousa and Germain, 1995), it is possible that these other particles also modulate levels of lysosome damage.

Figure 2.1

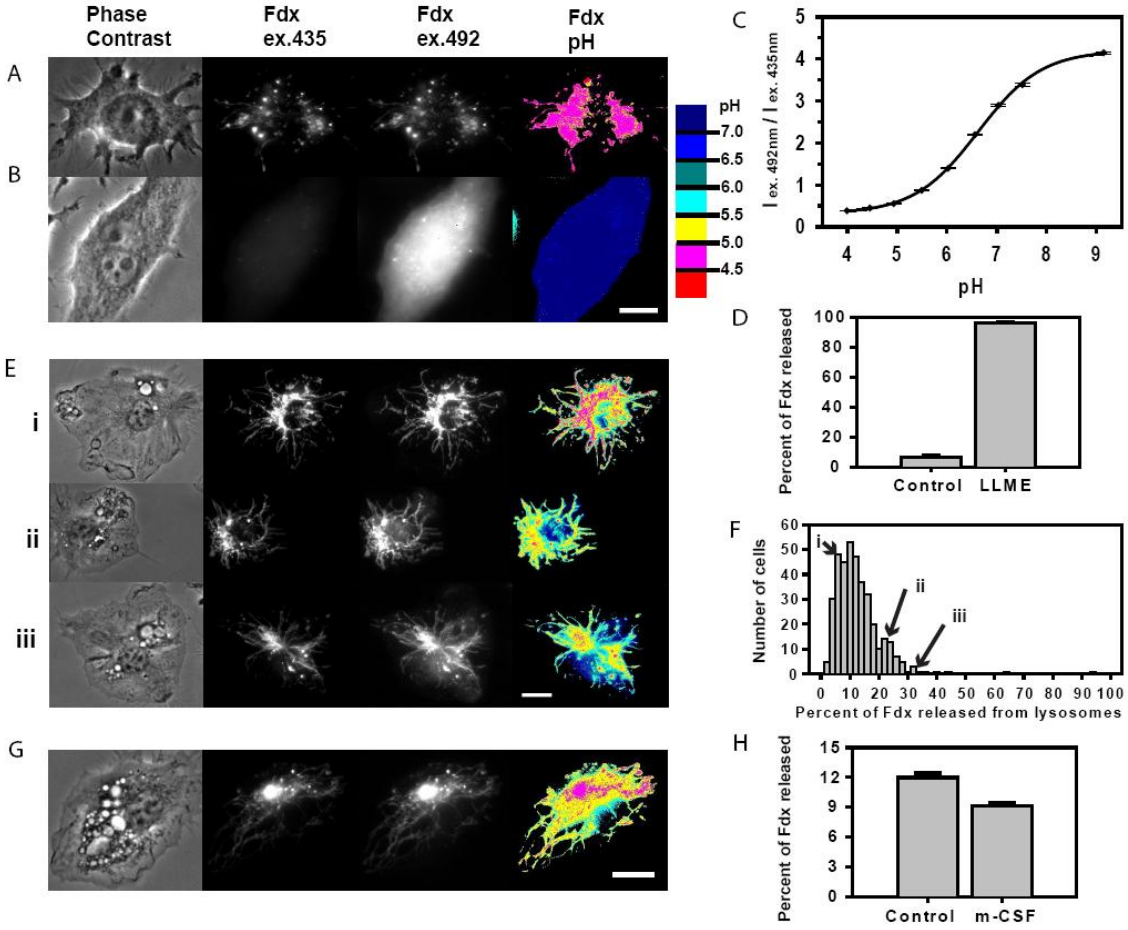

Figure 2.1. Detection of Fdx released from lysosomes. RAW macrophage lysosomes were loaded overnight with Fdx then chased for several hours in fresh medium. Cells were left untreated (A) or incubated with Leu-Leu-OMe for 30 min (B), then epi-fluorescence images were collected. All pH images are color-coded such that warm colors (red, pink, yellow) represent Fdx in acidic compartments and cool colors (cyan, dark cyan, blue and dark blue) represent Fdx in pH neutral compartments. ex. 492 nm / ex. 435 nm ratios were converted to pH using calibration curves generated by measuring ex. 492 nm / ex. 435 ratios at fixed pHs (C). The brightness of the Fdx ex. 435 nm and ex. 492 nm images are identically scaled in all micrograph sets. (D) The percentage of Fdx released from the lysosomes is plotted as mean ± SEM of ≥70 cells ($p<0.0001$). Murine BMM were loaded and imaged as above. (E) Epi-fluorescence images of otherwise unperturbed macrophages were then collected. Images of unperturbed cells depicting very low (i. 7.7%), slight (ii. 22.4%) and moderate (iii. 31.6%) lysosome release. (F) Lysosome release from all the negative control images acquired for Figures 2.1G and 2.2. (G) Typical images of BMM following M-CSF-induced macropinocytosis. Scale bars in A, E and G represent 10 μm. (H) Lysosome release from all the cells in each group were calculated and the averages plotted. Error bars are SEMs. Data are pooled averages of three experiments with n ≥ 200 cells total. $p<0.0001$

Figure 2.2

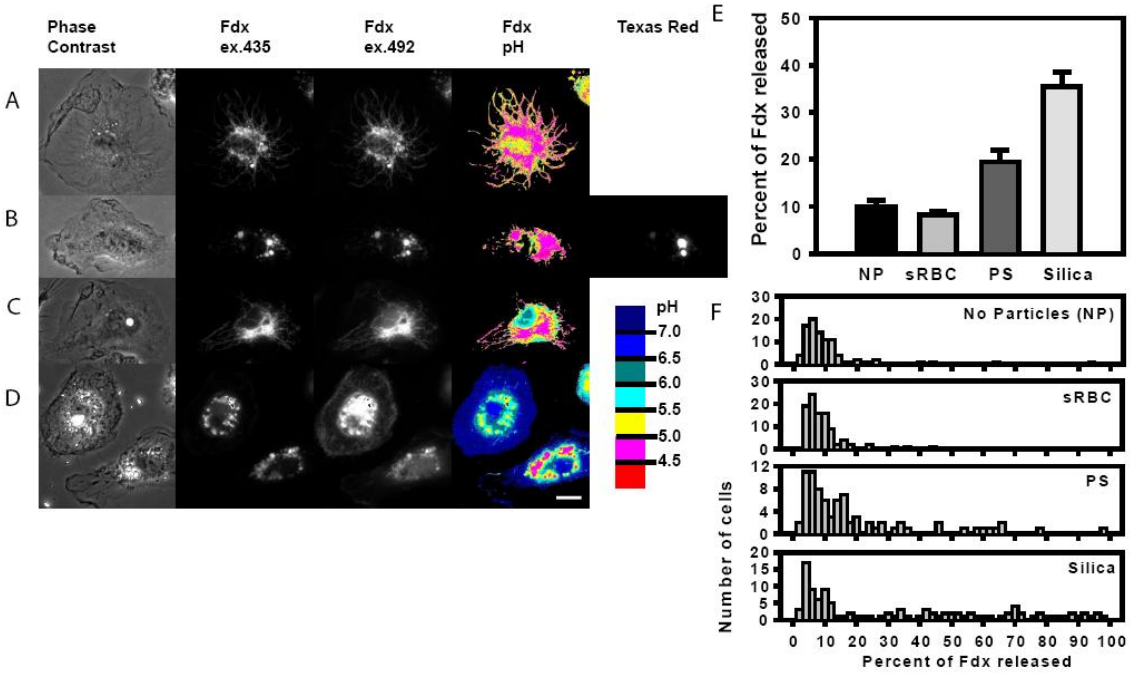

Figure 2.2. Lysosome damage following phagocytosis. Murine BMM lysosomes were labeled with Fdx. Cells were fed (A) no particles, (B) IgG-opsonized sheep red blood cell ghosts (labeled with Texas red dextran; sRBC $3.3x10^6$ sRBC/ mL), (C) PS beads ($2x10^5$ PS beads/mL), or (D) ground silica (170 μg/mL) and imaged one hour later. These particle doses were determined empirically to yield images with 1-5 particles per cell. Texas red images were used to identify cells containing sRBC ghosts. Scale bar represents 10 μm. (E) The average percent of lysosome release was calculated for each condition. Data represents mean ± SEM for three separate experiments with at least 80 cells examined in each condition. All conditions are significantly different ($p<0.0005$) from each other, except for no particle (NP) versus sRBC ghost. (F) The data from (E) replotted as histograms with percent of Fdx released (x-axis) compared to the number of cells containing a given level of Fdx release (Y-axis)

Figure 2.3

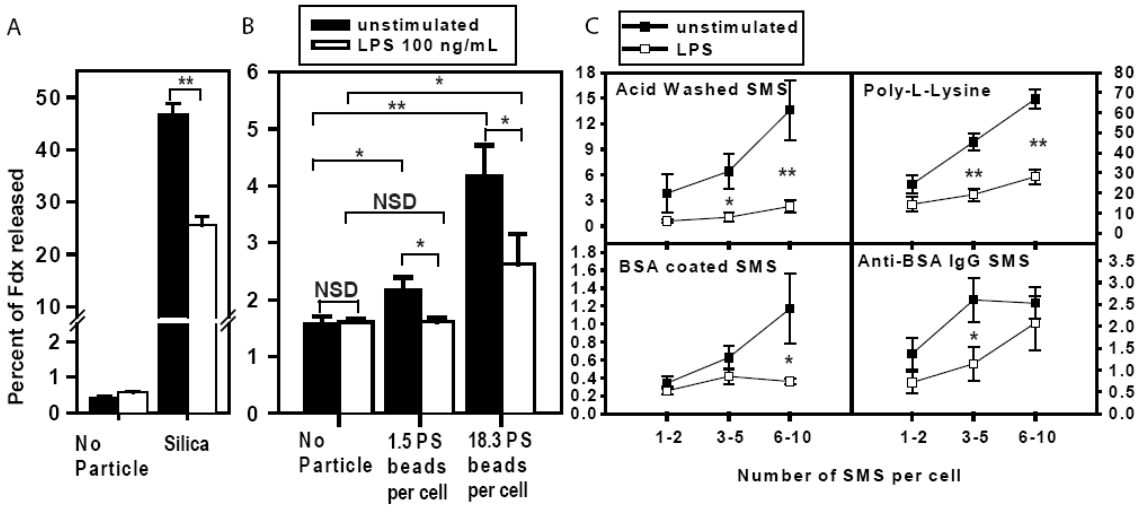

Figure 2.3. LPS treatment decreases lysosome release following phagocytosis. Murine BMM were labeled with Fdx and chased in unlabeled medium with (open bars) or without (closed bars) 100 ng/mL LPS. Cells were fed particles, imaged, and the average percent of lysosome release was calculated for each condition. Y-axis for all graphs plot the average percent of Fdx released. (A) LPS-stimulated or naïve BMM were fed 200 μg/mL ground silica and lysosome damage was measured. (B) The number of PS beads per cell was counted and indicated for each PS bead dose. For (A) and (B), bars are pooled averages from three experiments with at least 170 cells per condition (means±SEM). (C) Cells were fed acid-washed SMS coated with nothing (upper left), poly-l-lysine (upper-right), BSA (lower-left) or BSA and anti-BSA IgG (lower-right). Cells were imaged and the number of phagocytosed SMS was recorded for each cell. Cells were grouped by number of SMS phagocytosed and mean ± SEM was plotted for each group. Statistical comparisons in A and B are as indicated with brackets and in C are between unstimulated and LPS-prestimulated groups within each SMS type and count. p-values: NSD = not significantly different, * = $p<0.05$, ** = $p<0.0001$.

Figure 2.4. Caspase-1 activation correlates with lysosome damage. Murine BMM were treated overnight with or without LPS then fed ground silica at 57, 170 or 500 μg/mL, or were left unfed (no particles). (A and B) Cells were then stained for an additional hour using the caspase-1 FLICA reagent; propidium iodide was added for the last 10 minutes to detect cells with permeabilized plasma membranes. Active caspase-1 (FLICA) and propidium iodide were imaged and quantified. (A) Sample images of LPS pretreated cells fed 170 μg/mL of ground silica. The cell on the right shows high levels of caspase-1 activation detected by FLICA, nuclear PI staining, and a phase-dark nucleus while the cell on the left contains silica but is negative for FLICA, PI and nuclear condensation. Scale bar represents 10 μm. (B) Data is displayed as histograms with integrated FLICA signal for individual cells plotted on the horizontal axis. (C) Murine BMM lysosomes were labeled with Fdx in LPS-containing medium. Macrophages were fed silica as above and imaged one hour later. Data are the pooled results of three independent experiments ($n \geq 400$ total cells per condition). (D) Murine BMM treated with LPS were fed nothing (no particles), PS beads, ground silica, or sRBC ghosts for one hour, then stained for active caspase-1. Histograms show integrated caspase-1 FLICA signal for individual cells plotted on the horizontal axis. Data are pooled results of three independent experiments with at least 400 total cells examined per condition. (E) Data from LPS prestimulated BMM (Fig. 2.3) is replotted as histograms for comparison to (D).

Figure 2.4

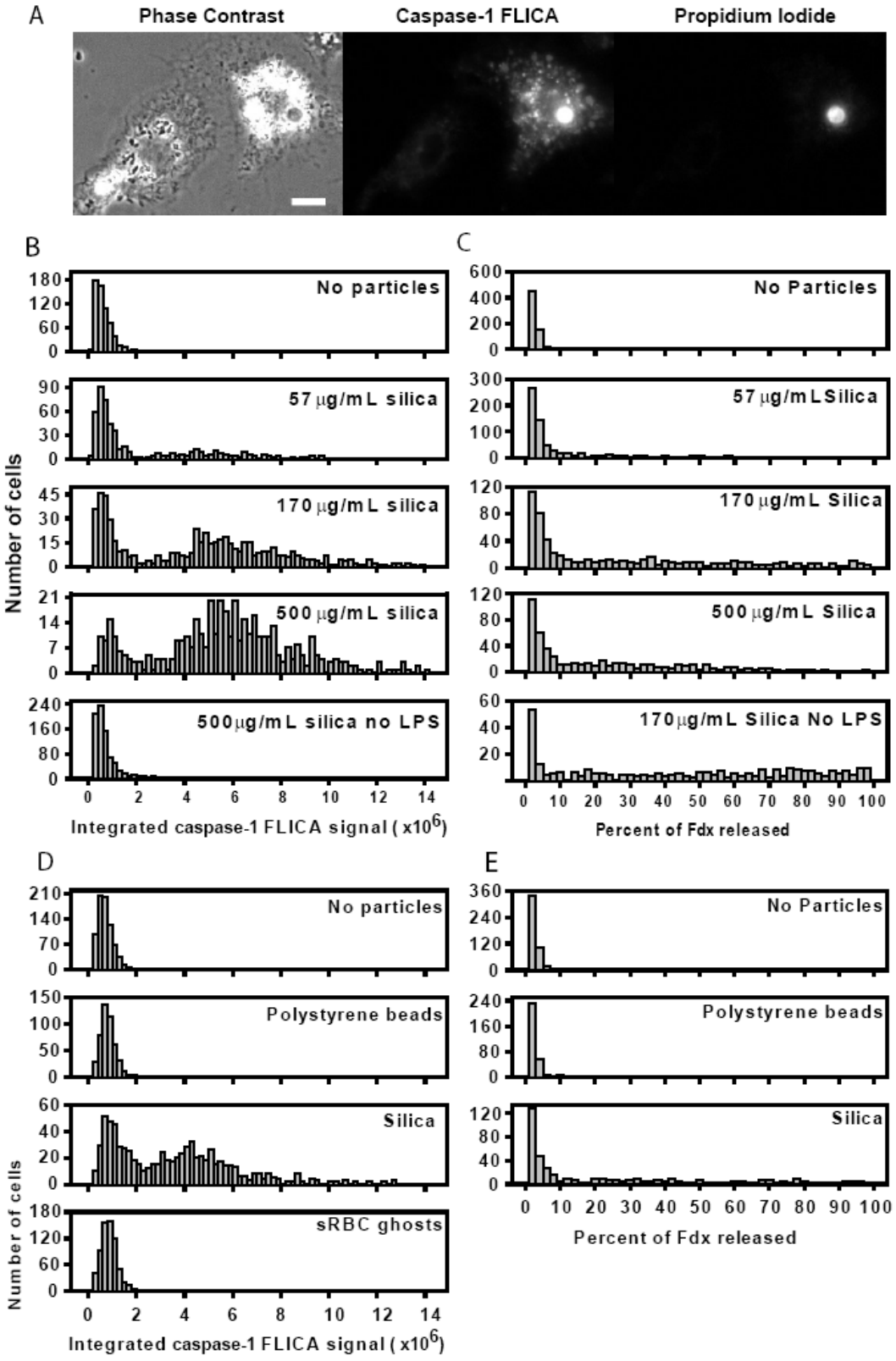
A
Phase Contrast
Caspase-1 FLICA
Propidium Iodide
B
No particles
57 μg/mL silica
170 μg/mL silica
500 μg/mL silica
500μg/mL silica no LPS
Number of cells
Integrated caspase-1 FLICA signal (x10^6)
C
No Particles
57 μg/mL Silica
170 μg/mL Silica
500 μg/mL Silica
170μg/mL Silica No LPS
Percent of Fdx released
D
No particles
Polystyrene beads
Silica
sRBC ghosts
Number of cells
Integrated caspase-1 FLICA signal (x10^6)
E
No Particles
Polystyrene beads
Silica
Percent of Fdx released

Figure 2.5

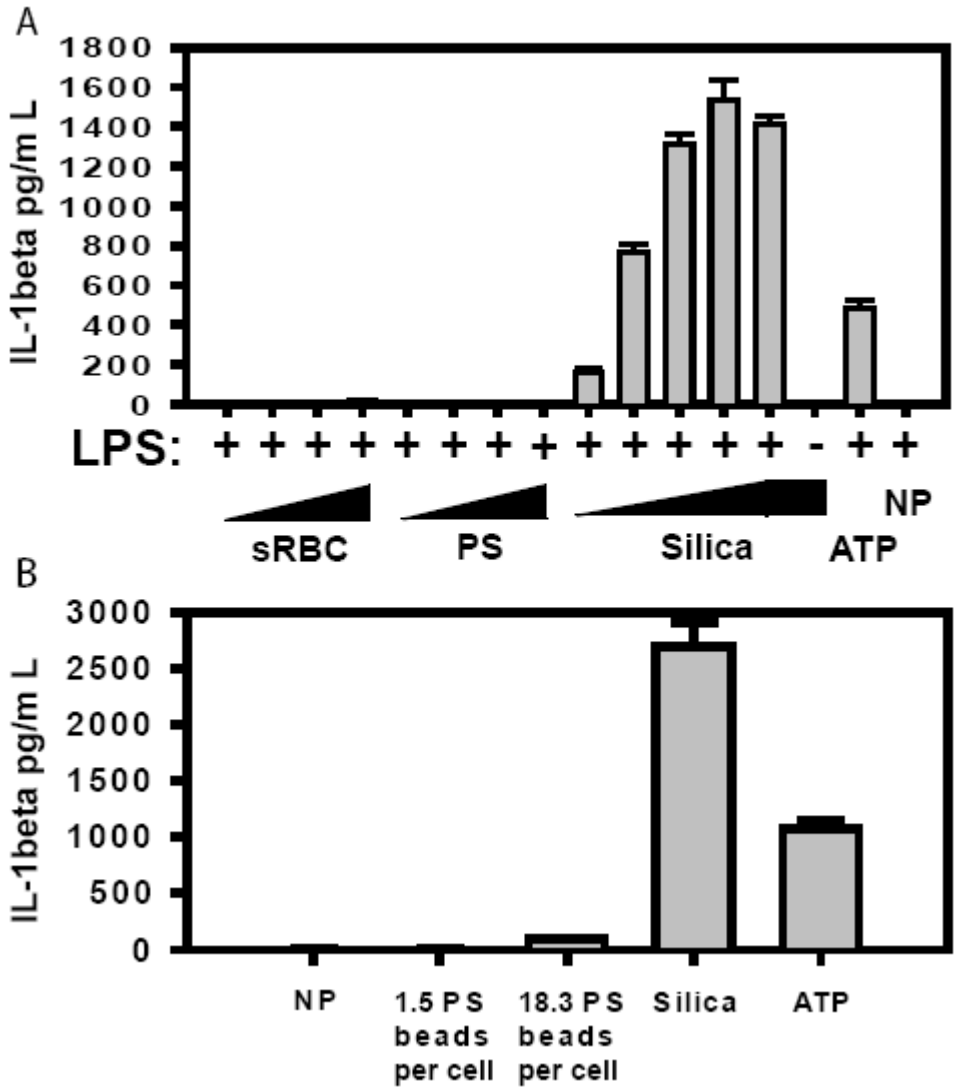

Figure 2.5. Secretion of IL-1β following particle phagocytosis is proportional to lysosome damage. BMM pretreated with LPS were fed opsonized sRBC ghosts, PS beads or silica. After four hours, culture supernatants were harvested and analyzed for IL-1β content. Data are averaged results from three independent experiments.

Table

		Lysosome Release			Caspase-1 activation					IL-1β secretion
Particle	dose	% of cells positive for LD	% of cells positive for LD or PDN	% of Fdx released	% of cells positive for FLICA	Mean FLICA Fluorescence Intensity	% of cells positive for PI	% of FLICA+ cells that were PI+	% of FLICA+ cells that were PDN+	pg/mL
No Particles	0	0	0	2	0	5.9E+05	1	†	†	2
sRBC ghosts	2.5 ghosts/cell	ND	ND	ND	1	7.8E+05	0	†	†	1
PS beads	1.5 beads/cell	0	0	2	1	7.4E+05	0	†	†	1
PS beads	18.3 beads/cell	2	2	3	ND	ND	ND	ND	ND	95
Silica	57 µg/mL	29	30	14	32	2.2E+06	32	90	98	772
Silica	170 µg/mL	50	54	28	64	4.0E+06	66	96	96	1309
Silica	500 µg/mL	56	65	30	85	5.8E+06	88	97	98	1537
Silica No LPS	170 µg/mL	45	45	28	ND	ND	ND	ND	ND	ND
Silica No LPS	500 µg/mL	ND	ND	ND	9	9.8E+05	6	69	70	0

Table. Compiled numerical data. Data are from LPS-stimulated BMM, except where noted. Cells with lysosome release greater than ten percent and with caspase-1 FLICA signal greater than $2x10^6$ fluorescence units were considered positive for lysosome damage and caspase-1 activation respectively. LD: for lysosome damage; PDN: phase-dark nuclear morphology. † indicates that the sample size is very small (less than 10 FLICA-positive cells) and ND indicates conditions for which there are no data.

Chapter 3
Inducible lysosome renitence limits *Listeria monocytogenes* escape in murine macrophages.

3.1 Abstract

In macrophages, mechanical lysosome damage can lead to release of inflammatory mediators, cell death and, entry of some pathogens into the macrophage cytoplasm. In previous work, we developed a ratiometric, live cell microscopy technique for measuring lysosome damage and showed that LPS-stimulated macrophages were resistant to damage induced by phagocytosis of ground silica or silica microspheres (SMS). In this work we characterized the mechanism of mechanical damage to lysosomes and the inducible lysosome protective phenotype. Lysosome damage was reduced when the cells were pre-incubated with a reactive oxygen inhibitor or exogenous antioxidants, but was independent of the phagocyte oxidase, implying that non-phagosomal reactive oxygen intermediates contribute to SMS-mediated damage. Maximal resistance to damage required 18 hours of LPS stimulation preceding SMS challenge. Stimulation of macrophages with peptidoglycan, TNF-α, IFN-γ or hemolysin-deficient *Listeria monocytogenes* (Δ*hly L.m.*) also conferred protection to subsequent SMS challenge. Pre-stimulation with LPS or IFN-γ also increased resistance of lysosomes to photodamage. The role of this inducible lysosome renitence (resistance to mechanical damage) was tested in *L.m.* infection which is capable of damaging

macrophage lysosomes. IFN-γ-stimulated macrophages derived from mice lacking the phagosomal oxidase inhibited *L.m.* escape, implying that inducible lysosome renitence represents a novel activity of activated macrophages which protects endocytic compartments from mechanical damage and membrane-damaging toxins.

3.2 Introduction

Classical macrophage activation, sometimes termed M1 macrophage activation, was originally identified from the ability of a sub-lethal infection with *Listeria monocytogenes* (*L.m*.) to protect mice from subsequent infectious challenges (Mackaness, 1962). This effect was independent of humoral acquired immunity and dependent on differentiation of macrophages (Mackaness, 1962). Macrophages become activated in response to combinations of soluble bacterial products, including lipopolysaccharide (LPS) and bacterial cell wall molecules, and host-derived signals, especially IFN-γ. In addition to their role in *L.m*. infection (reviewed in (Shaughnessy and Swanson, 2007)), activated macrophages are important in defense against HIV (Cassol et al., 2010; Herbein and Varin, 2010; Verani et al., 2005), *Yersina pestis* (Bergsbaken and Cookson, 2009), and protozoan parasite (Lykens et al., 2010) infection, as well as in sepsis (Lin and Yeh, 2005), cancer (Hallam et al., 2009) and atherosclerosis (Wilson, 2010).

While this activation leads to dramatic changes in gene regulation (Martinez et al., 2006), only a few anti-microbial mechanisms have been identified in activated macrophages (Trost et al., 2009). One formidable mechanism by which activated macrophages oppose infection is the up-regulation of the phagosomal NADPH oxidase system which synthesizes superoxide in the phagosomal lumen (Babior, 2004). Superoxide and other reactive oxygen species are toxic microbicides. Activated

macrophages also catalyze the production of reactive nitrogen species which can function as microbicides (MacMicking et al., 1997). Other strategies employed by activated macrophages include increased phagosome-lysosome fusion and increased antigen presentation (Trost et al., 2009). As only a fraction of the activation-regulated genes have been implicated in any of these processes, there may exist other important activities which macrophages use to combat infection. In this study we identify lysosome renitence, the resistance of lysosomal membranes to mechanical forces, as an activity which activated macrophages employ to resist *L.m.* infection.

L.m. is a Gram-positive facultative intracellular pathogen which can cause gastrointestinal disease in most individuals or more serious invasive infections in pregnant women, neonates or immuno-compromised individuals (Shaughnessy and Swanson, 2007). *L.m.* uses a unique cholesterol-dependent cytolysin, lysteriolysin O (LLO), to escape from macrophage phagosomes into the cell cytosol where *L.m.* divides and nucleates F-actin to invade neighboring cells. *L.m.* typically escapes macrophage phagosomes before phagosome-lysosome fusion and *L.m.* escape from macrophage lysosomes is inefficient (Henry et al., 2006). Wildtype *L.m.*, but not *L.m.* lacking the LLO gene (Δ*hly*), can disrupt pH and calcium gradients across phagosomal membranes, which allows *L.m.* to delayed phagosome-lysosome fusion for phagosomes containing bacteria (Henry et al., 2006; Shaughnessy et al., 2006).

Activation of macrophages significantly alters the dynamics of *L.m.* infection (Shaughnessy and Swanson, 2007). IFN-γ has a critical role in protecting mice from *L.m.* infection (Kiderlen et al., 1984). In tissue culture *L.m.* infection models, maximal protection is observed in macrophages pre-activated with LPS, IFN-γ, and a neutralizing

antibody against IL-10, and IL-6 (Myers et al., 2003). Reactive oxygen and nitrogen species produced by activated macrophages inhibit *L.m*. escape from the macrophage vacuole (Myers et al., 2003).

In previous work, we presented a fluorescence microscopy-based method for measuring lysosome damage (Davis and Swanson, 2010), which we used to confirm previous studies linking lysosome damage with inflammasome activation (Hornung et al., 2008). Pre-stimulation with LPS was necessary for IL-1β secretion and cell death following phagocytosis of ground silica. Unexpectedly, LPS-stimulated macrophages showed less lysosome damage after phagocytosis of ground silica than did unstimulated macrophages (Davis and Swanson, 2010). While silica-induced lysosome damage activates potentially damaging immune responses, loss of lysosome integrity in the context of an infection carries other consequences. Intracellular pathogens such as viruses and some bacteria must access host cell cytosol from endocytic compartments. Damage to membranes of endocytic compartments is essential to such infections. Increased resistance to such membrane-damaging activities by activated macrophages would be a novel mechanism of resistance to infection.

In this work we characterized the mechanism of particle-induced lysosome damage and the inducible mechanism of damage resistance. The lysosome protective effect observed with LPS pretreatment was also induced by other stimuli, including toll-like receptor ligands, cytokines and whole bacteria. As induced lysosome renitence protects lysosomes from a variety of damaging agents including ground silica, silica microspheres, and light-induced toxicity, we believe that this novel activity indicates a general lysosome membrane protection mechanism. Induced lysosome renitence was

also capable of reducing *L.m*. escape, independent of the phagosomal oxidase, implying that inducible lysosome renitence is a clinically relevant novel activity of activated macrophages.

3.3 Materials and methods

3.3.1 Materials

Fluorescein-dextran (Fdx) average molecular weight 3000 Daltons, RPMI 1640, certified heat-inactivated fetal calf serum (FCS), penicillin/streptomycin solution, valinomycin, nigericin, recombinant mouse IL-10, recombinant mouse IL-1β, SNARF-1 carboxylic acid acetate succinimidyl ester, Cell trace CFSE cell proliferation kit (carboxyfluotescein diacetate succinimidyl ester), Texas red-dextran average molecular weight 10,000 Daltons, Texas red-phalloidin, and gentamicin solution were purchased from Invitrogen (Carlsbad, CA, USA). Recombinant human IFN-β, diphenyleneiodonium (DPI), and n-acetyl-l-cystiene (NAC), were purchased from Sigma Chemical Co. (St. Louis, MO. USA). Lipopolysaccharide #225 *Salmonella typhurium* was from List Biological Laboratories INC (Campbell, CA, USA). Oxide silica 3 μm microspheres were purchased from Microspheres-Nanospheres (Cold Spring, NY, USA). 35 mm coverslips with attached 14 mm coverglass were purchased from MatTek Corp (Ashland, MA, USA). Peptidoglycan (PGN) from *Escherichia coli* 0111:B4 was purchased from Invivogen (San Diego, CA, USA). Recombinant IFN-γ was from R&D Systems (Minneapolis, MN, USA). Recombinant TNF-α was purchased from eBiosciences (San Diego, CA, USA). Recombinant mouse IL-6 was purchased from Calbiochem (San Diego, CA, USA). MIN-U-SIL-15 ground silica was a generous gift from U.S. Silica (Berkeley Springs, WV, USA).

3.3.2 Bone marrow-derived macrophages

C57BL/6J (wildtype) and B6.129S-*Cybb*^{tm1Din}/J (Nox-2 deficient) mice were purchased from Jackson Labs (Bar Harbor, ME, USA). Marrow from MyD88-deficient mice was a gift from the laboratory of Dr. Chung-Hee Chang at the University of Michigan. Differentiation of macrophages from mouse bone marrow cells has been previously described (Davis and Swanson, 2010; Swanson, 1989). Briefly, suspended marrow cells extracted from mouse femurs were cultured in the presence of M-CSF for six days. M-CSF was from 30% L-cell conditioned medium included in the differentiation medium. Bone marrow-derived macrophages (BMM) were then resuspended, frozen, and stored at -130^{o} C as aliquots in M-CSF-containing medium with 10% DMSO, then thawed as needed for experiments. 8x10^{4} cells were plated onto the bottom of each Mat-tek dish in RPMI 1640 with 10% FCS and penicillin/streptomycin.

3.3.3 Loading macrophage lysosomes and stimulation of cells

After allowing BMM to attach and recover for several hours, medium was replaced with fresh RPMI 1640 with 10% FCS and penicillin/streptomycin containing 150 µg/mL fluorescein-dextran (Fdx) and cultured overnight. BMM were then rinsed and chased in fresh RPMI 1640 with 10% FCS and penicillin/streptomycin for at least 3 hours to ensure all Fdx was trafficked into lysosomes. Penicillin/streptomycin was omitted from BMM to be infected with *L.m.* Cytokines and toll-like receptor ligands used to stimulate BMM were included in both the Fdx pulse medium and the subsequent Fdx-free chase medium, except as indicated in Figure 3.1A. The concentrations of these molecules were as follows; LPS was used at 100 ng/mL, PGN at 2.5 µg/mL, IFN-γ at 100

U/mL, TNF-α at 100 ng/mL, IL-6 at 5 ng/mL, IL-10 at 100 ng/mL, IL-1β at 10 ng/mL and IFN-β at 100 U/mL.

After Fdx was chased into BMM lysosomes, some cells were fed ground silica or silica microspherses (SMS). SMS were acid washed overnight in 1 N HCl then rinsed several times in distilled water. For some experiments, SMS were coated with 0.1 M poly-L-lysine (PLL) for 30 minutes. BMM medium was replaced with medium containing particles and incubated for an hour before imaging. Uncoated SMS were fed to BMM in serum-free medium while PLL-coated SMS were fed to cells in medium containing 10% FCS.

3.3.4 Measurement of lysosome damage

Lysosome damage was measured in live BMM using epi-fluorescence ratiometric microscopy, as described previously (Davis and Swanson, 2010). Briefly, cells were rinsed and imaged in Ringer's buffer (155 mM NaCl, 5 mM KCl, 2 mM CaCl2, 1 mM MgCl2, 2 mM NaH2PO4, 10 mM Hepes, and 10 mM glucose), using a Nikon TE300 inverted microscope equipped with a mercury arc lamp, 60x plan-apochromat 1.4-numerical aperture objective, a cooled digital CCD camera (Quantix Photometrics, Tucson, AZ, USA), a temperature controlled stage and a Fura/FITC ratiometric dichroic mirror (Omega Optical, Brattleboro, VT, USA). Three images were acquired for each field of cells: one phase-contrast image and two fluorescence images, which used the same emission filter but two different excitation band pass filters (centered at 440 nm and 485 nm). Filters were mounted in computer-controlled filter wheels (Sutter Instruments, Novato, CA, USA). Metamorph software (from Molecular Devices, Downingtown, PA, USA) was used for image capture and analysis.

The Fdx signal in the 440 nm excitation channel is relatively insensitive to pH, whereas the signal in the 485 channel varies significantly between pH 4.5 and 7.5. Thus the ratio of Fdx fluorescence in the 485 nm channel divided by that in the 440 nm channel is related to the pH of Fdx molecules in any sub-region of an image (pixel). 485 nm/440 nm ratios were converted to pH by calibrating the microscope, as described previously (Christensen et al., 2002; Davis and Swanson, 2010; Shaughnessy et al., 2006). Briefly, 485 nm /440 nm ratios were measured in cells with intracellular pH fixed at pH 9.0, 7.5, 7.0, 6.5, 6.0, 5.5, 5.0, 4.5 and 4.0, using clamping buffers (130 mM KCl, 1 mM $MgCl_2$, 15 mM Hepes, 15 mM MES). A 4-variable sigmoidal standard curve was then constructed using Sigmaplot software (San Jose, CA, USA). Areas showing pH greater than pH 5.5 were taken to indicate lysosome release. The percent of Fdx released in cells was calculated by summing the 440 nm intensity of pixels in regions of pH above 5.5 and dividing this value by the summed 440 nm intensity for the whole cell. This value (multiplied by 100) was the percent of Fdx released.

3.3.5 Photo-oxidative damage of lysosomes

This technique is based on that published in Kirkegaard et al. 2010 (Kirkegaard et al., 2010). BMM were co-loaded with 150 µg/mL Fdx along with 75 µg/mL Texas Red-dextran (TRdx). LPS and IFN-γ stimulation was performed for 18 hours, as described above. TRdx was used as a photosensitizer while Fdx imaging was used to monitor lysosome damage. BMM were rinsed with Ringer's buffer, mounted onto the microscope heated stage, and allowed to equilibrate for 5 minutes. Once a frame was selected for imaging, an initial Fdx image set was acquired. Using a 580 nm excitation filter the cells were then exposed to bright TRdx light in regular, 5-second exposures. Between each

580 nm photo-exposure, Fdx images at 440 nm and 485 nm were acquired to measure lysosome damage. This process was repeated for 60 total seconds of 580 nm photo-exposure. Percent Fdx release was then calculated for each time point.

3.3.6 Infection of cells with *Listeria monocytogenes*

Wildtype *Listeria monocytogenes (L.m.)* strain was DP-L10403 while Δ*hly* denotes *hly* deletion strain DP-L2161 (provided by Daniel Portnoy, University of California, Berkeley). *L.m.* cultures were grown overnight at room temperature then diluted and grown 75 minutes at 37 degrees with shaking which typically resulted in an O.D. 600nm of 0.8. Bacterial concentration was calculated by measuring the optical density of the culture at 600 nm before staining. One mL of bacterial culture was then centrifuged (2 min at 5000g) and resuspended in Ringer's buffer. Bacteria were stained using SNARF-1 or CFSE dye by adding these dyes to the Ringer's buffer and incubating for another 15 min in a shaking 37^{o} incubator. The culture was then washed three times in Ringer's buffer. BMM were infected by adding bacteria to 200 µL of culture medium without antibiotics and replacing the BMM culture medium with this infection mix. All infections were 10 minutes followed by rinsing in Ringer's buffer and chasing in culture medium containing gentamicin to kill any remaining extracellular *L.m.* After 90-120 minutes of culture, infected cells were either imaged for lysosome damage or fixed to measure escape.

3.3.7 Measurement of vacuole escape by *Listeria monocytogenes*

BMM infected with CFSE-stained *L.m.* were fixed using cytoskeleton fix (2% paraformelahyde, 30mM Hepes, 10mM EGTA, 0.5 mM EDTA, 5 mMMgSO4, 33 mM potassium acetate, 5% polyethylene glycol 400) and permeabilized in 0.1% Triton X-100

in PBS. Coverslips were blocked in PBS containing 2% goat serum and stained using Texas Red-phalloidin and DAPI. Cells were imaged and the number of total and escaped bacteria was recorded for each infected macrophage.

3.3.8 Statistical methods

All statistical tests were Student's T-Tests, performed on groups of cells containing similar numbers of SMS, *L.m*. or photostimulation.

3.4 Results

3.4.1 Reactive oxygen species contribute to particle-mediated lysosome damage.

The LPS-inducible lysosome protective activity may consist of mechanisms which defend the membrane itself from damage, which repair minor damage, or which prevent damage by interfering directly with the mechanism(s) by which particles cause damage. To examine the role of damage interference, the mechanism by which silica induces lysosome damage was explored. We first examined the role of reactive oxygen species (ROS) in silica-induced lysosome damage. Some groups have implicated ROS in silica induced NLRP3 activation (Cassel et al., 2008; Hu et al., 2010), while others have disputed this role (Hornung et al., 2008).

Diphenyleneiodonium (DPI) is a potent inhibitor of most ROS-generating activities in macrophages, including the phagocyte oxidase (NOX2) and the mitochondrial electron transport chain (Li and Trush, 1998; O'Donnell et al., 1993; Stuehr et al., 1991). Macrophages loaded with Fdx and pre-incubated in DPI or control medium were fed ground silica (Fig. 3.1A) or SMS (Fig. 3.1B) and the extent of damage was assessed. In both cases DPI reduced the lysosome damage following phagocytosis. The damage reduction was independent of any DPI effect on the efficiency of

phagocytosis, as DPI-dosed BMM which had phagocytosed SMS showed less lysosome damage than control cells which had ingested equivalent numbers of particles (Fig. 3.1B). These data indicate that ROS mediate lysosome damage after phagocytosis. This conclusion was also tested in BMM fed SMS in medium containing the exogenous antioxidant n-acyl-cysteine (NAC). Antioxidants like NAC interfere with radical chemistries by breaking the free radical reaction chain or by detoxifying free radical reaction products. BMM pre-incubated in NAC showed less SMS-mediated lysosome damage than did control cells (Fig. 3.1C) confirming the role of ROS in silica-mediated lysosome damage.

A major source of ROS in the phagosomal lumen is the phagosomal NADPH oxidase (Nox2). Once assembled this complex converts luminal oxygen into superoxide radicals by oxidizing cytosolic NADPH. One essential component of Nox2 is the cytochrome gp91*phox* (Babior, 2004). BMM were derived from mice lacking the gp91*phox* gene (Nox2 -/-). These *nox2*-deficient BMM and wildtype controls were loaded with Fdx and fed ground silica or SMS as lysosomal challenge. No difference in lysosome damage was observed between wildtype and *nox2*-deficient BMM fed ground silica (Fig. 3.1D), or SMS (Fig. 3.1E), indicating that the phagocyte oxidase does not contribute to particle-mediated lysosome damage. Taken together, these data indicate that phagosomal oxidase-independent ROS plays an important role in silica-induced lysosome damage.

3.4.2 Macrophage activation stabilizes lysosomes.

Previous studies established that particle-mediated lysosome damage was reduced when cells were pre-stimulated with LPS (Davis and Swanson, 2010), indicating that the

same signals which up-regulate pro-IL-1β, NLRP3, and other genes necessary for the inflammasome response to lysosome damage also protect lysosomes from damage. To analyze this inducible response, we first measured the time course of the LPS protective effect. Following Fdx loading of lysosomes and LPS pre-stimulation of variable time, BMM lysosomes were damaged using SMS. Stimulating BMM with LPS for 1 or 2 hours was insufficient to induce lysosome renitence (Fig. 3.2A). Full lysosome protection required 18 hours of LPS stimulation (Fig. 3.2A). This long time delay indicates that lysosome protection may require changes in gene expression, autocrine/paracrine signaling and/or the accumulation of metabolites. The requirement of novel translation could be tested by inhibiting translation with cycloheximide and the role of paracrine signaling could be probed using neutralizing antibodies against potential signaling intermediates, such as TNF-α.

We hypothesized that other stimuli also induce lysosome renitence. BMM lysosomes were loaded with Fdx and stimulated with LPS, peptidoglycan (PGN), IFN-γ, TNF-α, IL-6, IL-10, IL-1β, or IFN-β (Fig. 3.2B & C) then the lysosome damage induced by phagocytosis of SMS was measured. LPS, PGN, IFN-γ, and TNF-α protected lysosomes from SMS challenge, IL-6, IL-10, IL-1β, and IFN-β did not. TNF-α-induced protection of lysosomes has been reported for other systems (Persson and Vainikka, 2010). Thus lysosome renitence can be induced by different signaling inputs leading to classical macrophage activation.

To measure the contribution of Myd88 to signaling that induces lysosome protection, BMM from Myd88-deficient mice were loaded with Fdx, pre-stimulated with LPS or TNF-α, and then challenged with SMS. Lysosome damage was similar between

wildtype and Myd88-deficient BMM when the cells were unstimulated or stimulated with TNF-α. For LPS, lysosome damage was significantly decreased in BMM lacking MyD88, compared to unstimulated cells, (Fig. 3.2D). This is consistent with the known properties of TLR4 signaling, in that TRIF signaling can partially compensate for MyD88-deficiency (Akira and Takeda, 2004).

To examine the relevance of inducible lysosome renitence for infections we measured the ability of whole live bacteria to induce lysosome resistance to damage. BMM were fed Δ*hly L.m.*, then loaded with Fdx then assayed 18 hours later for lysosome damage after phagocytosis of SMS. *L.m.* lacking the *hly* gene, which encodes the pore-forming cytolysin, Listeriolysin O, cannot escape the macrophage vacuole and are killed in lysosomes (Portnoy et al., 1988). BMM fed Δ*hly L.m.* showed less lysosome damage after phagocytosis of SMS than did unstimulated BMM (Fig. 3.2E). This protection was similar to that induced by LPS. Those BMM exposed to Δ*hly L.m.* which did not ingest bacteria showed lysosome damage levels comparable to unstimulated cells (Fig. 3.2F), indicating that the Δ*hly L.m.* activated this lysosome protective mechanism inside the cells that ingested them, rather than through some secreted factor. Thus, macrophages possess an inducible system for the protection of lysosomes which can be elicited by soluble bacterial mediators, the phagocytosis of bacteria or activation signals from other cells of the immune system.

3.4.3 Inducible lysosome renitence protects lysosomes against photo-oxidative damage.

Lysosome protection was also measured in a non-particulate lysosome damaging system. BMM lysosomes were co-loaded with Texas red-dextran (TRdx), as a

photosensitizer, and Fdx, to monitor lysosome integrity, then damaged by exposure to light, as in the methods of Kirkegaard et al. (Kirkegaard et al., 2010). Cells were illuminated with 580 nm light, which excites TRdx but not Fdx. While most of this excited TRdx returns to the ground state via fluorescence, some fraction of these excited TRdx will take part in photo-oxidation chemistries which damage cell membranes. BMM were loaded with TRdx and Fdx and prestimulated with LPS or IFN-γ. The cells were illuminated with 580 nm light in five-second increments. Lysosome integrity was measured by imaging Fdx after each 580 nm exposure. In unstimulated BMM, lysosome damage was detectable as early as 25 seconds of 580 nm exposure and was nearly complete by 50 seconds (Fig. 3.3A & B). This measurement was actual lysosome damage and not photobleaching of the Fdx as BMM not loaded with photosensitizer but exposed to the same 580 nm light failed to show any neutral Fdx throughout the experiment (Fig. 3.3A & B). LPS- or IFN-γ-stimulated BMM were protected from phototoxic lysosome damage as the average lysosome damage in these conditions was reduced in LPS-or IFN-γ-stimulated BMM between 30 and 55 seconds. Thus the lysosome protective activity induced in macrophages applies to lysosome damage other than that caused by silica (Fig. 3.3A & B).

3.4.4 Lysosome renitence protects activated BMM from *L.m*. escape and lysosome damage.

We hypothesized that induced lysosome renitence could inhibit the escape of invasive pathogens from macrophage vacuoles. The ability of lysosome renitence to limit *L.m*. escape in a BMM tissue culture model was assayed. The escape of *L.m.* from macrophage phagosomes into the host cell cytosol is a critical step in the life cycle of this

invasive bacterial pathogen (Shaughnessy and Swanson, 2007). Previous data suggested that in a low multiplicity of infection (MOI) BMM infection model most *L.m*. vacuolar escape occurs before vacuoles fuse with lysosomes (Henry et al., 2006). Fdx-loaded BMM were fed SNARF-1-labeled wildtype or Δ*hly L.m*. Wildtype *L.m.* induced high levels of lysosome damage at higher bacterial loads (Fig. 3.4A, B, &C). Some cells which contained fewer (1-7) bacteria had high levels of lysosome damage indicating that low numbers of bacteria could induce a detectable signal. Generally, however, cells containing fewer than seven bacteria showed low amounts of lysosome damage (Fig. 4C). When other BMM coverslips were infected with identical doses of *L.m*. and scored for *L.m*. escape using phalloidin (Fig. 3.4D), amounts of escape and lysosome damage were both dose-dependent and correlated (Fig. 3.4E). BMM infected with Δ*hly L.m*. showed neither lysosome damage nor *L.m*. escape, confirming that lysosome damage is dependent on the bacterial cytolysin LLO. Of note, cells containing low numbers of wildtype *L.m*. more frequently had escaped bacterium than lysosome damage. This difference decreased at higher bacterial loads until there was no difference in the group with the highest numbers of *L.m.* (Fig. 3.4F). These data suggest that while *L.m*.-induced lysosome damage is dependent on LLO, escape itself may not be the primary cause of lysosome damage in this system.

Inducible lysosome renitence may reduce either of these potentially harmful outcomes. Previous work has shown that activated macrophages use the *nox2* phagosomal oxidase to inhibit *L.m*. escape (Myers et al., 2003). *Nox2* was not critical to the induction of damage as lysosome damage levels in macrophages lacking the *nox2* phagosomal oxidase were identical to control cells (Fig 3.1 D&E). To determine if

induced lysosomal renitence inhibits *L.m.* escape in activated macrophages, wildtype and *nox2*-deficient BMM were loaded with Fdx, activated with IFN-γ, then infected with wildtype *L.m*. Although IFN-γ-activated *nox2*-deficient BMM could not inhibit escape as well as IFN-γ activated wildtype BMM, they were significantly better than unactivated cells (Fig. 3.4H). IFN-γ-activated, *nox2*-deficient BMM also showed reduced levels of lysosome damage after *L.m.* infection compared to unactivated *nox2*-deficient cells (Fig. 3.4I). Together these data imply that inducible lysosome renitence can inhibit *L.m.* escape and LLO-induced lysosome damage. Thus lysosome renitence is a novel activity employed by activated macrophages to limit invasive pathogen escape as well as intracellular damage.

3.5 Discussion

Lysosome renitence is a novel mechanism of activated macrophages which protects cells from harmful lysosome disruption. This protection is important in part because lysosome damage can have grave consequences for host cells. Aside from allowing access of microbes or virulence factors to an immune-privileged niche, lysosome damage induces a pro-inflammatory cell death program in activated macrophages. Lysosome damage-dependent inflammasome activation requires NLRP3 and results in IL-1β release and cell death (Davis and Swanson, 2010; Hornung et al., 2008). Lysosome damage is important in several diseases of crystal or particle accumulation such as silicosis (ground silica crystals) (Cassel et al., 2008; Hornung et al., 2008) and arteriosclerosis (cholesterol crystals) (Duewell et al., 2010) and may also be important for gout (monosodium-urate crystals) and asbestosis. As there are significant negative consequences of excessive lysosome damage, there may be evolutionary

pressure to minimize lysosome damage in situations of pre-existing inflammation. On the other hand, lysosome damage in unactivated cells results in less inflammatory cell death (Boya and Kroemer, 2008). This dichotomy between the results of lysosome damage in activated and unactivated cells may explain why renitence correlates with macrophages activation: low lysosome renitence in non-infectious settings and high renitence in situations where pathogens have been detected. Some level of lysosome permeability may even be beneficial in some circumstances, as it may facilitate the cross presentation of exogenous antigens on MHC class I molecules. Indeed, low levels of background lysosome release have been observed in some systems (Davis and Swanson, 2010).

One way cells may circumvent inflammatory sensing of lysosome damage is by sampling earlier endocytic compartments. The lysosomal damage ligand recognized by the NLRP3 inflammasome and its localization are unclear at this time, especially as there is some uncertainty as to the role of cathepsins and cathepsin inhibitors in activating inflammasomes (Dostert et al., 2009; Hornung et al., 2008; Newman et al., 2009). If early endocytic compartments are not under this innate immune surveillance, then some pathogens may avoid detection by entering cytoplasm from early endosomal compartments. For instance, preferential escape of *L.m.* from pre-lysosomal compartments (Henry et al., 2006) may lessen inflammasome activation. In cells containing low numbers of bacteria, *L.m.*-induced lysosome damage is less frequent than *L.m.* vacuolar escape, suggesting that some *L.m.* are capable of accessing host cell cytosol without significantly damaging lysosomes. In addition to minimizing the bacterium's

exposure to microbicidal lysosomal conditions, early endosomal escape may enable pathogens to evade this immune sensing mechanism.

Inflammasome activation in *L.m.* tissue culture infection is dependent on the expression of LLO, as bacteria lacking this toxin do not induce IL-1β secretion (Warren et al., 2008). However, in addition to lysosome damage bacterial escape also delivers other inflammasome activators into the host cell cytosol. Some inflammasome activation was observed to be IPAF- and flagellin- dependent (Warren et al., 2008; Way et al., 2004). AIM2 inflammasomes can also sense *L.m*. DNA in host cell cytosol (Kim et al., 2010). NLRP3- and ASC- dependent inflammasome activation are independent of IPAF and AIM2, suggesting that lysosome damage is sensed during in *L.m.* infection.

Bacterial load may affect lysosome damage-sensing by macrophages. Figure 3.4 shows that lysosome damage is proportional to the number of *L.m*. phagocytosed. At low doses of *L.m.*, lysosome damage was less frequent than escape and typically low while at higher bacterial loads lysosome damage was extensive and as frequent as escape. It could be that infection of macrophages by one or two bacteria evades innate immune surveillance better than infections with higher bacterial loads, such as later in infections.

While lysosome damage induced by single *L.m*. bacteria was infrequent and on average low, some macrophages containing only one bacterium were positive for lysosome damage (Fig. 3.4 and data not shown). These data imply that ratiometric detection of released Fdx is sensitive enough to detect the Fdx released by a single *L.m.* escape event and that escape only infrequently results in lysosome damage. While lysosome damage and escape were completely dependent on the pore-forming toxin LLO (Fig. 3.4C & E), the mechanism by which LLO and *L.m*. induce lysosome damage

remains unknown. Although single escape events only infrequently induced lysosome damage, perhaps multiple escape events in cells infected with many bacteria do induce lysosome damage. Alternatively, LLO may damage lysosomes in processes outside of proper bacterial escape. LLO secreted into the endosomal lumen by bacterium prior to escape or by the fraction of *L.m*. that do not escape (about 75%; Fig. 3.4H) may be trafficked to lysosomes and attack membranes there. The fate of LLO secreted into the cytosol by *L.m.* is unknown (Schnupf and Portnoy, 2007). Perhaps this cytosolic LLO attacks the cytosolic face of lysosomal membranes. While *L.m*. escape from lysosomes may be inefficient (Henry et al., 2006), LLO may nonetheless damage lysosomes by other mechanisms.

Lysosome renitence was observed in a variety of different lysosome-damaging conditions. Ground or microsphere silica particles damaged lysosomes mechanically (Fig. 3.2), while *L.m*. damaged lysosomes by the pore-forming toxin LLO. In addition to protecting cells from these particles, induced lysosome renitence protected macrophage lysosomes from damage induced by photo-oxidation of a pre-loaded photo-sensitizer independent of any particles (Fig. 3.3). These observations demonstrate that lysosome renitence inhibits lysosome damage from a variety of insults. Thus, lysosome renitence is unlikely to involve mechanisms specific to any one damaging stimulus but is instead a general pathway which re-enforces lyososomal membranes against mechanical and chemical damage. This novel activity of activated macrophages was induced by the TLR ligands LPS and PGN, whole bacteria, as well as the cytokines IFN-γ and TNF-α (Fig. 3.1). That these stimuli derive from disparate sources re-enforces that lysosome renitence

is probably induced in a variety of situations and is a novel common feature of classical macrophage activation.

Macrophages cultures fed *Δhly L.m.* induced lysosome renitence (Fig. 3.2E). Induction of lysosome renitence required phagocytosis of bacteria as bystander cells were not protected (Fig. 3.2F). This indicates that the secondary secretion of soluble factors, such as TNF-α, was not responsible for this induction. A recent study showed that *Δhly L.m.* induced TNF-α secretion by macrophages nearly as well as wildtype *L.m.* (Dewamitta et al., 2010) suggesting that bystander cells could be protected by TNF-α induced renitence in some circumstances. Our studies used sparsely cultured cells, whereas the Dewamitta study involved a higher density macrophage culture. Thus dilution of secreted cytokines may have prevented any bystander protection. In the setting of a *L.m.* infection, these data suggest that macrophages which survive an early infection by *L.m.* are protected from subsequent infection. Figure 3.2E used *Δhly L.m.* to activate macrophages, as wildtype *L.m.* would have killed the macrophages. Thus, the use of mutant bacteria insured a robust population of surviving cells and also reduced the role of inflammatory mediators released by death of the macrophages.

The question of whether lysosome-damaging agents themselves induce lysosome renitence in surviving cells is yet unanswered. Ground silica induces TNF-α secretion in a macrophage like cell line which is not killed by lysosome damage induced pyroptosis (Claudio et al., 1995). This suggests that ground silica also induces renitence in survivor and bystander cells. As induced renitence protects macrophage lysosomes from various insults, lysosome renitence induced after surviving one infection could provide some measure of protection in a subsequent infection with a different intracellular pathogen.

Accordingly, macrophages which survive a *L.m.* infection should be protected in a subsequent infection with *Mycobacterium tuberculosis*, which requires some lysosome-cytosol contact but does not typically escape out of the vacuole (Teitelbaum et al., 1999).

The mechanisms by which macrophages induce lysosome renitence remain unknown. The role of ROS in the various lysosome damaging mechanisms tested here is mixed. Non-phagosomal ROS was important to damage induced by silica particles (Fig. 3.2) while luminally generated ROS from the TRdx photo-stimulation probably account for a portion of the phototoxic damage (Fig. 3.3). In cells infected with *L.m*., phagosome-derived ROS protected lysosome integrity (Fig. 3.4I) and inhibited escape of *L.m*. from the macrophage phagosome (Myers et al., 2003). Thus, while modulation of ROS remains a possible mechanism for modulating lysosome damage, this is unlikely to be the main mechanism of lysosome renitence.

The data presented here show that induced lysosome renitence is a novel pathway induced in activated macrophages which reduces the access of intracellular pathogens to macrophage cytosol. This activity also reduced irritant particle-induced lysosome damage, indicating that therapeutic interventions which increase renitence, preferably independent of inflammation, could be efficacious against infection by intracellular pathogens or for individuals exposed to harmful lysosome-damaging particles.

Figure 3.1

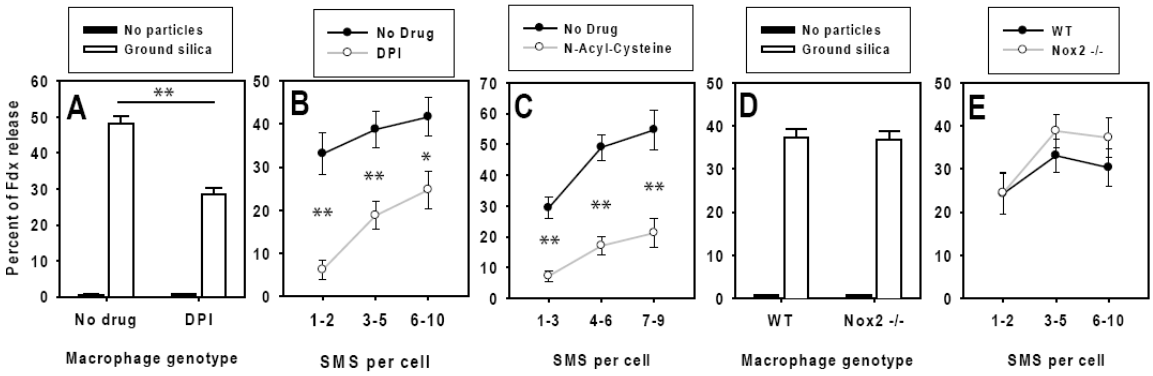

Figure 3.1. Non-phagosomally generated reactive oxygen intermediates contribute to silica-mediated lysosome damage. BMM were loaded with Fdx then fed ground silica (A and D) or PLL-coated silica microspheres (SMS) (C,B&E). 5μM diphenyleneiodium (DPI) (A & B) or 50 mM N-acyl-cysteine were added in the medium with the particles. D) and E) BMM were derived from wildtype or *Nox2* deficient (*Nox2* -/-) mice, loaded with Fdx and fed particles. After one hour, cells were imaged and lysosome damage measured. All data points represent mean±SEM Fdx release with n>200 BMM for A,B,D and E and n>50 BMM for C. * $p<0.05$, ** $p<0.001$.

Figure 3.2

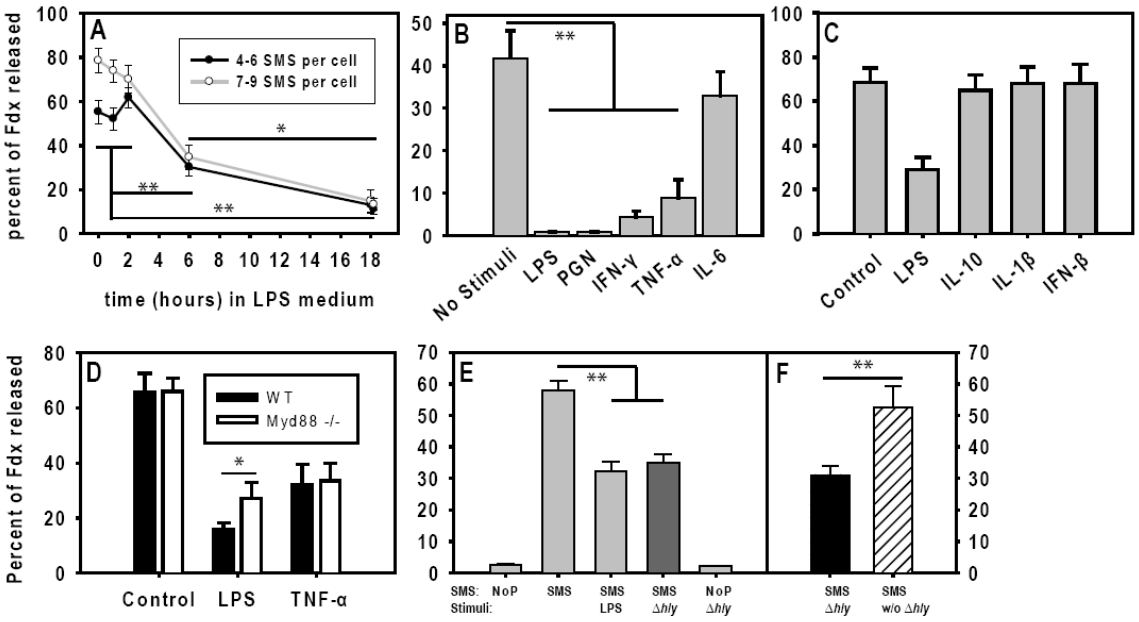

Figure 3.2. Macrophage activation increases lysosome renitence. BMM were loaded with Fdx then chased for at least 3 hours in medium without Fdx. BMM were then fed SMS and imaged after one hour to measure lysosome damage. Following imaging the number of SMS phagocytosed by each BMM was counted and groups of BMM which contained similar numbers of SMS were plotted together. Bars and data points are the average percent of Fdx released for at least 100 cells in all cases. Error bars represent SEM. BMM were stimulated during loading and chase with various stimuli. A) 100 ng/mL LPS was included in the loading and or chase medium for various times. BMM stimulated for 18 or 6 hours were significantly different from those stimulated for 1 or 2 hours or those left unstimulated ($p<0.001$) and BMM stimulated for 18 hours were significantly different than cells stimulated for 6 hours ($p<0.05$). B) 100 ng/mL LPS, 2.5 μg/mL peptidoglycan (PGN), 100 U/mL IFN-γ, 100 ng/mL TNF-α, 5 ng/mL IL-6 C) 100 ng/mL IL-10, 10 ng/mL IL-1β, or 100 U/mL IFN-β were included in the loading and chase medium of select BMM. D) BMM were derived from C57/BL6 (WT; dark bars) and *myd88*-deficient (Myd88 -/-; open bars) mice. These BMM were dosed with 100 ng/mL LPS or 100 ng/mL TNF-α in loading and chase medium. E) BMM were infected with SNARF-1 stained *hly* deficient *L.m.* (Δ*hly*) or stimulated with 100 ng/mL LPS or left unstimulated. These cells were then lysosomaly challenged with SMS or left unchallenged. F) Re-plotted data from the Δ*hly*–primed SMS-fed condition in E) (darkest bar). Using the SNARF-1 signal, BMM were separated into cells which had phagocytosed at least one bacterium (Δ*hly*; dark bar) and those cells in the same coverslips which had no SNARF-1 signal (w/o Δhly; striped bar). Bars in B-D represent cells which contained between 7 and 9 SMS while Bars in E & F represent cells which contained between 1 and 3 SMS. * $p<0.05$ ** $p<0.001$.

Figure 3.3

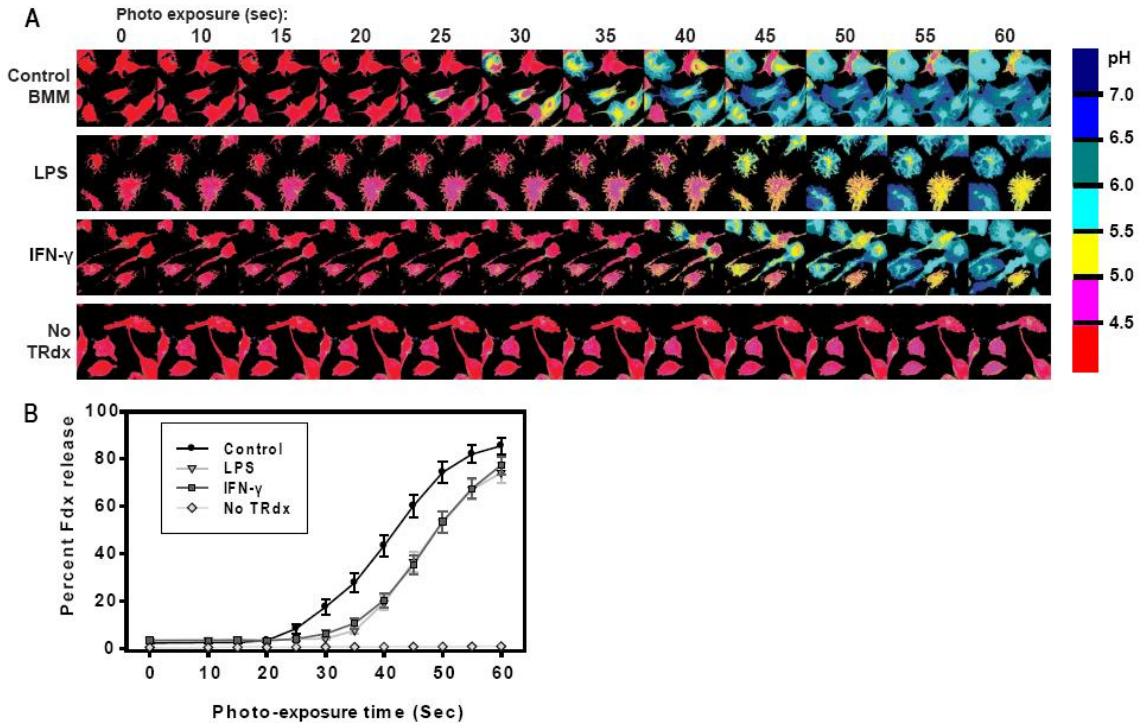

Figure 3.3. Inducible lysosome renitence protects lysosomes against photodamage. BMM lysosomes were loaded with Fdx and TRdx overnight and chased as in previous figures. As in Figure 3.1, LPS (100 ng/mL) or IFN-γ (100 U/mL) were included in the loading and chase medium as indicated. Coverslips were mounted onto the stage of an epi-fluorescent microscope. Chosen fields were then exposed to bright 580 nm light from the microscope arc lamp in 5-second pulses with Fdx pH images acquired in between each pulse. A) Sample pH maps of fields of photostimulated BMM with pH color key. B) Percent of Fdx released was calculated for each cell. Average percent release for each time point is plotted ± SEM. Note LPS and IFN-γ curves are nearly identical making them difficult to distinguish. At least 50 cells were analyzed for each condition. * $p<0.05$ ** $p<0.001$ noted comparisons are between control cells and LPS and IFN-γ.

Figure 3.4. Lysosome renitence protects IFN-γ activated macrophages from *L.m.* escape and damage. A-C) C57/BL6 BMM were loaded with Fdx overnight and then chased in dye and antibiotic-free medium for at least 3 hours. BMM were infected with SNARF-1 labeled wildtype or Δ*hly L.m.* for 10 min then chased in gentamicin-containing medium. 90 minutes later BMM were imaged to measure lysosome damage and the number of bacteria in each cell counted using the SNARF-1 signal. A) Fdx pH map of a BMM infected with wildtype *L.m.* B) Fdx pH map of a BMM infected with Δ*hly L.m* and pH color key. Scale bar in A) represents 10μm while green pseudo-color in A), B) and G) labels SNARF-1 labeled *L.m.* C) Average ± SEM percent Fdx release for BMM plotted in groups of cells containing similar numbers of total wildtype (filled bars) or Δ*hly* (open bars) *L.m.* D) Sample image of BMM infected with CFSE stained *L.m.* (pseudo-colored green) then fixed and stained with phalloidin for F-actin (pseudo-colored red) and DAPI (pseudo-colored blue) E) Fdx release data from C) re-plotted with average number of escaped (phalloidin positive) *L.m.* ± SEM plotted on the x-axis for each category of BMM grouped by total number of *L.m.* Filled circles represent groups of BMM infected with wildtype *L.m.* while open symbols near the origin represent all three groups of Δ*hly L.m.* which have background Fdx release and no escape. F) Average percent of cells positive for at least one event of *L.m.* endosomal escape (filled bars) or greater than five percent Fdx release (striped bars). Bars are average percentages from at least 6 different coverslips ± SEM. G) Example Fdx pH map of *nox2* deficient BMM pre-stimulated with 100 U/mL of IFN-γ depicting reduced lysosome damage. H) and I) C57/BL6 (WT) and *nox2*-deficient (Nox2 -/-) BMM were pre-stimulated with IFN-γ (open bars) or left un-simulated (dark bars) and for I) loaded with Fdx. BMM were infected as above with wildtype *L.m.* and after 120 minutes were fixed and stained with phalloidin for *L.m.* escape H) or imaged for Fdx release I). Bars in H) are average percent of phalloidin positive *L.m.* and error bars are SEMs with about 150 cells analyzed for each bar. Bars in I) are average percent of Fdx released ± SEMs of BMM containing 1 to 7 *L.m.* per cell. About 150 cells were analyzed for each bar. * $p<0.05$ ** $p<0.001$

Figure 3.4

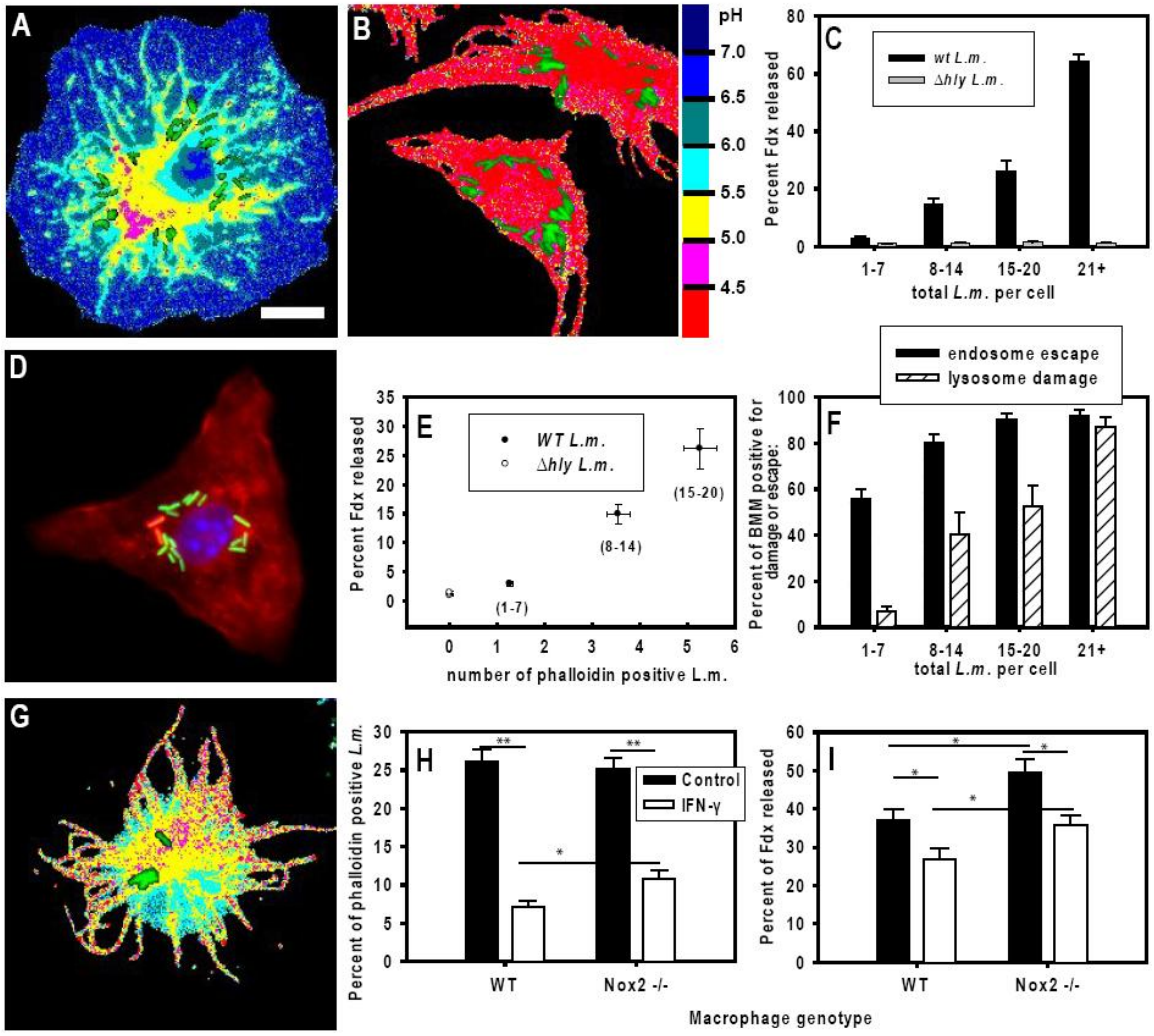
A
B
pH
7.0
6.5
6.0
5.5
5.0
4.5
C
wt L.m.
Δhly L.m.
Percent Fdx released
1-7
8-14
15-20
21+
total L.m. per cell
D
E
WT L.m.
Δhly L.m.
(1-7)
(8-14)
(15-20)
Percent Fdx released
number of phalloidin positive L.m.
F
endosome escape
lysosome damage
Percent of BMM positive for damage or escape:
total L.m. per cell
G
H
Control
IFN-γ
Percent of phalloidin positive L.m.
WT
Nox2 -/-
I
Percent of Fdx released
Macrophage genotype

Chapter 4
Mechanisms of lysosome damage and repair.

4.1 Abstract

Lysosome renitence may consist of mechanisms which reduce membrane-damaging chemistries, which increase membrane resistance to damage or which repair damaged organelles. We therefore examined several possible mechanisms of membrane stabilization and repair. Exogenously added HSP70 protected macrophage lysosomes and pharmacological inhibition of HSP70 activity reversed lysosome renitence, indicating a role for HSP70 in lysosome stabilization. Although previous studies showed that inhibition of acid sphingomyelinase (ASM) destabilized fibroblast lysosome membranes, the same ASM inhibitory drug did not alter silica microsphere (SMS)-mediated lysosome damage in macrophages. To examine possible lysosome repair mechanisms in lysosome renitence, we tested two possible repair mechanisms: calcium-mediated membrane patching and autophagy. Chelation of lysosomal but not extracellular calcium increased SMS-mediated lysosome damage, suggesting that luminal calcium protects lysosomes from damage. Time-lapse studies of phagocytosis indicated the existence of rapid membrane –sealing activities on phagosomes. GFP-Lc3, a marker of autophagosomes, localized to a fraction of phagolysosomes which contained lysosome-damaging SMS. GFP-Lc3 did not localize to phagolysosomes containing a different variety of SMS which

did not damage lysosomes. Together these data suggest that lysosome repair mechanisms contribute to lysosome renitence.

4.2 Introduction

The mechanism of inducible lysosome renitence is unknown. Lysosome damage resistance could involve inducible mechanisms which reinforce lysosome membranes, which repair modestly damaged lysosomes before damage becomes severe, or which interfere with the mechanisms which cause lysosome damage. In this chapter we examine several possible mechanisms which may mediate lysosomes renitence.

One possible mechanism for lysosome renitence is that activation induces changes in lysosomal membrane composition which alter chemical reactivity and or biophysical properties of the lysosomal membrane. Kirkegaard et al (Kirkegaard et al., 2010) recently showed endocytosed HSP70 activates acid sphingomyelinase (ASM) in lysosomes. ASM-catalyzed synthesis of ceramide protects fibroblast lysosomes and inhibition of ASM destabilizes lysosomes. ASM converts sphingomyelin at the luminal face of lysosomal membranes into ceramide which can increase acyl-packing (Holopainen et al., 1998), putatively conferring some membrane renitence. We hypothesized that a similar system operates in BMM and may be regulated by macrophage activation.

BMM repair damaged plasma membranes by a process which reduces membrane tension, docks endomembranes, and stimulates endocytosis all at the site of membrane damage (Idone et al., 2008; McNeil and Steinhardt, 2003). When plasma membranes are damaged, calcium (Ca^{2+}) flows into the cytosol from the extracellular environment and triggers all three of these mechanisms. Plasma membrane repair occurs in a wide variety

of cells including macrophages (McNeil and Steinhardt, 2003). Moreover, some pathogens inhibit plasma membrane repair in macrophages (Divangahi et al., 2009). As lysosomes are known to contain higher Ca^{2+} concentrations than the cytosol (Christensen et al., 2002), lysosome damage may trigger a lysosome active membrane repair activity analogous to the Ca^{2+}-dependent plasma membrane repair mechanisms. Here we test this hypothesis by probing SMS-mediated lysosome damage in situations which modify lysosomal calcium levels.

Another option for lysosome repair or renitence is the autophagy system, reviewed in (Mehrpour et al., 2010). Autophagy is a cytosolic pathway in which organelles or cytosolic proteins become enclosed by vesicular membranes. These double membrane-enclosed compartments, termed autophagosomes, fuse with lysosomes, leading to the degradation of the autophagosome contents. Autophagy-related proteins have also been shown to localize to phagosomes to a higher degree in TLR-activated cells, suggesting that conditions which induce lysosome renitence may also induce autophagy (Delgado et al., 2008; Mehrpour et al., 2010; Sanjuan et al., 2007). We hypothesized that damaged lysosomes may trigger autophagy mechanisms that repair the lysosomes or engulf the damaged membrane in an autophagosome which would fuse with an intact lysosome. In this chapter we show that GFP-Lc3 chimeras are recruited to phagosomes containing silica microspheres (SMS) which damage lysosomes but not to phagosomes containing SMS which do not damage lysosomes.

4.3 Materials and Methods

4.3.1 Materials

Fluorescein-dextran, RPMI medium and fetal bovine serum was purchased from Invitrogen (Carlsbad, CA, USA). Buthionine sulfoximine (BSO), Desipramine (des), EGTA and BAPTA were purchased from Sigma-Aldrich (St. Louis, MO. USA). Silica microspheres (SMS), uncoated, and amine-coated were purchased from Microparticles-Nanoparticles.com (Cold Spring, NY, USA). Uncoated SMS were washed in 1 M hydrochloric acid overnight then rinsed thoroughly in distilled water before use. Recombinant HSP70 and the HSP70-modifying pharmacological agents, 115-7c, Ym1 and Myr were generous gifts from the Jason Gestwicki lab at the University of Michigan.

4.3.2 Fdx loading and drug treatment of macrophages

The preparation of bone marrow-derived macrophages (BMM), pulse-chase Fdx loading, SMS preparation, and lysosome damage calculations were performed as described in (Davis and Swanson, 2010) and chapters 2 and 3. Microscopic imaging was performed as described in chapter 3. Buthionine sulphoximine was included in Fdx loading and chase medium while desipramine was added one or three hours before addition of SMS. Both drugs were included in medium used to feed BMM with SMS. Recombinant HSP70 (300 nM) or the HSP70-acting drugs 115-7c (100 µM), Ym1 (20 µM) and Myr (25 µM) were included in the macrophage medium for 5 hours.

4.3.3 Time lapse imaging of macrophages

Macrophages with Fdx-labeled lysosomes were fed SMS and incubated for ten minutes. Excess SMS were then rinsed away and coverslips were mounted onto the heated stage of a microscope. After a suitable field was found images were acquired every 5 minutes using short exposure times to minimize photobleaching. pH calculations were performed as described in chapter 2 (Davis and Swanson, 2010). Regions of

interest were drawn over cells and phagosomes and the data transferred to Excel for analysis.

4.3.4 Lysosomal Calcium modification

BMM were prepared and Fdx loaded as in (Davis and Swanson, 2010) and chapters 2 and 3. One hour before SMS addition, cells were rinsed in Ringer's buffer (RB) (Davis and Swanson, 2010) or RB lacking $CaCl_2$ (Ca^{2+} free-RB). BMM were then incubated with RB, Ca^{2+} free-RB or Ca^{2+} free-RB with 10 mM EGTA or 3 mM BAPTA for one hour. SMS were then added in the same buffer. After one hour cells were imaged for lysosome damage in this same buffer.

4.3.5 Imaging of GFP-Lc3

GFP-Lc3 transgenic mice (Mizushima and Kuma, 2008) were the generous gift of Dr. Michele Swanson. GFP imaging was performed on the microscope described in chapter 3. Because GFP signal in GFP-Lc3 BMM was extremely dim, live cell imaging was performed with a 485 nm excitation filter and without any other emission filter. Phase-contrast images were also acquired for each frame.

4.4 Results

4.4.1 HSP70 protects lysosomes

To determine whether HSP70 contributes to induced lysosome renitence, macrophages were incubated with either recombinant HSP70, a pharmacological activator of HSP70 called 115-7c (Jinwal et al., 2009; Koren et al., 2010), or LPS and lysosome damage after SMS phagocytosis was measured. Recombinant HSP70 and HSP70 activator 115-7c reduced lysosome damage to levels comparable to that induced by LPS (Fig. 4.1A). As HSP70 has been observed to interact directly with lysosomal

membrane components (Sanjuan et al., 2007), these data suggest that HSP70 mediates induced lysosome renitence. To test this hypothesis, macrophages were loaded with Fdx and left unstimulated or stimulated with LPS for 5 or 18 hours. For the last 5 hours of this stimulation, cells were dosed with HSP70 inhibitors, Ym1 and Myr (Jinwal et al., 2009; Koren et al., 2010; Wadhwa et al., 2000). LPS-stimulated macrophages not exposed to drug were protected from lysosome damage, and macrophages stimulated with LPS for 5 hours in the presence of either HSP70 inhibitor showed higher lysosome damage than did LPS-stimulated cells without drug (Fig. 4.1B 5hrs). The HSP70 inhibitor Ym1 reversed LPS-induced renitence (Fig. 4.1B 18 hrs). These data indicate that HSP70 may function as a mediator of LPS-induced lysosome renitence, perhaps by interacting with lysosomal membrane components.

4.4.2 The role of acid sphingomyelinase in lysosome renitence

Recent data has shown that HSP70 mediates lysosome protection in fibroblasts by activating ASM activity in fibroblast lysosomes. The ASM inhibitor, desipramine, reversed HSP70-mediated lysosome protection in fibroblasts (Kirkegaard et al., 2010). To determine the role of ASM in induced lysosome renitence, Fdx-loaded BMM were pre-incubated with desipramine for 1 or 3 hours then fed SMS with or without desipramine in the medium before measuring lysosome damage. While LPS activation reduced lysosome damage, desipramine-treated BMM did not show increased lysosome damage either in naïve or LPS-activated cells (Fig. 4.2). Interestingly desipramine-dosed BMM not fed SMS had higher lysosome damage compared to control BMM not fed SMS. These data suggest that ASM inhibition does not impact lysosomal stability in

macrophages, indicating that lysosome stability may be regulated differently than in fibroblasts.

4.4.3 Macrophages repair minor phagolysosome damage

Mammalian cells possess the ability to repair damaged plasma membranes (Idone et al., 2008; McNeil and Steinhardt, 2003). Thus we sought to extend these results to the repair of the lysosomal membranes. Fdx-loaded macrophages were fed SMS for ten minutes, then mounted on a microscope for time-lapse imaging. Images were acquired every five minutes for one hour. A variety of outcomes were observed in these phagolysosomes, from no damage (Fig. 4.3A, Cii and D) to high levels of Fdx release (Fig. 4.3B, Ciii and G). Some SMS phagosomes progressed through phagocytosis, phagosome fusion with an acidic lysosome, followed by a damage event which resulted in neutralization of the phagolysosome without Fdx release (Fig. 4.3E, F, H and I). A population of these neutral phagolysosomes was observed to proceed to full release of Fdx (Fig. 4.3B & Ciii) while another group of phagosomes was observed to re-acidify without lysosomal Fdx release (Fig. 4.3A & Ci). This re-acidification suggests that these phagolysosomes repaired the minor damage allowing the vacuolar ATPase to acidify the lysosomal lumen. Roughly equal numbers of phagosomes re-acidified as proceeded to lysosome release (Fig. 4.4) suggesting that lysosome repair occurs in a significant fraction of damaged phagolysosomes.

It should be noted that dilution of Fdx upon phagolysosome fusion was ruled out in the case of repair type phagosomes since only phagolysosomes which containing Fdx in an acidic environment for at least one frame prior to neutralization were considered strong evidence for repair (such as Fig. 4.3 A,C,D & E phagosome i). Neutralized

phagosomes without a preceeding frame depicting an acidic phagolysosome were also acquired (Fig. 4.3A 20 min. upper right of image and Fig. 4.4) but were not considered definitive data depicting phagolysosome repair.

4.4.4 Lysosomal calcium chelation potentiates SMS lysosome damage

The repair of plasma membranes is initiated by the influx of extracellular Ca^{2+} into the low calcium cytosol, through patching of the plasma membrane damage by intracellular membrane stores (Idone et al., 2008; McNeil and Steinhardt, 2003). As lysosomes contain high concentrations of calcium (Ca^{2+}) (Christensen et al., 2002), we hypothesized that release of lysosomal Ca^{2+} could trigger a lysosome repair mechanism analogous to that which repairs plasma membrane. BMM lysosomes were loaded with Fdx and the cells were incubated for one hour in buffer containing high or low Ca^{2+} concentrations. BMM were then fed SMS and imaged an hour later in the same buffer. BMM maintained in 2 mM Ca^{2+} showed moderate levels of lysosome damage following phagocytosis of SMS (Fig. 4.5, Solid-dark bars). Cells in buffer without added Ca^{2+} showed slightly higher levels of lysosome damage than did cells in Ca^{2+}-containing buffer (Fig. 4.5), BMM in Ca^{2+}-free buffer with the calcium chelator BAPTA showed greater damage (Fig. 4.5, hatched bars). Thus chelation of Ca^{2+} in BMM lysosomes increased lysosome damage, consistent with a Ca^{2+}-dependent repair mechanism. To test the specificity of this Ca^{2+} requirement, BMM were also assayed in buffer containing EGTA, a Ca^{2+} chelator which efficiently binds Ca^{2+} at neutral pH but only binds Ca^{2+} weakly at the low pH of lysosomes (Fig. 4.5, solid gray bars, EGTA). BMM in EGTA buffer had lysosome damage equivalent to that induced in Ca^{2+}-free buffer consistent with a role for lysosomal calcium in damage repair.

4.4.5 A role for autophagy in lysosome renitence

The components of this damage repair system remain unknown. The process of autophagy is an attractive possible mechanism for lysosome repair, as autophagy is known to sequester damaged mitochondria. We tested the role of autophagy in lysosome repair using BMM from mice expressing GFP-Lc3 as a transgene chimera (Mizushima and Kuma, 2008). The Lc3 protein is an important component of autophagy, as it is covalently attached to phosphatidylethanolamine and is inserted transiently into membranes of autophagosomes (Mehrpour et al., 2010). Thus, GFP-Lc3 can be used to localize autophagic membranes in living cells. BMM were fed uncoated or amine-coated SMS. Fdx-loaded BMM fed uncoated, acid-washed, SMS (AW) showed high levels of lysosome damage, while those fed amine-coated SMS (AC) showed very low levels of lysosome damage (Fig. 4.6A). GFP-Lc3 transgenic BMM fed AW SMS showed high levels of GFP-Lc3 recruited to a subset of phagolysosomes, while cells fed AC SMS failed to recruit high levels of GFP-Lc3 (Fig. 4.6 B & C). While the majority of cells fed either particle showed low levels of recruitment, a subset of cells of fed AW SMS showed high levels of GFP-Lc3 recruitment, no cells fed AC SMS showed such high levels of recruitment (Fig. 4.6D&E). This difference in recruitment led to significant differences in the mean intensity of GFP-Lc3 on SMS phagosomes (Fig. 4.6F) and in the percentage of SMS containing phagosomes showing high levels of recruitment (Fig. 4.6G). Thus SMS which damage lysosomes also induce the localization of GFP-Lc3, consistent with a mechanism in which autophagy contributes to lysosome repair.

4.5 Discussion

These studies examined possible mechanisms for induced lysosome renitence. Inhibition of ASM (Fig. 4.2) did not increase lysosome damage after phagocytosis. Chelating lysosomal calcium increased lysosome damage (Fig. 4.5). A marker of autophagy (GFP-Lc3) localized to phagolysosomes containing lysosome-damaging SMS but not to inert SMS (Fig. 4.6). Time-lapse microscopy provided evidence of a rapid repair mechanism operating inside macrophages (Fig. 4.3 &4.4). The role of lysosome repair in inducible lysosome renitence remains an intriguing possibility meriting further study.

One mechanism by which lysosomes become resistant to damage is through ASM (Holopainen et al., 1998). Recently, ASM was shown to be activated by endocytosed HSP70, which protected fibroblast lysosomes (Kirkegaard et al., 2010). Our observation that HSP70 protected BMM from lysosome damage (Fig. 4.1), suggested that macrophage activation may increase ASM activity, either through HSP70 or by other means, and that increased ASM activity would increase lysosome renitence. However, pharmacological inhibition of ASM did not increase phagolysosome damage; but rather it decreased lysosome damage after phagocytosis (Fig. 4.2). These data indicate a second role for ASM or its product ceramide. Increased ceramide levels reduce the release of TNF-α from LPS-stimulated macrophages (Jozefowski et al., 2010; Rozenova et al., 2010), suggesting that ceramide may be involved in macrophage differentiation. Thus, the decrease in SMS-mediated lysosome damage observed following ASM inhibition (Fig. 4.2) may be due to altered activation signals as opposed to biophysical changes in membrane properties. ASM inhibition did increase lysosome damage in cells not fed

SMS (Fig.4.2), perhaps indicating that there may be a weakening of resting lysosome membrane integrity.

HSP70 may contribute to lysosome renitence, especially if activation of BMM increases HSP70 expression. Cytosolic HSP70 may act on the cytosolic face of lysosomal membranes. Alternatively, HSP70 could be secreted from activated macrophages leading to endocytic re-uptake and trafficking to the lysosomes. A third possibility is that HSP70 is sequestered from cytoplasm into autophagosomes and trafficked into lysosomes. Secreted HSP70 may also protect cells surrounding the BMM, via endocytosis and delivery into lysosomes. The expression or secretion of HSP70 by activated and naïve BMM is an interesting topic for further study.

Time-lapse imaging studies illustrated re-acidification of neutralized phagolysosomes in SMS-fed BMM, indicating that macrophages can rapidly re-seal damaged lysosomes (Figs. 4.3 & 4.4). Plasma membrane damage is repaired by a patching mechanism regulated by extracellular calcium, which enters cytoplasm through the damaged membrane. This increased cytosolic calcium binds to synaptotagmin VII, which activates V-SNARE-mediated vesicle fusion with the damaged membrane (Idone et al., 2008; McNeil and Steinhardt, 2003). As lysosomes have higher calcium concentrations than the cytosol, calcium released from damaged lysosomes may induce a repair program similar to that which repairs plasma membrane. Chelation of lysosomal calcium increased SMS-mediated lysosome damage, suggesting the existence of a calcium-dependent lysosome repair pathway. These data suggest that synaptotagmin VII and V-SNARES may be interesting targets for future study. Also, the regulation of these components by macrophage activation may affect their roles in inducible lysosome

renitence. Other calcium sensors, such as classical protein kinases C or calmodulin, may also play a role in lysosome damage repair and merit future consideration.

We also obtained evidence that autophagy contributes to lysosome repair. Autophagy is the process by which cells sequester their damaged organelles or bulk cytosol into endomembranes, creating a double membrane structure with the damaged organelle or cytosol inside. Fusion of these structures with lysosomes recycles damaged organelles and proteins. We found that the marker for autophagosome formation, GFP-Lc3, localized selectively to some phagolysosomes containing a type of SMS which induced high levels of lysosome damage (Fig. 4.6). Although GFP-Lc3 localized to phagosomes infrequently (Fig. 4.6G), that may be due to the assay conditions. Whereas the lysosome damage assay reports any lysosome release that takes place after the Fdx is loaded into the cells, GFP-Lc3 localization shows only the Lc3 localizing at the time examined. If lysosome damage repair is transient then GFP-Lc3 localization should be transient, as well. Thus, at any one time only a fraction of cells may be actively repairing organelles, even in situations where high lysosome damage is observed. Further, experiments are required to confirm that GFP-Lc3 is indeed localized to the damaged phagosomes, to determine the timing of localization relative to damage and the role of macrophage activation in the regulation of autophagic repair of lysosomes. Activation of macrophages has been shown to result in increased autophagy (Xu et al., 2007) suggesting that autophagy-mediated repair may be increased by activation as well. Inhibition of autophagy with gene deletion, siRNA, or small molecule inhibitors would be predicted to reverse the induction of lysosome renitence and result in increased lysosome damage following SMS challenge.

Occasionally one particle (SMS or *L.m.*) was sufficient to trigger complete lysosome release. These rare cases may be intact lysosomes fusing with damaged lysosomes and spilling even more lysosomal contents into the cytosol. Plasma membrane repair mechanisms use lysosome membrane exocytosis to repair plasma membrane damage. In the case of lysosome repair, other lysosomes recruited to repair damaged lysosomes may result in additional lysosome content release. Alternatively cells may repair lysosomes using an autophagy-like pathway, in which the damaged organelle, including the SMS, is bound into a autophagosome, which fuses with a lysosome which the SMS may damage anew. Thus, lysosome repair mechanisms have the potential to modulate lysosome damage levels in interesting ways which merit future exploration.

Figure 4.1

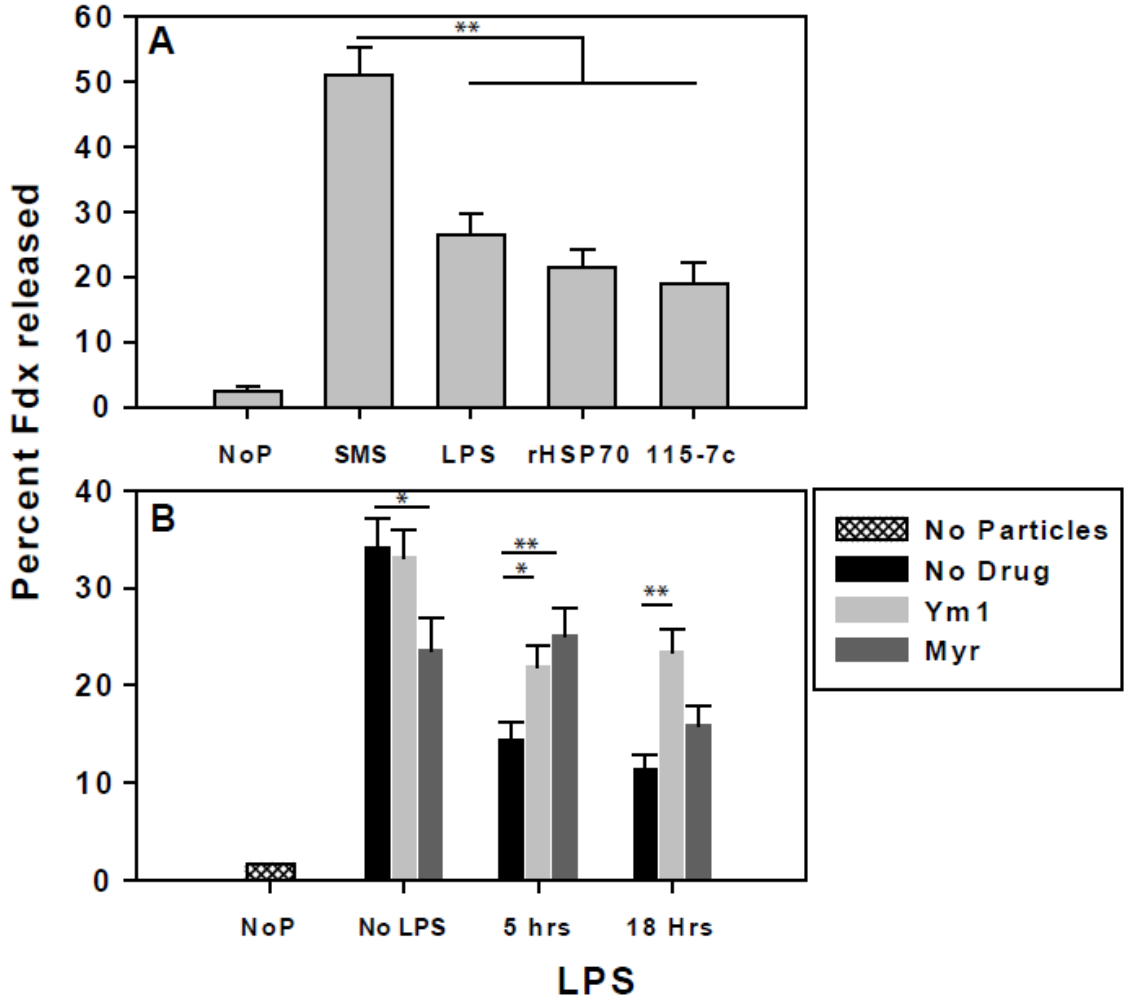

Figure 4.1. HSP70 protects SMS phagolysosomes. Fdx was loaded into BMM lysosomes as described (Davis and Swanson, 2010). A) Loaded BMM were exposed to 100ng/mL LPS, 300 nM recombinant HSP70 or 100 µM HSP70 activator 115-7c for 5 hours each. Cells were rinsed and fed SMS for one hour then imaged for lysosome release as in (Davis and Swanson, 2010). B) BMM were exposed to LPS for 5 or 18 hours or left untreated. Ym1 (20 µM) or Myr (25 µM) were included for the last 5 hours of stimulation. Bars are population averages (± SEM) of BMM. * $p<0.05$, ** $p<0.001$

Figure 4.2

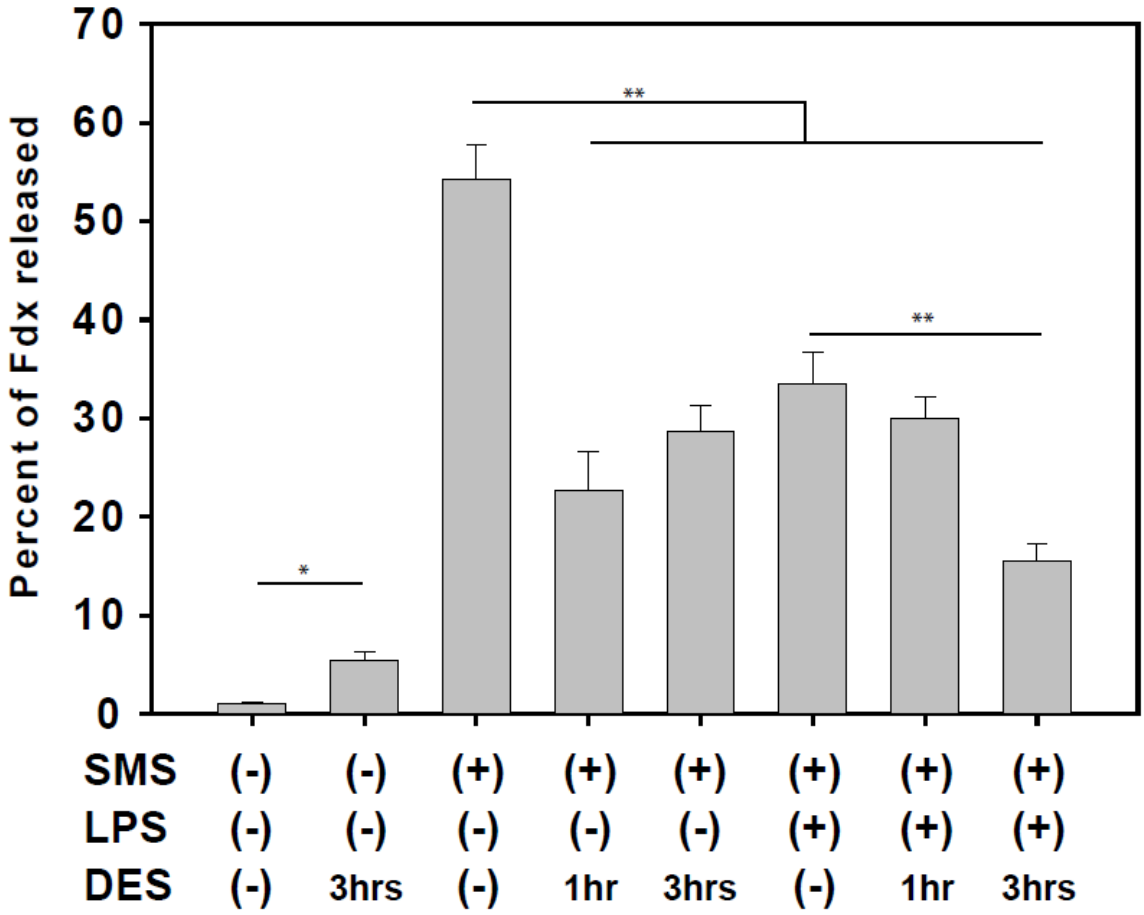

Figure 4.2. Inhibition of acid sphingomyelinase does not potentiate SMS-mediated lysosome damage. BMM lysosomes were loaded with Fdx and chased as described (Davis and Swanson, 2010). Where indicated, 100 ng/mL LPS was included in the loading and chase medium. BMM were pre-incubated in 12.5 μM desipramine (DES) for one or three hours before SMS addition (also in the presence of DES). One hour after SMS addition, cells were analyzed for Fdx release into cytoplasm. Bars are population averages (± SEM) of BMM containing 1-3 SMS per cell of at least 100 cells per condition. * $p<0.05$, ** $p<0.001$

Figure 4.3. Phagolysosome damage can be repaired in BMM. BMM lysosomes were loaded with Fdx by endocytosis. Cells were fed SMS for ten minutes then rinsed, and time-lapse images were acquired every five minutes. A) Selected pH maps, phase-contrast, and Fdx fluorescent images showing phagolysosome repair (phagosomes i.1 and 1.2) and never show any lysosomes damage (phagosome ii). In phagosome i, phagosome-lysosome fusion was evident at 30 min., neutralization occurred at 40 min. followed by re-acidification at 45 min. B) Selected images from a cell with a SMS phagosome which proceeds from neutralization (35 min.) to full release (40 min.). C) Enlarged pH maps of phagosomes i,ii and iii from the cells in A) and B), at all time points imaged. D) and G) show the percent lysosome release calculated from regions of interest drawn around the cells and phagosomes in A) and B) respectively. E) and H) show the mean pH calculated from regions of interest drawn around the cells and phagosomes in A) and B) respectively. F) and I) show the mean fluorescence intensity in the 440nm channel calculated from regions of interest drawn around the cells and phagosomes in A) and B) respectively.

Figure 4.3

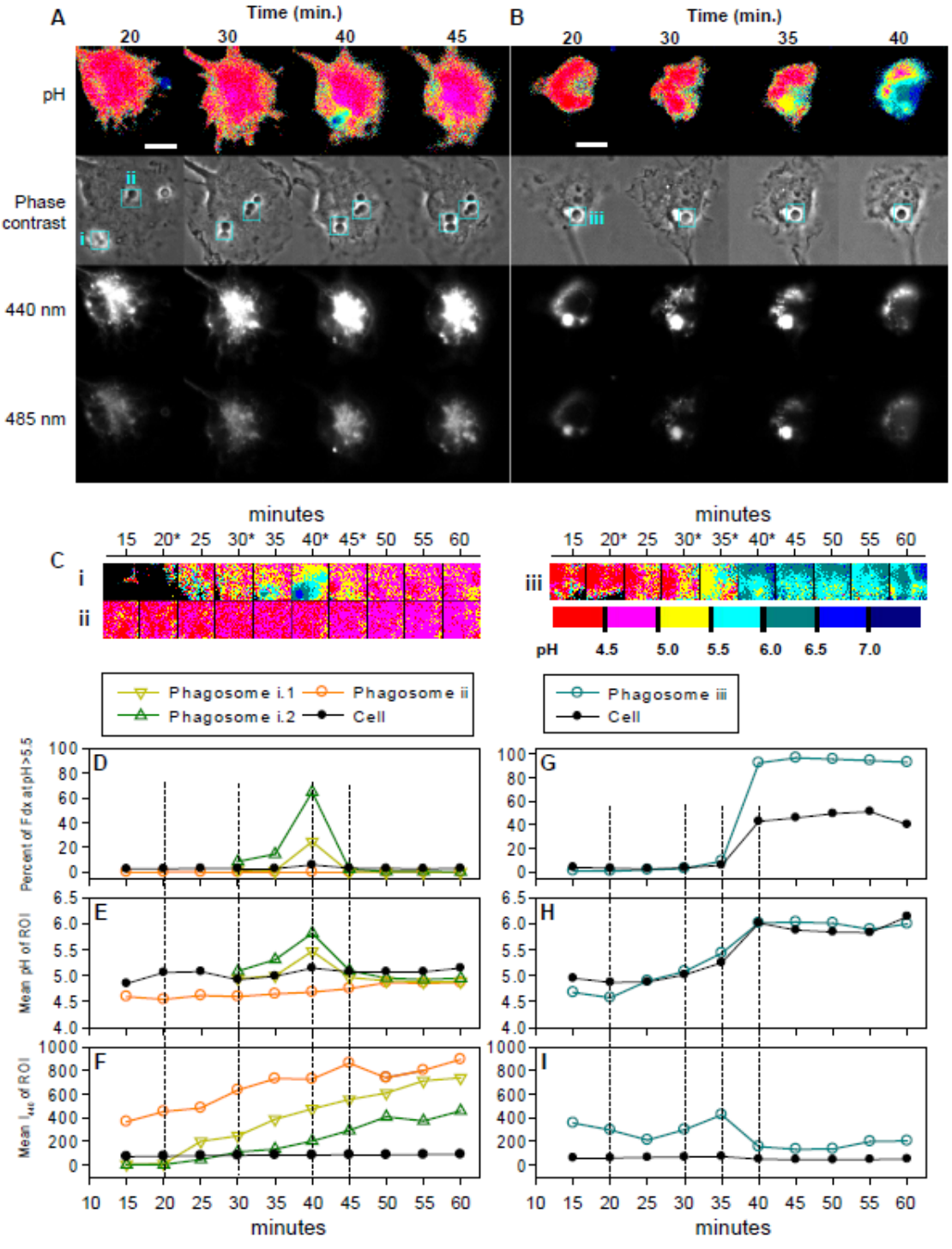
A
Time (min.)
20
30
40
45
B
Time (min.)
20
30
35
40
pH
Phase contrast
440 nm
485 nm
i
ii
iii
C
minutes
15 20* 25 30* 35 40* 45* 50 55 60
pH 4.5 5.0 5.5 6.0 6.5 7.0
Phagosome i.1
Phagosome ii
Phagosome i.2
Cell
Phagosome iii
Cell
D
E
F
G
H
I
Percent of F dx at pH>5.5
Mean pH of ROI
Mean I440 of ROI
10 15 20 25 30 35 40 45 50 55 60
minutes

Figure 4.4

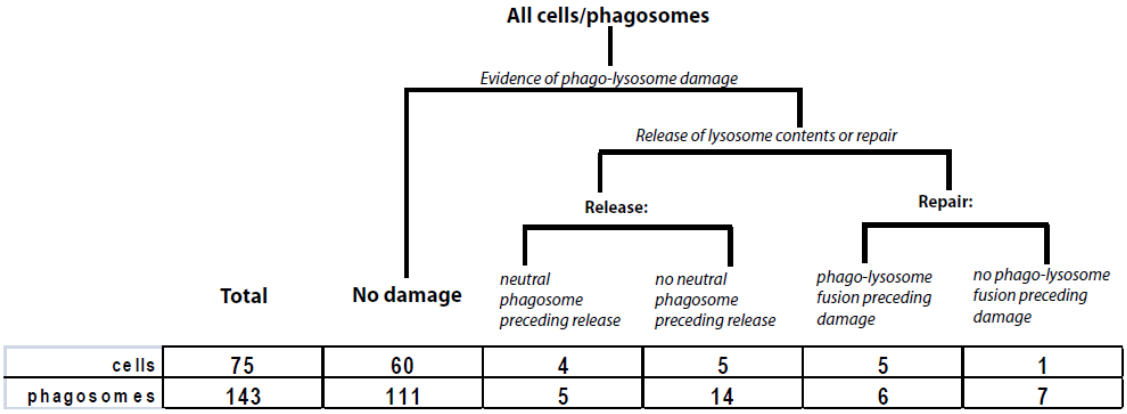

	Total	No damage	neutral phagosome preceding release	no neutral phagosome preceding release	phago-lysosome fusion preceding damage	no phago-lysosome fusion preceding damage
cells	75	60	4	5	5	1
phagosomes	143	111	5	14	6	7

Figure 4.4. Lysosome release and phagolysosome repair are potential outcomes of damage. Combined data from time-lapse imaging studies described in figure 4. Data represent 18 movies collected over 3 days. Examples of repair and release were observed all three days. Data are broken down based on the number of cells (top row) or phagosomes (bottom row) which displayed phagosomal pH profiles consistent with no damage, release or repair. Phagosomes with "no damage" were those which never displayed any neutral Fdx at any time point (phagosomes ii from figure 4 is an example of this type of event). Release was characterized as cells with greater than 10% released Fdx after the 60 minute image. These events were distinguished as those where a neutral phagosome was obvious a frame before lysosome release was detectable (phagosomes iii from figure 4) and those where there was no observed neutral phagosome. Repaired phagosomes were those in which a neutral phagosome later acidified. These events were broken down into those where this neutralization was preceded by phagosome-lysosome fusion (phagosomes i from figure 4) or where there was not phagosome-lysosome fusion preceding phagosome neutralization. Phagosome-lysosome fusion was indicated by acidic Fdx surrounding the SMS particle.

Figure 4.5

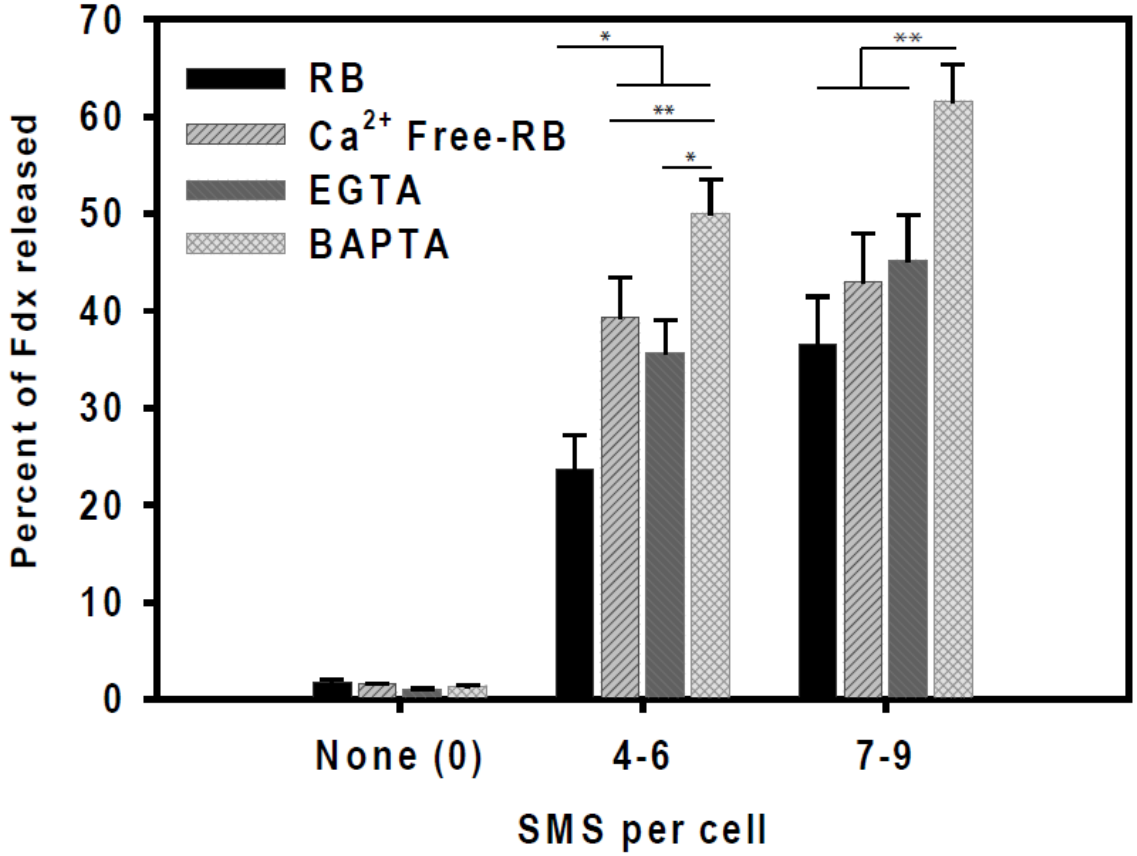

Figure 4.5. Chelation of lysosomal calcium increases SMS phagolysosome damage. BMM lysosomes were loaded with Fdx as described (Davis and Swanson, 2010). BMM chase medium was then exchanged for Ringer's buffer, Ca^{2+}-free Ringer's buffer, Ca^{2+}-free Ringer's buffer with 10 mM EGTA, or Ca^{2+}-free Ringer's buffer with 3 mM BAPTA. SMS were then fed to the BMM in these same buffers and one hour later cells were imaged. SMS were counted and lysosome damage measured. Bars are population averages ± SEMs of BMM containing the indicated SMS per cells. * $p<0.05$, ** $p<0.001$

Figure 4.6

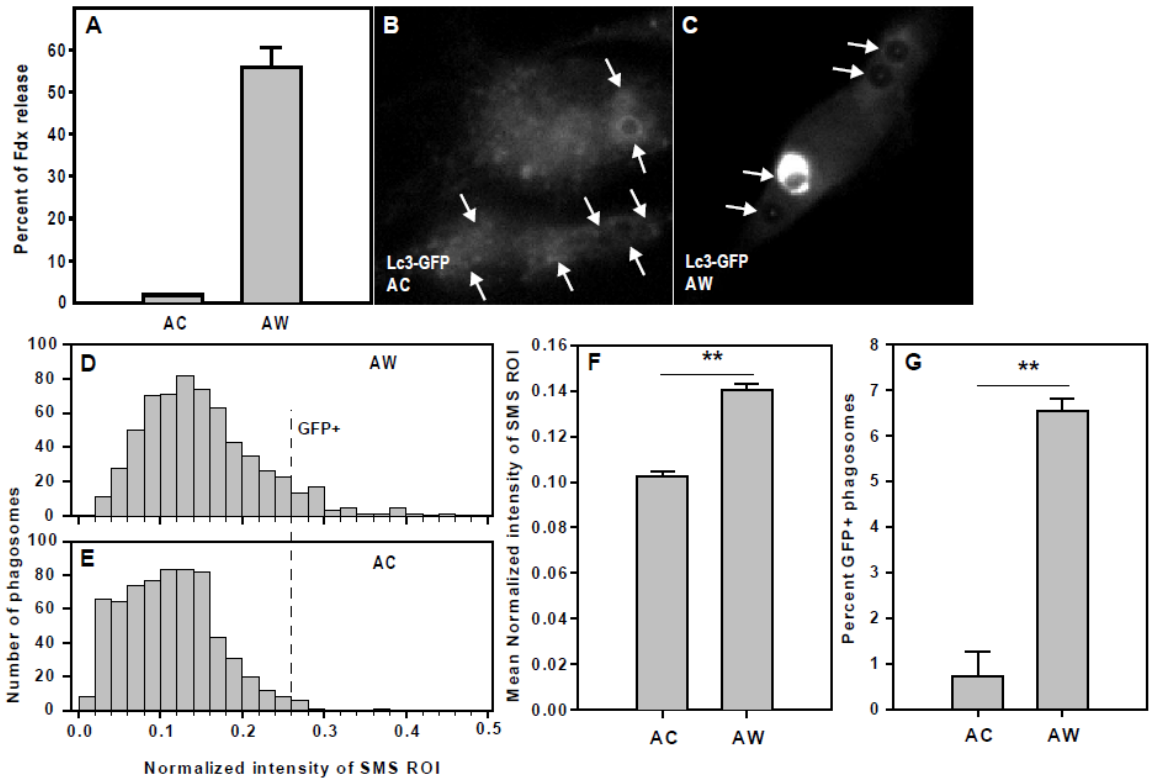

Figure 4.6. Lc3-GFP is recruited to damaging but not inert SMS suggesting autophagic involvement in lysosome repair. For A), BMM were preloaded with Fdx and chased in fresh medium for 3 hours. Macrophages were then fed amine coated (AC) or uncoated acid-washed (AW) SMS. After 1 hour cells were imaged and lysosome damage calculated for cells containing 1-3 SMS. Bars are average lysosome release for n<50 cells and error bars indicate SEM. B-G) BMM from GFP-Lc3 transgenic mice were fed AC or AW SMS and imaged 30 minutes later. Sample GFP fluorescence images of Lc3-GFP BMM fed AC (B) or AW (C) SMS. Recruitment of GFP-Lc3 was calculated for each imaged SMS phagosome as the fraction of total GFP-Lc3 signal which was in a region of interest drawn surrounding the phagosomes. D&E) Histograms with normalized GFP-Lc3 intensity on the horizontal axis and phagosome count on the vertical axis. D) Data from cells fed un-coated SMS (AW). E) Data from amine-coated SMS (AC). F) Average GFP intensity for all recorded phagosomes. G) The percent of phagosomes with GFP-Lc3 recruitment above a threshold level indicated by dashed line in D&E). ** $p<0.001$

Chapter 5
Discussion

5.1 Summary of findings

A novel technique was developed to explore lysosome damage following phagocytosis in macrophages. Macrophage endosomes were pulse-loaded with fluorescein-dextran (Fdx), which was then chased into lysosomes. Live-cell, epi-fluorescence ratiometric microscopy was used to measure the distribution and pH of Fdx simultaneously. The pH measurements were used to distinguish Fdx contained in acidic lysosomes from that released into neutral cytosol. The percent of Fdx released into cytosol could be calculated as a quantitative measure of lysosome damage.

This technique has several advantages over previous methods which only detect lysosome damage by dye redistribution. In all of the previous methods, dye redistribution indicates the transition from intact lysosomes to a diffuse signal after release into the cytosol. By using Fdx, fluorescence from dye which remains in intact lysosomes indicated the acidic lumen of lysosomes, while Fdx released from lysosomes reported the neutral pH of the cytosol. This method has three main advantages over the previous techniques: (1) sensitivity in the detection of low levels of lysosome release, (2)

a method for classifying dye as inside of or outside of lysosomes, and (3) quantification which derives from combining the previous two factors.

The increased sensitivity of this system is due to the large increase in 485nm excitation efficiency of fluorescein at neutral pH, compared to the relatively inefficient 485nm excitation obtained at acidic pH. Upon release of Fdx from the acidic lysosome to the neutral cytosol, the 485 nm signal from each Fdx molecule increases. The signal from Fdx can be processed into quantitative data using pH calibration. This increased signal sensitivity is a significant improvement in the detection of low levels of Fdx release compared to other fluorescent molecules, such as that used in (Hornung et al., 2008). As Fdx fluorescence in the 440nm channel is less sensitive to pH this channel illustrates dye redistribution without any additional sensitivity; observing just this channel is similar to previous dye redistribution methods. The pH-dependent spectral shift of fluorescein increases the per-Fdx-molecule 485nm fluorescence at the higher pH of cytoplasm. Figure 2.2D illustrates this difference in signals. This cell has significant lysosome damage, displayed in the pH and 485 nm images, but cytoplasmic Fdx cannot be observed in the pH insensitive 440 nm channel. As other techniques for detecting lysosome damage lack this sensitivity boost most of the lysosome damage reported in other works probably only represents the highest levels of damage. Thus the role of lower levels of damage and the amounts of damage necessary for the induction of downstream signals are unknown.

Quantization of lysosome damage allowed various aspects of populations to be compared. While macrophages fed certain damaging particles such as ground silica showed high average levels of lysosome damage, individual cells showed lysosome

damage from the entire spectrum of possible lysosome damage states: from no damage, despite high levels of internalized ground silica, to complete release of all loaded Fdx. While lysosome damage and inflammasome activation were correlated at the population level (Chapter 2), lysosome damage and inflammasome activation could not be monitored in the same cells. Thus, the dynamics of lysosome damage which subsequently lead to downstream signaling have not yet been demonstrated. It is unknown if a threshold level of lysosome damage exists which triggers inflammasome activation. The level of inflammasome activation necessary to induce cell death is also unknown. Figures 2.4 and 2.5 show that macrophages fed low doses of ground silica had some cells with higher lysosome damage, low FLICA activation and IL-1β secretion, whereas polystyrene beads failed to induce lysosome damage higher than 10%, elicited-no FLICA signal and no IL-1β release. Using 10% Fdx release as a threshold and a similarly set threshold for FLICA signal yielded similar percentages of cells positive for both lysosome damage, caspase-1 activation and cell death in all the various conditions tested. This suggests that greater than 10% lysosomal content release in LPS-stimulated macrophages commits the cells to inflammasome activation and cell death. This hypothesis could be tested in cells simultaneously stained for lysosome damage and caspase-1 activation. These experiments may also show the fate of cells with sub-threshold levels of lysosome damage which have been hypothesized to undergo other types of programmed cell death (Boya and Kroemer, 2008).

Sensitive detection of lysosome damage in individual cells allowed a more careful examination of the types of particles which induce lysosome damage after phagocytosis. The average level of lysosome damage following phagocytosis was found to depend on

the type of particle phagocytosed. The particle coating was especially important, as silica microspheres coated with various materials induced different levels of lysosome damage; hence lysosome damage is not a common outcome of phagocytosis but is instead triggered by chemistries present on only some phagocytic targets.

While the vast majority of resting macrophages which had not been fed particles showed background levels of lysosome damage, a few cells showed higher levels of lysosome damage. Background levels of lysosome damage were typically low but were mostly non-zero, indicating that some level of lysosome damage exists in otherwise healthy cell populations, and higher lysosome damage in a sub-population of cells. This could explain how endocytosed material can access cytoplasm leading to the cross-presentation of exogenous antigens on MHC class I molecules. In all cases this background was low enough to allow comparisons with experimental conditions.

Figures 2.2 and 2.3 showed that some particles mediated at least some lysosome damage. These data provide a potential mechanism for the phenomena of particle phagocytosis increasing the efficiency of exogenous antigen cross-pressentation on class I MHC (Harding and Song, 1994; Kovacsovics-Bankowski et al., 1993; Oh et al., 1997; Reis e Sousa and Germain, 1995). One prediction is that induced lysosome renitence would decrease the access of exogenous antigens to host cytosol and perhaps decrease the efficiency of presentation of these exogenous antigens on MHC class I. This effect may be confused by other consequences of macrophage activation such as increased efficiency of antigen processing and MHC protein up-regulation.

Lysosome renitence was examined more thoroughly in chapter 3. Treatment of macrophages with LPS, peptidoglycan, interferon-γ and tumor necrosis factor-α (TNF- α)

reduced subsequent lysosome damage induced by particle phagocytosis. Stimulation with these molecules resulted in protection from lysosome damage induced by a wide variety of agents. Induced lysosome renitence reduced the escape of *Listeria monocytogenes* (*L.m.*) from macrophage endosomes and reduced lysosome damage induced by *L.m.* infection, indicating that inducible lysosome renitence is a novel activity utilized by activated macrophages to resist infection by intracellular pathogens. While lysosome damage resistance has been shown in other contexts (Kirkegaard et al., 2010; Persson and Vainikka, 2010), this is the first description of lysosome renitence as an activity that can inhibit infection. Kirkegaard (2010) showed that exogenous HSP70 could protect fibroblast lysosomes from damage by activating acid sphingomyelinase. In our studies, macrophage lysosomes were protected by HSP70 but inhibition of acid sphingomyelinase in macrophages did not inhibit lysosome renitence (chapter 4), suggesting that acid sphingomyelinase does not function in macrophages as it does in fibroblasts. Alternatively, the acid sphingomyelinase inhibitor may alter membrane trafficking, or another process involved in lysosome damage, which may function differently in macrophages and fibroblasts.

TNF-α may exert different effects on lysosomes in different cell types. While TNF-α induces lysosome damage and cell death in some cell types, it is protective in a Fe-ROS-mediated lysosome damage system in macrophages (Persson and Vainikka, 2010) as well as in our system. In Persson (2010), this protection was mainly mediated by increasing the cellular defenses against ROS, specifically increasing levels of anti-oxidants and endogenous iron chelators. The protective roles for TNF-α and

sphingomyelinase may be linked, as sphingomyelin is involved in the release of TNF-α in some cells (Jozefowski et al., 2010; Rozenova et al., 2010).

Lysosome damage measured during *Listeria monocytogenes* (*L.m.*) infection (Fig. 3.4) was unexpected, as previous work had shown that *L.m.* escape from vacuoles before they fully fuse with lysosomes (Henry et al., 2006). The observed lysosome damage may have resulted from the small fraction of bacteria which did escape from the lysosomes. Alternatively, *L.m.*-induced lysosome damage could have been caused by listeriolysin O (LLO) secreted from the *L.m.* which were trafficked into lysosomes but unable to escape. LLO secreted while bacteria reside in early endosomes may go to lysosomes via vesicular trafficking. Alternatively, Fdx release may have resulted from intact lysosomes fusing with vacuoles already damaged during *L.m.* escape. In all cases, lysosome damage was dependent on LLO (chapter 3 figure 4). Lysosome damage following *L.m.* may also be induced by secondary signaling events which only occur after *Listeria* escape, such as those which eventually lead to cell death. Certain apoptotic stimuli can induce lysosome damage. Thus the role of the Bcl-2 family members and mitochondrial integrity in *Listeria*-induced lysosome damage may be interesting to investigate in the future.

Reactive oxygen species (ROS) can have a mixed role in lysosome integrity depending on the particle and circumstances. ROS inhibitors and anti-oxidants reduced silica-induced lysosome damage (chapter 3), indicating that ROS contributed to that damage. As the *nox2* phagosomal oxidase was excluded as a source of ROS causing silica-mediated lysosome damage, perhaps ROS from mitochondria induce lysosome damage. Thus, the localization of mitochondria, especially damaged mitochondria, may be an important determinant for lysosome damage. Although the phagosomal oxidase

inhibited *L.m.* escape, (chapter 4) and shown previously (Myers et al., 2003), it had no impact on silica-mediated lysosome damage (chapter 3) reinforcing that the role of ROS is context or perhaps location-dependent.

Chapter 4 provided evidence of a phagolysosome damage-repair system. Time-lapse images showed that some phagosomes undergo temporary neutralization following phagosome-lysosome fusion. Some of these phagosomes went on to show release of Fdx from lysosomes. Others re-acidified, implying that the membrane damage which allowed the pH to equilibrate with cytoplasm was repaired. While repair of plasma membrane has been previously described (Idone et al., 2008; McNeil and Steinhardt, 2003), this is the first report of the repair of an intracellular membrane. Plasma membrane repair requires calcium (Idone et al., 2008; McNeil and Steinhardt, 2003). Similarly, chelation of lysosomal calcium increased silica particle-mediated lysosome damage, suggesting that the mechanisms of plasma membrane repair may be involved in repairing lysosomes. Repair of damaged lysosomes could involve autophagy, which envelopes damaged organelles in membranes and delivers them to lysosomes for degradation. We observed autophagy markers recruited to phagolysosomes containing membrane-damaging particles, but not to those containing non-damaging particles (Chapter 4). The complete process of autophagy may be induced by damaged lysosomes, alternatively autophagy proteins may be involved in a repair response to lysosome damage. Autophagy proteins have been implicated in membrane binding and fusion (Mehrpour et al., 2010). That could explain why autophagy-related proteins were recruited to some phagosomes independent of full autophagy (Sanjuan et al., 2007). Full repair of damaged lysosomes still containing the damaging stimulus may re-initiate membrane damage and ultimately

lead to increased levels of lysosome release. The role of calcium and autophagy in phagolysosome repair has yet to be fully resolved and would be an interesting topic of further research.

Other mechanisms responsible for lysosome renitence may exist. Regulated changes of membrane composition could stabilize membranes and reduce lysosome damage upon challenge. Kirkegaard (2010) suggested that HSP70 mediated protection was mediated by the activation of lysosomal sphingomyelinase which converts sphingomyelin to ceramide. Thus, increases in ceramide or reductions in sphingomyelin in the luminal face of the lysosomal membrane may stabilize the compartment. Accumulation of sphingosine is known to damage lysosomes (Kagedal et al., 2001a; Kagedal et al., 2001b; Werneburg et al., 2002) so reduction of lysosomal sphingosine may improve lysosomal stability. Lipid rafts are membrane sub-domains of increased rigidity, composed of high concentrations of sphingolipids and cholesterol. Thus membrane rigidity may be involved in the sphingolipid effect on lysosomal membrane stability. Indeed, depletion of cholesterol can decrease lysosome stability (Hao et al., 2008). Other changes in membrane lipid content may also regulate lysosome stability as lysophosphatidycholine, a phospholipid produced in some phospholipase reactions, can also reduce lysosomal membrane stability (Hu et al., 2007). Future research into the regulation of these species during macrophage activation may illuminate the role of membrane composition in induced lysosome renitence.

Lysosome renitence may also have important implications for lysosome storage disorders. The widespread activation of macrophages and macrophage-like cells present in many lysosome storage disorders may induce renitence and account for the relative

absence of lysosome damage in these patients. However, lysosome damage has been reported for Niemann-Pick patients and mouse models of the disease (Kirkegaard et al., 2010). HSP70, shown in chapter 4 to be important for lysosome renitence, is thought to induce lysosome protection by activating acid sphingomyelinase. Thus patients with Niemann-Pick, which have mutations in acid sphingomyelinase, may be unable to fully activate lysosome renitence. Alternatively, lysosome renitence may not get activated in Niemann-Pick due to a lack of inflammatory mediator secretion. Niemann-Pick alveolar macrophages did not have elevated TNF-α levels compared to normal cells and cells from other lysosome storage disorder models (Dhami et al., 2001).

Our studies suggest a model of phagolysosome damage progression (Summarized in figure 5.1). Initially, a phagocytosed particle is trafficked through the various endosomes until its phagosome fuses with lysosomes. Some aspect of the particle's chemistry damages the lysosomal membrane. In the case of silica this damage is mediated by phagosomal oxidase-independent ROS. *L.m.* induces lysosome damage through the action of the pore-forming toxin LLO. In the photo-damage model, lysosome damage is initiated by photo-oxidative damage due to the fluorophore Texas-red. Initial damage is typically minor and results in phagolysosome neutralization without substantial dye release. A fraction of these damaged lysosomes are repaired and re-acidify while others proceed into complete rupture. Activation of macrophages reduced lysosome damage in multiple models. The mechanism of this resistance is unknown, but could involve mechanisms that reduce the initial damage, enhance membrane repair or inhibit the transition from neutralized phagosomes to fully ruptured lysosomes.

5.2 Experimental limitations

5.2.1 Limitations with lysosome damage assay

Although ratiometric imaging of released Fdx provides an improvement over previous techniques, some experimental caveats remain. The image processing protocols which measure the percent of Fdx released harvests data from all regions where the pH of the Fdx containing compartments is above 5.5. Thus the protocol does not necessarily differentiate diffuse from compartmental staining, implying that conditions which neutralize but do not rupture lysosomes could produce an artificially high percentage of Fdx released. Therefore it is important to confirm that cells with neutral pixels also show diffuse staining typical of release. In practical terms this has not been a significant problem with this system, as normal healthy cells maintain an acidic lysosomal pH. Neutral pH pixels in intact lysosomes were only observed when lysosomotropic agents such as ammonium chloride were added at a sufficient concentration to raise the lysosomal pH.

Another limitation of ratiometric imaging on an epi-fluorescence microscope comes from fluorophores above or below the focal plane of the lysosomes. As lysosomes are maintained at a pH of about 4.75 and the cytosol is maintained at around neutral, pH 7.0, the Fdx signal should be near one of these two values. Instead, a range of pH is observed in cells due to the mixing of fluorescence from Fdx in intact lysosomes and the released Fdx above or below the lysosome. The nucleus is a good place to look for released Fdx, as there are relatively few lysosomes above or below the nucleus. In some cells, this may result in an undercounting of the released Fdx signal as the relatively bright lysosomes may overwhelm the signal from the diluted released Fdx. Moreover,

changes in cell shape may result in different amounts of averaging which may result in different regions showing pH greater than the pH 5.5 cut-off used for measuring lysosome release. This was taken into account by gathering data from cells of many different shapes for each data set.

The method could be improved. One way to possibly reduce the z-axis averaging would be to collect through-focus image stacks and perform 3-D reconstructions of the cells. This technique also has some limitations as Fdx is easily photo-bleached and the light used to image cells would have to be minimized which may reduce signal levels at each plane. Another drawback is that current 3-D reconstruction algorithms do not maintain quantitative values across multiple fluorescent channels. New computer algorithms would need to be developed to maintain proper pH ratios throughout de-convolution. Another possible improvement is based on the assumption above that all cellular Fdx is in compartments at pH 4.75 or pH 7.0. Spectral un-mixing algorithms could be designed to calculate the relative contributions from neutral (pH 7.0) and acidic (pH 4.75) compartments.

5.2.2 Membrane and endosomal trafficking

Another drawback to this method is that endosomal trafficking is required to load lysosomes. Measurements of lysosomal pH or damage in cells with trafficking defects may be difficult to interpret. Trafficking and membrane fusion may also be important for increasing lysosome damage by increasing lysosome fusion with phagosomes containing damaging particles. Intact lysosomes may also fuse with damaged compartments and result in increased lysosome release. This could also be reduced in situations of altered trafficking. Thus drugs and mutations which drastically alter intracellular trafficking may

have complicated and potentially counter-intuitive phenotypes in regards to lysosome damage and protection. This is an especially important consideration when interpreting data regarding sphingomyelinase inhibition such as that in Kirkegaard (2010) and chapter 4, figure 3, as membrane sphingomyelin and ceramide concentrations can alter membrane trafficking and fusion (Choudhury et al., 2004; Leventhal et al., 2001; Liscum, 2000).

5.3 Future experimental directions

Several interesting questions are prompted by the findings in this thesis. There are probably many other medically relevant particles and conditions which involve lysosome damage. As lysosome damage is known to activate the NLRP3 inflammasome (Halle et al., 2008; Hornung et al., 2008), molecules which activate the NLRP3 inflammasome may also damage lysosomes. A number of diseases and pathologies rely on NLRP3 signaling, including dextran sulfate sodium-induced colitis, which may depend on NLRP3 signaling (Bauer et al., 2010; Zaki et al., 2010).

Intracellular pathogens likely damage lysosomes. Intracellular bacteria such as *Franciscella, Salmonella, Mycobacteria* and other *Listeria* species could all be tested for lysosome damage during infection. While over-expression of some viral proteins such as HIV NEF (Laforge et al., 2007) can induce lysosome damage, it is not known if viral invasion damages lysosomes. Even if lysosome damage does not occur at low MOI, higher MOI infection or viruses that traffic to lysosomes could trigger lysosome damage. Lysosome damage resulting from infection may serve a trigger which overcomes immune evasion.

To screen a large variety of molecules for lysosome damage activity, this damage assay could be adapted into a high through-put, high-content imaging technique. Imaging

platforms exist which could be used for fast low magnification imaging in two fluorescent channels. Such methods could be used to identify other conditions and signals which induce lysosome renitence. One broad category of molecules which has not been tested for the induction of lysosome renitence are lipid immune mediators. Arachidonic acid derivatives are powerful immune modulators which may affect lysosome stability. The molecules identified so far which induce lysosome renitence are associated with classical activation of macrophages. Conditions which alternatively activate macrophages have not yet been explored for inducing lysosome renitence. Although interleukin-10 did not induce lysosome renitence, other cytokines which reduce or resolve inflammation remain to be tested. Resolution type signals are associated with the fibrotic diseases which result from exposure of lysosome damaging particles, such as silica, suggesting that resolution type signals may modify lysosome stability.

Common signaling intermediates may mediate lysosome renitence. The molecules which induce lysosome renitence are involved in classical activation in macrophages. TNF-α may itself be a common intermediate as it is induced in LPS (Carswell et al., 1975), PGN (Gupta et al., 1995) or IFN-γ- (Collart et al., 1986) stimulated macrophages. By blocking TNF-α using an antibody, or using TNF-α-deficient mutant mice, one could determine if TNF-α is an intermediate in lysosome renitence induced by other stimuli. Secreted HSP70 could be another common extracellular mediator of lysosome renitence. HSP70 released from activated macrophages could even induce lysosome renitence in cells which lack receptors for inflammatory immune molecules.

The mechanisms responsible for lysosome renitence and or repair could be explored. Common intracellular signaling proteins could be identified using siRNA or mutant mice. While lysosome repair and, perhaps, secreted HSP70 are important mediators of lysosome renitence, other mechanisms may be involved. Changes in membrane composition can affect membrane stability. Many systems implicated in lysosome damage in this work and others may alter membrane dynamics and composition. ROS species can form peroxide membrane phospholipids which can destabilize membrane. Sphingomyelin, ceramide and sphingosine can stabilize or damage membranes and have been implicated in HSP70-mediated lysosome stability (Kirkegaard et al., 2010).

In chapter 2 it was noted that, after one hour of exposure to ground silica, cells stimulated with LPS displayed lower levels of lysosome damage but much higher levels of cell death compared to unstimulated cells, which had high levels of lysosome damage and almost no cell death. Thus macrophage stimulation had profound effect on the trajectory of silica-mediated cell death. The details of this cell death phenotype have not been explored further. While it seems likely from other studies that unstimulated macrophages with high levels of lysosome damage would eventually die by apoptosis, this death has not been characterized for this system. One hypothesis is that macrophage activation acts as a switch which converts lysosome damage-mediated cell death from a slow non-inflammatory apoptotic type to a fast version of pyroptosis which results in the release of IL-1β and other inflammatory signals. This would be contrary to current beliefs where lysosome damage levels are assumed to be responsible for such a switch

from apoptosis to necrosis or pyroptosis (Boya and Kroemer, 2008). If TNF-α or IFN-γ mediate such a switch in cell death characteristics is also unknown.

5.4 Potential therapeutics suggested from this thesis

Further study of inducible lysosome renitence may result in new treatments for disease. Molecules which induce lysosome renitence could be used to combat infection by intracellular pathogens or to delay or reduce inflammation caused by particulates such as silica or asbestos. To be most useful, induction of lysosome renitence would have to be separated from the inflammation associated with the molecules identified here with classical macrophage activation. This strategy may be especially useful in immuno-suppressed individuals. The general prevention of inflammation by immune-suppression regimens may circumvent normal levels of lysosome renitence in these individuals, leading to increased susceptibility to intracellular infection. One common strategy for immuno-suppression is to use an antibody against TNF-α. This may directly reduce lysosome renitence which could be repaired using a specific inducer of lysosome renitence. While we have not tested for inflammatory induction, the HSP70 ATPase activator assayed in figure 4.1, 115-7c is a promising start to the identification of lysosome renitence activators.

Molecules which reduce lysosome renitence may also be useful. Such molecules would have to be used carefully but could be useful in situations where delivery of hydrophilic compounds into the cell cytosol is critical such as in vaccines where cellular CD8 immunity is important. The delivery of macromolecular drugs into cell cytosol, such as siRNA or proteins, may also be enhanced by inhibitors of lysosome renitence.

5.5 Conclusion

This thesis explores the process of lysosome damage after phagocytosis and the novel inducible resistance to this damage in macrophages. The novel lysosome damage measurement system described here has the potential to open new avenues of study in the fields of inflammation and cell death. Inducible lysosome renitence is a novel activity of activated macrophages which could be targeted with novel therapeutics which oppose intracellular pathogens and or reduce irritant-induced inflammation. Repair of intracellular membranes, demonstrated here as repair of lysosomes, is a novel ability of macrophages which merits further study.

Figure 5.1

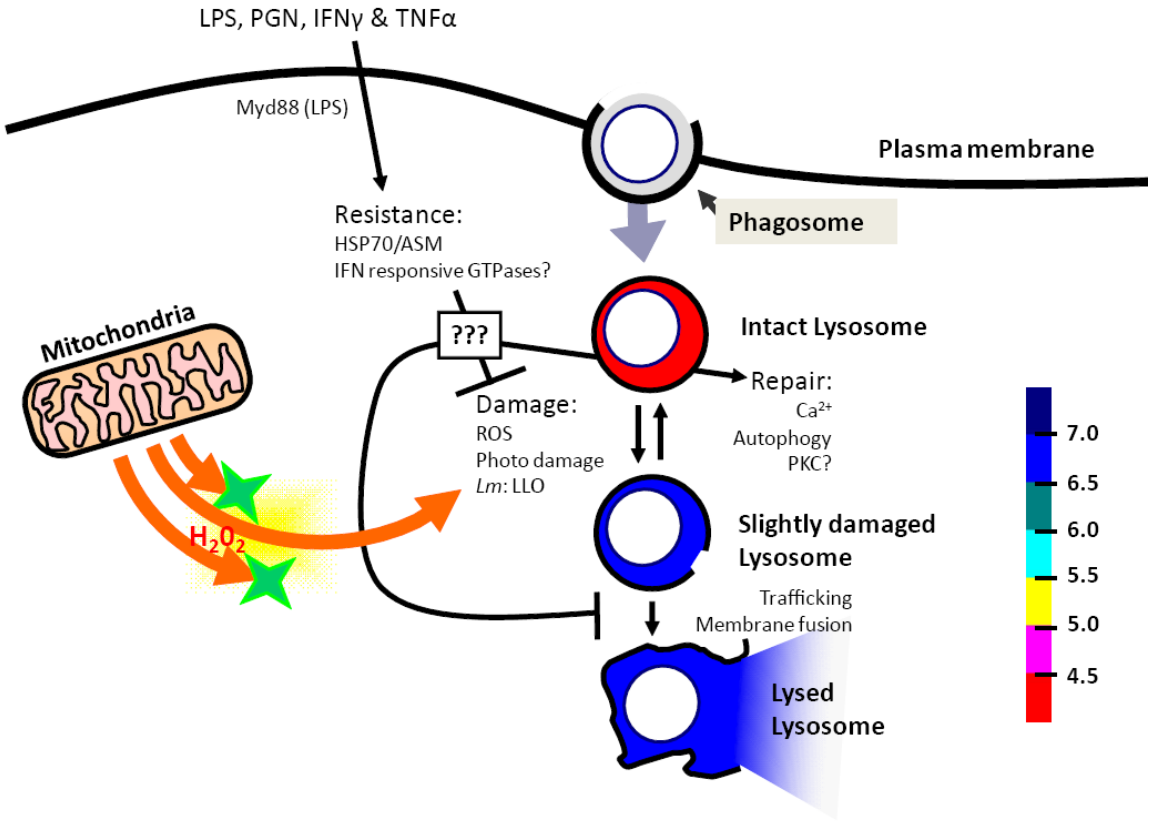

Figure 5.1 Summary of the process of phagolysosome damage. Following phagocytosis and fusion of the phagosome with lysosomes, particle associated chemistries damage the lysosomal membrane resulting in pH equilibration of the phagolysosome with the cytosol. This minor damage can be repaired or proceed to full lysosome rupture. Macrophage activation reduces lysosome damage by preventing initial damage, increasing repair or by inhibiting the progression from minor damage to full rupture.

Bibliography

Akira, S., and K. Takeda. 2004. Toll-like receptor signalling. *Nat Rev Immunol*. 4:499-511.

Allen, M.J., B.J. Myer, A.M. Khokher, N. Rushton, and T.M. Cox. 1997. Pro-inflammatory cytokines and the pathogenesis of Gaucher's disease: increased release of interleukin-6 and interleukin-10. *QJM*. 90:19-25.

Antunes, F., E. Cadenas, and U.T. Brunk. 2001. Apoptosis induced by exposure to a low steady-state concentration of H2O2 is a consequence of lysosomal rupture. *Biochem J*. 356:549-555.

Babior, B.M. 2004. NADPH oxidase. *Curr Opin Immunol*. 16:42-47.

Ballabio, A., and V. Gieselmann. 2009. Lysosomal disorders: from storage to cellular damage. *Biochim Biophys Acta*. 1793:684-696.

Bauer, C., P. Duewell, C. Mayer, H.A. Lehr, K.A. Fitzgerald, M. Dauer, J. Tschopp, S. Endres, E. Latz, and M. Schnurr. 2010. Colitis induced in mice with dextran sulfate sodium (DSS) is mediated by the NLRP3 inflammasome. *Gut*. 59:1192-1199.

Bergsbaken, T., and B.T. Cookson. 2009. Innate immune response during Yersinia infection: critical modulation of cell death mechanisms through phagocyte activation. *J Leukoc Biol*. 86:1153-1158.

Bergsbaken, T., S.L. Fink, and B.T. Cookson. 2009. Pyroptosis: host cell death and inflammation. *Nat Rev Microbiol*. 7:99-109.

Bidere, N., H.K. Lorenzo, S. Carmona, M. Laforge, F. Harper, C. Dumont, and A. Senik. 2003. Cathepsin D triggers Bax activation, resulting in selective apoptosis-inducing factor (AIF) relocation in T lymphocytes entering the early commitment phase to apoptosis. *J Biol Chem*. 278:31401-31411.

Bivik, C., I. Rosdahl, and K. Ollinger. 2007. Hsp70 protects against UVB induced apoptosis by preventing release of cathepsins and cytochrome c in human melanocytes. *Carcinogenesis*. 28:537-544.

Boya, P., and G. Kroemer. 2008. Lysosomal membrane permeabilization in cell death. *Oncogene*. 27:6434-6451.

Bradova, V., F. Smid, B. Ulrich-Bott, W. Roggendorf, B.C. Paton, and K. Harzer. 1993. Prosaposin deficiency: further characterization of the sphingolipid activator protein-deficient sibs. Multiple glycolipid elevations (including lactosylceramidosis), partial enzyme deficiencies and ultrastructure of the skin in this generalized sphingolipid storage disease. *Hum Genet*. 92:143-152.

Broker, L.E., C. Huisman, S.W. Span, J.A. Rodriguez, F.A. Kruyt, and G. Giaccone. 2004. Cathepsin B mediates caspase-independent cell death induced by microtubule stabilizing agents in non-small cell lung cancer cells. *Cancer Res*. 64:27-30.

Burgdorf, S., and C. Kurts. 2008. Endocytosis mechanisms and the cell biology of antigen presentation. *Curr Opin Immunol*. 20:89-95.

Carswell, E.A., L.J. Old, R.L. Kassel, S. Green, N. Fiore, and B. Williamson. 1975. An endotoxin-induced serum factor that causes necrosis of tumors. *Proc Natl Acad Sci U S A*. 72:3666-3670.

Caruso, J.A., P.A. Mathieu, A. Joiakim, H. Zhang, and J.J. Reiners, Jr. 2006. Aryl hydrocarbon receptor modulation of tumor necrosis factor-alpha-induced apoptosis and lysosomal disruption in a hepatoma model that is caspase-8-independent. *J Biol Chem*. 281:10954-10967.

Cassel, S.L., S.C. Eisenbarth, S.S. Iyer, J.J. Sadler, O.R. Colegio, L.A. Tephly, A.B. Carter, P.B. Rothman, R.A. Flavell, and F.S. Sutterwala. 2008. The Nalp3 inflammasome is essential for the development of silicosis. *Proc Natl Acad Sci U S A*. 105:9035-9040.

Cassol, E., L. Cassetta, M. Alfano, and G. Poli. 2010. Macrophage polarization and HIV-1 infection. *J Leukoc Biol*. 87:599-608.

Chen, W., N. Li, T. Chen, Y. Han, C. Li, Y. Wang, W. He, L. Zhang, T. Wan, and X. Cao. 2005. The lysosome-associated apoptosis-inducing protein containing the pleckstrin homology (PH) and FYVE domains (LAPF), representative of a novel family of PH and FYVE domain-containing proteins, induces caspase-independent apoptosis via the lysosomal-mitochondrial pathway. *J Biol Chem*. 280:40985-40995.

Chipuk, J.E., T. Kuwana, L. Bouchier-Hayes, N.M. Droin, D.D. Newmeyer, M. Schuler, and D.R. Green. 2004. Direct activation of Bax by p53 mediates mitochondrial membrane permeabilization and apoptosis. *Science*. 303:1010-1014.

Choudhury, A., D.K. Sharma, D.L. Marks, and R.E. Pagano. 2004. Elevated endosomal cholesterol levels in Niemann-Pick cells inhibit rab4 and perturb membrane recycling. *Mol Biol Cell*. 15:4500-4511.

Christensen, K.A., J.T. Myers, and J.A. Swanson. 2002. pH-dependent regulation of lysosomal calcium in macrophages. *J Cell Sci*. 115:599-607.

Christomanou, H., A. Chabas, T. Pampols, and A. Guardiola. 1989. Activator protein deficient Gaucher's disease. A second patient with the newly identified lipid storage disorder. *Klin Wochenschr*. 67:999-1003.

Cirman, T., K. Oresic, G.D. Mazovec, V. Turk, J.C. Reed, R.M. Myers, G.S. Salvesen, and B. Turk. 2004. Selective disruption of lysosomes in HeLa cells triggers apoptosis mediated by cleavage of Bid by multiple papain-like lysosomal cathepsins. *J Biol Chem*. 279:3578-3587.

Claudio, E., F. Segade, K. Wrobel, S. Ramos, and P.S. Lazo. 1995. Activation of murine macrophages by silica particles in vitro is a process independent of silica-induced cell death. *Am J Respir Cell Mol Biol*. 13:547-554.

Coffey, J.W., and C. De Duve. 1968. Digestive activity of lysosomes. I. The digestion of proteins by extracts of rat liver lysosomes. *J Biol Chem*. 243:3255-3263.

Collart, M.A., D. Belin, J.D. Vassalli, S. de Kossodo, and P. Vassalli. 1986. Gamma interferon enhances macrophage transcription of the tumor necrosis factor/cachectin, interleukin 1, and urokinase genes, which are controlled by short-lived repressors. *J Exp Med*. 164:2113-2118.

Conner, S.D., and S.L. Schmid. 2003. Regulated portals of entry into the cell. *Nature*. 422:37-44.

Conzelmann, E., and K. Sandhoff. 1978. AB variant of infantile GM2 gangliosidosis: deficiency of a factor necessary for stimulation of hexosaminidase A-catalyzed degradation of ganglioside GM2 and glycolipid GA2. *Proc Natl Acad Sci U S A*. 75:3979-3983.

Daugaard, M., T. Kirkegaard-Sorensen, M.S. Ostenfeld, M. Aaboe, M. Hoyer-Hansen, T.F. Orntoft, M. Rohde, and M. Jaattela. 2007a. Lens epithelium-derived growth factor is an Hsp70-2 regulated guardian of lysosomal stability in human cancer. *Cancer Res*. 67:2559-2567.

Daugaard, M., M. Rohde, and M. Jaattela. 2007b. The heat shock protein 70 family: Highly homologous proteins with overlapping and distinct functions. *FEBS Lett*. 581:3702-3710.

Davis, M.J., and J.A. Swanson. 2010. Technical advance: Caspase-1 activation and IL-1beta release correlate with the degree of lysosome damage, as illustrated by a novel imaging method to quantify phagolysosome damage. *J Leukoc Biol*. 88:813-822.

de Duve, C. 1983. Lysosomes revisited. *Eur J Biochem*. 137:391-397.

de Duve, C. 2005. The lysosome turns fifty. *Nat Cell Biol*. 7:847-849.

De Duve, C., B.C. Pressman, R. Gianetto, R. Wattiaux, and F. Appelmans. 1955. Tissue fractionation studies. 6. Intracellular distribution patterns of enzymes in rat-liver tissue. *Biochem J*. 60:604-617.

De Milito, A., E. Iessi, M. Logozzi, F. Lozupone, M. Spada, M.L. Marino, C. Federici, M. Perdicchio, P. Matarrese, L. Lugini, A. Nilsson, and S. Fais. 2007. Proton pump inhibitors induce apoptosis of human B-cell tumors through a caspase-independent mechanism involving reactive oxygen species. *Cancer Res*. 67:5408-5417.

Delgado, M.A., R.A. Elmaoued, A.S. Davis, G. Kyei, and V. Deretic. 2008. Toll-like receptors control autophagy. *EMBO J*. 27:1110-1121.

Dewamitta, S.R., T. Nomura, I. Kawamura, H. Hara, K. Tsuchiya, T. Kurenuma, Y. Shen, S. Daim, T. Yamamoto, H. Qu, S. Sakai, Y. Xu, and M. Mitsuyama. 2010. Listeriolysin O-dependent bacterial entry into the cytoplasm is required for

calpain activation and interleukin-1 alpha secretion in macrophages infected with Listeria monocytogenes. *Infect Immun*. 78:1884-1894.
Dhami, R., X. He, R.E. Gordon, and E.H. Schuchman. 2001. Analysis of the lung pathology and alveolar macrophage function in the acid sphingomyelinase--deficient mouse model of Niemann-Pick disease. *Lab Invest*. 81:987-999.
Di Piazza, M., C. Mader, K. Geletneky, Y.C.M. Herrero, E. Weber, J. Schlehofer, L. Deleu, and J. Rommelaere. 2007. Cytosolic activation of cathepsins mediates parvovirus H-1-induced killing of cisplatin and TRAIL-resistant glioma cells. *J Virol*. 81:4186-4198.
Dierks, T., B. Schmidt, L.V. Borissenko, J. Peng, A. Preusser, M. Mariappan, and K. von Figura. 2003. Multiple sulfatase deficiency is caused by mutations in the gene encoding the human C(alpha)-formylglycine generating enzyme. *Cell*. 113:435-444.
Dinarello, C.A. 2009. Immunological and inflammatory functions of the interleukin-1 family. *Annu Rev Immunol*. 27:519-550.
Divangahi, M., M. Chen, H. Gan, D. Desjardins, T.T. Hickman, D.M. Lee, S. Fortune, S.M. Behar, and H.G. Remold. 2009. Mycobacterium tuberculosis evades macrophage defenses by inhibiting plasma membrane repair. *Nat Immunol*. 10:899-906.
Dostert, C., G. Guarda, J.F. Romero, P. Menu, O. Gross, A. Tardivel, M.L. Suva, J.C. Stehle, M. Kopf, I. Stamenkovic, G. Corradin, and J. Tschopp. 2009. Malarial hemozoin is a Nalp3 inflammasome activating danger signal. *PLoS One*. 4:e6510.
Dostert, C., V. Petrilli, R. Van Bruggen, C. Steele, B.T. Mossman, and J. Tschopp. 2008. Innate immune activation through Nalp3 inflammasome sensing of asbestos and silica. *Science*. 320:674-677.
Doulias, P.T., S. Christoforidis, U.T. Brunk, and D. Galaris. 2003. Endosomal and lysosomal effects of desferrioxamine: protection of HeLa cells from hydrogen peroxide-induced DNA damage and induction of cell-cycle arrest. *Free Radic Biol Med*. 35:719-728.
Dudeja, V., N. Mujumdar, P. Phillips, R. Chugh, D. Borja-Cacho, R.K. Dawra, S.M. Vickers, and A.K. Saluja. 2009. Heat shock protein 70 inhibits apoptosis in cancer cells through simultaneous and independent mechanisms. *Gastroenterology*. 136:1772-1782.
Duewell, P., H. Kono, K.J. Rayner, C.M. Sirois, G. Vladimer, F.G. Bauernfeind, G.S. Abela, L. Franchi, G. Nunez, M. Schnurr, T. Espevik, E. Lien, K.A. Fitzgerald, K.L. Rock, K.J. Moore, S.D. Wright, V. Hornung, and E. Latz. 2010. NLRP3 inflammasomes are required for atherogenesis and activated by cholesterol crystals. *Nature*. 464:1357-1361.
Eder, C. 2009. Mechanisms of interleukin-1beta release. *Immunobiology*. 214:543-553.
Eisenbarth, S.C., O.R. Colegio, W. O'Connor, F.S. Sutterwala, and R.A. Flavell. 2008. Crucial role for the Nalp3 inflammasome in the immunostimulatory properties of aluminium adjuvants. *Nature*. 453:1122-1126.
Feldstein, A.E., N.W. Werneburg, A. Canbay, M.E. Guicciardi, S.F. Bronk, R. Rydzewski, L.J. Burgart, and G.J. Gores. 2004. Free fatty acids promote hepatic lipotoxicity by stimulating TNF-alpha expression via a lysosomal pathway. *Hepatology*. 40:185-194.

Feldstein, A.E., N.W. Werneburg, Z. Li, S.F. Bronk, and G.J. Gores. 2006. Bax inhibition protects against free fatty acid-induced lysosomal permeabilization. *Am J Physiol Gastrointest Liver Physiol*. 290:G1339-1346.

Fernandes-Alnemri, T., J.W. Yu, C. Juliana, L. Solorzano, S. Kang, J. Wu, P. Datta, M. McCormick, L. Huang, E. McDermott, L. Eisenlohr, C.P. Landel, and E.S. Alnemri. 2010. The AIM2 inflammasome is critical for innate immunity to Francisella tularensis. *Nat Immunol*.

Fink, S.L., and B.T. Cookson. 2006. Caspase-1-dependent pore formation during pyroptosis leads to osmotic lysis of infected host macrophages. *Cell Microbiol*. 8:1812-1825.

Firestone, R.A., J.M. Pisano, P.J. Bailey, A. Sturm, R.J. Bonney, P. Wightman, R. Devlin, C.S. Lin, D.L. Keller, and P.C. Tway. 1982. Lysosomotropic agents. 4. Carbobenzoxyglycylphenylalanyl, a new protease-sensitive masking group for introduction into cells. *J Med Chem*. 25:539-544.

Franchi, L., and G. Nunez. 2008. The Nlrp3 inflammasome is critical for aluminium hydroxide-mediated IL-1beta secretion but dispensable for adjuvant activity. *Eur J Immunol*. 38:2085-2089.

Futerman, A.H., and G. van Meer. 2004. The cell biology of lysosomal storage disorders. *Nat Rev Mol Cell Biol*. 5:554-565.

Garnett, T.O., M. Filippova, and P.J. Duerksen-Hughes. 2007. Bid is cleaved upstream of caspase-8 activation during TRAIL-mediated apoptosis in human osteosarcoma cells. *Apoptosis*. 12:1299-1315.

Giam, M., D.C. Huang, and P. Bouillet. 2008. BH3-only proteins and their roles in programmed cell death. *Oncogene*. 27 Suppl 1:S128-136.

Gonzalez-Noriega, A., J.H. Grubb, V. Talkad, and W.S. Sly. 1980. Chloroquine inhibits lysosomal enzyme pinocytosis and enhances lysosomal enzyme secretion by impairing receptor recycling. *J Cell Biol*. 85:839-852.

Groth-Pedersen, L., M.S. Ostenfeld, M. Hoyer-Hansen, J. Nylandsted, and M. Jaattela. 2007. Vincristine induces dramatic lysosomal changes and sensitizes cancer cells to lysosome-destabilizing siramesine. *Cancer Res*. 67:2217-2225.

Guicciardi, M.E., S.F. Bronk, N.W. Werneburg, X.M. Yin, and G.J. Gores. 2005. Bid is upstream of lysosome-mediated caspase 2 activation in tumor necrosis factor alpha-induced hepatocyte apoptosis. *Gastroenterology*. 129:269-284.

Gupta, D., Y.P. Jin, and R. Dziarski. 1995. Peptidoglycan induces transcription and secretion of TNF-alpha and activation of lyn, extracellular signal-regulated kinase, and rsk signal transduction proteins in mouse macrophages. *J Immunol*. 155:2620-2630.

Gyrd-Hansen, M., T. Farkas, N. Fehrenbacher, L. Bastholm, M. Hoyer-Hansen, F. Elling, D. Wallach, R. Flavell, G. Kroemer, J. Nylandsted, and M. Jaattela. 2006. Apoptosome-independent activation of the lysosomal cell death pathway by caspase-9. *Mol Cell Biol*. 26:7880-7891.

Gyrd-Hansen, M., J. Nylandsted, and M. Jaattela. 2004. Heat shock protein 70 promotes cancer cell viability by safeguarding lysosomal integrity. *Cell Cycle*. 3:1484-1485.

Hallam, S., M. Escorcio-Correia, R. Soper, A. Schultheiss, and T. Hagemann. 2009. Activated macrophages in the tumour microenvironment-dancing to the tune of TLR and NF-kappaB. *J Pathol*. 219:143-152.

Halle, A., V. Hornung, G.C. Petzold, C.R. Stewart, B.G. Monks, T. Reinheckel, K.A. Fitzgerald, E. Latz, K.J. Moore, and D.T. Golenbock. 2008. The NALP3 inflammasome is involved in the innate immune response to amyloid-beta. *Nat Immunol*. 9:857-865.

Hannun, Y.A., and L.M. Obeid. 2002. The Ceramide-centric universe of lipid-mediated cell regulation: stress encounters of the lipid kind. *J Biol Chem*. 277:25847-25850.

Hao, S.J., J.F. Hou, N. Jiang, and G.J. Zhang. 2008. Loss of membrane cholesterol affects lysosomal osmotic stability. *Gen Physiol Biophys*. 27:278-283.

Harding, C.V., and R. Song. 1994. Phagocytic processing of exogenous particulate antigens by macrophages for presentation by class I MHC molecules. *J Immunol*. 153:4925-4933.

Hasilik, A., A. Waheed, and K. von Figura. 1981. Enzymatic phosphorylation of lysosomal enzymes in the presence of UDP-N-acetylglucosamine. Absence of the activity in I-cell fibroblasts. *Biochem Biophys Res Commun*. 98:761-767.

Heinrich, M., J. Neumeyer, M. Jakob, C. Hallas, V. Tchikov, S. Winoto-Morbach, M. Wickel, W. Schneider-Brachert, A. Trauzold, A. Hethke, and S. Schutze. 2004. Cathepsin D links TNF-induced acid sphingomyelinase to Bid-mediated caspase-9 and -3 activation. *Cell Death Differ*. 11:550-563.

Henry, R., L. Shaughnessy, M.J. Loessner, C. Alberti-Segui, D.E. Higgins, and J.A. Swanson. 2006. Cytolysin-dependent delay of vacuole maturation in macrophages infected with Listeria monocytogenes. *Cell Microbiol*. 8:107-119.

Herbein, G., and A. Varin. 2010. The macrophage in HIV-1 infection: from activation to deactivation? *Retrovirology*. 7:33.

Hers, H.G. 1963. alpha-Glucosidase deficiency in generalized glycogenstorage disease (Pompe's disease). *Biochem J*. 86:11-16.

Hickman, S., and E.F. Neufeld. 1972. A hypothesis for I-cell disease: defective hydrolases that do not enter lysosomes. *Biochem Biophys Res Commun*. 49:992-999.

Hishita, T., S. Tada-Oikawa, K. Tohyama, Y. Miura, T. Nishihara, Y. Tohyama, Y. Yoshida, T. Uchiyama, and S. Kawanishi. 2001. Caspase-3 activation by lysosomal enzymes in cytochrome c-independent apoptosis in myelodysplastic syndrome-derived cell line P39. *Cancer Res*. 61:2878-2884.

Hollak, C.E., L. Evers, J.M. Aerts, and M.H. van Oers. 1997. Elevated levels of M-CSF, sCD14 and IL8 in type 1 Gaucher disease. *Blood Cells Mol Dis*. 23:201-212.

Holopainen, J.M., M. Subramanian, and P.K. Kinnunen. 1998. Sphingomyelinase induces lipid microdomain formation in a fluid phosphatidylcholine/sphingomyelin membrane. *Biochemistry*. 37:17562-17570.

Hoppe, A., K. Christensen, and J.A. Swanson. 2002. Fluorescence resonance energy transfer-based stoichiometry in living cells. *Biophys J*. 83:3652-3664.

Hornung, V., F. Bauernfeind, A. Halle, E.O. Samstad, H. Kono, K.L. Rock, K.A. Fitzgerald, and E. Latz. 2008. Silica crystals and aluminum salts activate the

NALP3 inflammasome through phagosomal destabilization. *Nat Immunol*. 9:847-856.

Hu, J.S., Y.B. Li, J.W. Wang, L. Sun, and G.J. Zhang. 2007. Mechanism of lysophosphatidylcholine-induced lysosome destabilization. *J Membr Biol*. 215:27-35.

Hu, Y., K. Mao, Y. Zeng, S. Chen, Z. Tao, C. Yang, S. Sun, X. Wu, G. Meng, and B. Sun. 2010. Tripartite-Motif Protein 30 Negatively Regulates NLR Family, Pyrin Domain-Containing 3 Inflammasome Activation by Modulating Reactive Oxygen Species Production. *J Immunol*.

Huaux, F. 2007. New developments in the understanding of immunology in silicosis. *Curr Opin Allergy Clin Immunol*. 7:168-173.

Idone, V., C. Tam, and N.W. Andrews. 2008. Two-way traffic on the road to plasma membrane repair. *Trends Cell Biol*. 18:552-559.

Ishisaka, R., T. Utsumi, T. Kanno, K. Arita, N. Katunuma, J. Akiyama, and K. Utsumi. 1999. Participation of a cathepsin L-type protease in the activation of caspase-3. *Cell Struct Funct*. 24:465-470.

Jinwal, U.K., Y. Miyata, J. Koren, 3rd, J.R. Jones, J.H. Trotter, L. Chang, J. O'Leary, D. Morgan, D.C. Lee, C.L. Shults, A. Rousaki, E.J. Weeber, E.R. Zuiderweg, J.E. Gestwicki, and C.A. Dickey. 2009. Chemical manipulation of hsp70 ATPase activity regulates tau stability. *J Neurosci*. 29:12079-12088.

Johnson, G.B., G.J. Brunn, Y. Kodaira, and J.L. Platt. 2002. Receptor-mediated monitoring of tissue well-being via detection of soluble heparan sulfate by Toll-like receptor 4. *J Immunol*. 168:5233-5239.

Jozefowski, S., M. Czerkies, A. Lukasik, A. Bielawska, J. Bielawski, K. Kwiatkowska, and A. Sobota. 2010. Ceramide and ceramide 1-phosphate are negative regulators of TNF-alpha production induced by lipopolysaccharide. *J Immunol*. 185:6960-6973.

Kagedal, K., A.C. Johansson, U. Johansson, G. Heimlich, K. Roberg, N.S. Wang, J.M. Jurgensmeier, and K. Ollinger. 2005. Lysosomal membrane permeabilization during apoptosis--involvement of Bax? *Int J Exp Pathol*. 86:309-321.

Kagedal, K., U. Johansson, and K. Ollinger. 2001a. The lysosomal protease cathepsin D mediates apoptosis induced by oxidative stress. *FASEB J*. 15:1592-1594.

Kagedal, K., M. Zhao, I. Svensson, and U.T. Brunk. 2001b. Sphingosine-induced apoptosis is dependent on lysosomal proteases. *Biochem J*. 359:335-343.

Kaznelson, D.W., S. Bruun, A. Monrad, S. Gjerlov, J. Birk, C. Ropke, and B. Norrild. 2004. Simultaneous human papilloma virus type 16 E7 and cdk inhibitor p21 expression induces apoptosis and cathepsin B activation. *Virology*. 320:301-312.

Kiderlen, A.F., S.H. Kaufmann, and M.L. Lohmann-Matthes. 1984. Protection of mice against the intracellular bacterium Listeria monocytogenes by recombinant immune interferon. *Eur J Immunol*. 14:964-967.

Kim, S., F. Bauernfeind, A. Ablasser, G. Hartmann, K.A. Fitzgerald, E. Latz, and V. Hornung. 2010. Listeria monocytogenes is sensed by the NLRP3 and AIM2 inflammasome. *Eur J Immunol*. 40:1545-1551.

Kinchen, J.M., and K.S. Ravichandran. 2008. Phagosome maturation: going through the acid test. *Nat Rev Mol Cell Biol*. 9:781-795.

Kirkegaard, T., A.G. Roth, N.H. Petersen, A.K. Mahalka, O.D. Olsen, I. Moilanen, A. Zylicz, J. Knudsen, K. Sandhoff, C. Arenz, P.K. Kinnunen, J. Nylandsted, and M. Jaattela. 2010. Hsp70 stabilizes lysosomes and reverts Niemann-Pick disease-associated lysosomal pathology. *Nature*. 463:549-553.

Knapp, P.E., and J.A. Swanson. 1990. Plasticity of the tubular lysosomal compartment in macrophages. *J Cell Sci*. 95 (Pt 3):433-439.

Kool, M., V. Petrilli, T. De Smedt, A. Rolaz, H. Hammad, M. van Nimwegen, I.M. Bergen, R. Castillo, B.N. Lambrecht, and J. Tschopp. 2008. Cutting edge: alum adjuvant stimulates inflammatory dendritic cells through activation of the NALP3 inflammasome. *J Immunol*. 181:3755-3759.

Koren, J., 3rd, U.K. Jinwal, Y. Jin, J. O'Leary, J.R. Jones, A.G. Johnson, L.J. Blair, J.F. Abisambra, L. Chang, Y. Miyata, A.M. Cheng, J. Guo, J.Q. Cheng, J.E. Gestwicki, and C.A. Dickey. 2010. Facilitating Akt clearance via manipulation of Hsp70 activity and levels. *J Biol Chem*. 285:2498-2505.

Kovacsovics-Bankowski, M., K. Clark, B. Benacerraf, and K.L. Rock. 1993. Efficient major histocompatibility complex class I presentation of exogenous antigen upon phagocytosis by macrophages. *Proc Natl Acad Sci U S A*. 90:4942-4946.

Kumar, Y., and R.H. Valdivia. 2009. Leading a sheltered life: intracellular pathogens and maintenance of vacuolar compartments. *Cell Host Microbe*. 5:593-601.

Kurz, T., B. Gustafsson, and U.T. Brunk. 2006. Intralysosomal iron chelation protects against oxidative stress-induced cellular damage. *FEBS J*. 273:3106-3117.

Laforge, M., F. Petit, J. Estaquier, and A. Senik. 2007. Commitment to apoptosis in CD4(+) T lymphocytes productively infected with human immunodeficiency virus type 1 is initiated by lysosomal membrane permeabilization, itself induced by the isolated expression of the viral protein Nef. *J Virol*. 81:11426-11440.

Lamparska-Przybysz, M., B. Gajkowska, and T. Motyl. 2006. BID-deficient breast cancer MCF-7 cells as a model for the study of autophagy in cancer therapy. *Autophagy*. 2:47-48.

Leventhal, A.R., W. Chen, A.R. Tall, and I. Tabas. 2001. Acid sphingomyelinase-deficient macrophages have defective cholesterol trafficking and efflux. *J Biol Chem*. 276:44976-44983.

Li, N., Y. Zheng, W. Chen, C. Wang, X. Liu, W. He, H. Xu, and X. Cao. 2007. Adaptor protein LAPF recruits phosphorylated p53 to lysosomes and triggers lysosomal destabilization in apoptosis. *Cancer Res*. 67:11176-11185.

Li, Y., and M.A. Trush. 1998. Diphenyleneiodonium, an NAD(P)H oxidase inhibitor, also potently inhibits mitochondrial reactive oxygen species production. *Biochem Biophys Res Commun*. 253:295-299.

Lin, W.J., and W.C. Yeh. 2005. Implication of Toll-like receptor and tumor necrosis factor alpha signaling in septic shock. *Shock*. 24:206-209.

Liscum, L. 2000. Niemann-Pick type C mutations cause lipid traffic jam. *Traffic*. 1:218-225.

Lozano, J., S. Menendez, A. Morales, D. Ehleiter, W.C. Liao, R. Wagman, A. Haimovitz-Friedman, Z. Fuks, and R. Kolesnick. 2001. Cell autonomous apoptosis defects in acid sphingomyelinase knockout fibroblasts. *J Biol Chem*. 276:442-448.

Luzio, J.P., P.R. Pryor, and N.A. Bright. 2007. Lysosomes: fusion and function. *Nat Rev Mol Cell Biol*. 8:622-632.

Lykens, J.E., C.E. Terrell, E.E. Zoller, S. Divanovic, A. Trompette, C.L. Karp, J. Aliberti, M.J. Flick, and M.B. Jordan. 2010. Mice with a selective impairment of IFN-gamma signaling in macrophage lineage cells demonstrate the critical role of IFN-gamma-activated macrophages for the control of protozoan parasitic infections in vivo. *J Immunol*. 184:877-885.

Mackaness, G.B. 1962. Cellular resistance to infection. *J Exp Med*. 116:381-406.

MacMicking, J., Q.W. Xie, and C. Nathan. 1997. Nitric oxide and macrophage function. *Annu Rev Immunol*. 15:323-350.

Mariathasan, S., D.S. Weiss, K. Newton, J. McBride, K. O'Rourke, M. Roose-Girma, W.P. Lee, Y. Weinrauch, D.M. Monack, and V.M. Dixit. 2006. Cryopyrin activates the inflammasome in response to toxins and ATP. *Nature*. 440:228-232.

Martinez, F.O., S. Gordon, M. Locati, and A. Mantovani. 2006. Transcriptional profiling of the human monocyte-to-macrophage differentiation and polarization: new molecules and patterns of gene expression. *J Immunol*. 177:7303-7311.

Martinon, F., K. Burns, and J. Tschopp. 2002. The inflammasome: a molecular platform triggering activation of inflammatory caspases and processing of proIL-beta. *Mol Cell*. 10:417-426.

Martinon, F., A. Mayor, and J. Tschopp. 2009. The inflammasomes: guardians of the body. *Annu Rev Immunol*. 27:229-265.

Martinon, F., V. Petrilli, A. Mayor, A. Tardivel, and J. Tschopp. 2006. Gout-associated uric acid crystals activate the NALP3 inflammasome. *Nature*. 440:237-241.

McKee, A.S., M.W. Munks, M.K. MacLeod, C.J. Fleenor, N. Van Rooijen, J.W. Kappler, and P. Marrack. 2009. Alum induces innate immune responses through macrophage and mast cell sensors, but these sensors are not required for alum to act as an adjuvant for specific immunity. *J Immunol*. 183:4403-4414.

McNeil, P.L., and R.A. Steinhardt. 2003. Plasma membrane disruption: repair, prevention, adaptation. *Annu Rev Cell Dev Biol*. 19:697-731.

Mehrpour, M., A. Esclatine, I. Beau, and P. Codogno. 2010. Overview of macroautophagy regulation in mammalian cells. *Cell Res*. 20:748-762.

Michallet, M.C., F. Saltel, M. Flacher, J.P. Revillard, and L. Genestier. 2004. Cathepsin-dependent apoptosis triggered by supraoptimal activation of T lymphocytes: a possible mechanism of high dose tolerance. *J Immunol*. 172:5405-5414.

Mihara, M., S. Erster, A. Zaika, O. Petrenko, T. Chittenden, P. Pancoska, and U.M. Moll. 2003. p53 has a direct apoptogenic role at the mitochondria. *Mol Cell*. 11:577-590.

Miller, D.K., E. Griffiths, J. Lenard, and R.A. Firestone. 1983. Cell killing by lysosomotropic detergents. *J Cell Biol*. 97:1841-1851.

Minakami, R., and H. Sumimotoa. 2006. Phagocytosis-coupled activation of the superoxide-producing phagocyte oxidase, a member of the NADPH oxidase (nox) family. *Int J Hematol*. 84:193-198.

Mizushima, N., and A. Kuma. 2008. Autophagosomes in GFP-LC3 Transgenic Mice. *Methods Mol Biol*. 445:119-124.

Mossman, B.T., and A. Churg. 1998. Mechanisms in the pathogenesis of asbestosis and silicosis. *Am J Respir Crit Care Med*. 157:1666-1680.

Myers, J.T., A.W. Tsang, and J.A. Swanson. 2003. Localized reactive oxygen and nitrogen intermediates inhibit escape of Listeria monocytogenes from vacuoles in activated macrophages. *J Immunol*. 171:5447-5453.

Nagaraj, N.S., N. Vigneswaran, and W. Zacharias. 2006. Cathepsin B mediates TRAIL-induced apoptosis in oral cancer cells. *J Cancer Res Clin Oncol*. 132:171-183.

Nakanishi-Matsui, M., M. Sekiya, R.K. Nakamoto, and M. Futai. 2010. The mechanism of rotating proton pumping ATPases. *Biochim Biophys Acta*. 1797:1343-1352.

Neufeld, E.B., M. Wastney, S. Patel, S. Suresh, A.M. Cooney, N.K. Dwyer, C.F. Roff, K. Ohno, J.A. Morris, E.D. Carstea, J.P. Incardona, J.F. Strauss, 3rd, M.T. Vanier, M.C. Patterson, R.O. Brady, P.G. Pentchev, and E.J. Blanchette-Mackie. 1999. The Niemann-Pick C1 protein resides in a vesicular compartment linked to retrograde transport of multiple lysosomal cargo. *J Biol Chem*. 274:9627-9635.

Newman, Z.L., S.H. Leppla, and M. Moayeri. 2009. CA-074Me protection against anthrax lethal toxin. *Infect Immun*. 77:4327-4336.

Norbury, C.C., L.J. Hewlett, A.R. Prescott, N. Shastri, and C. Watts. 1995. Class I MHC presentation of exogenous soluble antigen via macropinocytosis in bone marrow macrophages. *Immunity*. 3:783-791.

Nylandsted, J., M. Gyrd-Hansen, A. Danielewicz, N. Fehrenbacher, U. Lademann, M. Hoyer-Hansen, E. Weber, G. Multhoff, M. Rohde, and M. Jaattela. 2004. Heat shock protein 70 promotes cell survival by inhibiting lysosomal membrane permeabilization. *J Exp Med*. 200:425-435.

O'Donnell, B.V., D.G. Tew, O.T. Jones, and P.J. England. 1993. Studies on the inhibitory mechanism of iodonium compounds with special reference to neutrophil NADPH oxidase. *Biochem J*. 290 (Pt 1):41-49.

Oh, Y.K., C.V. Harding, and J.A. Swanson. 1997. The efficiency of antigen delivery from macrophage phagosomes into cytoplasm for MHC class I-restricted antigen presentation. *Vaccine*. 15:511-518.

Ohkuma, S., and B. Poole. 1978. Fluorescence probe measurement of the intralysosomal pH in living cells and the perturbation of pH by various agents. *Proc Natl Acad Sci U S A*. 75:3327-3331.

Parkinson-Lawrence, E.J., T. Shandala, M. Prodoehl, R. Plew, G.N. Borlace, and D.A. Brooks. 2010. Lysosomal storage disease: revealing lysosomal function and physiology. *Physiology (Bethesda)*. 25:102-115.

Pelled, D., E. Lloyd-Evans, C. Riebeling, M. Jeyakumar, F.M. Platt, and A.H. Futerman. 2003. Inhibition of calcium uptake via the sarco/endoplasmic reticulum Ca2+-ATPase in a mouse model of Sandhoff disease and prevention by treatment with N-butyldeoxynojirimycin. *J Biol Chem*. 278:29496-29501.

Peri, P., K. Nuutila, T. Vuorinen, P. Saukko, and V. Hukkanen. 2011. Cathepsins are involved in virus-induced cell death in ICP4 and Us3 deletion mutant herpes simplex virus type 1-infected monocytic cells. *J Gen Virol*. 92:173-180.

Perregaux, D., and C.A. Gabel. 1994. Interleukin-1 beta maturation and release in response to ATP and nigericin. Evidence that potassium depletion mediated by these agents is a necessary and common feature of their activity. *J Biol Chem*. 269:15195-15203.

Persson, H.L. 2005. Iron-dependent lysosomal destabilization initiates silica-induced apoptosis in murine macrophages. *Toxicol Lett*. 159:124-133.

Persson, H.L., and L.K. Vainikka. 2010. TNF-alpha preserves lysosomal stability in macrophages: a potential defense against oxidative lung injury. *Toxicol Lett*. 192:261-267.

Petrilli, V., S. Papin, C. Dostert, A. Mayor, F. Martinon, and J. Tschopp. 2007. Activation of the NALP3 inflammasome is triggered by low intracellular potassium concentration. *Cell Death Differ*. 14:1583-1589.

Portnoy, D.A., P.S. Jacks, and D.J. Hinrichs. 1988. Role of hemolysin for the intracellular growth of Listeria monocytogenes. *J Exp Med*. 167:1459-1471.

Racoosin, E.L., and J.A. Swanson. 1989. Macrophage colony-stimulating factor (rM-CSF) stimulates pinocytosis in bone marrow-derived macrophages. *J Exp Med*. 170:1635-1648.

Rajamaki, K., J. Lappalainen, K. Oorni, E. Valimaki, S. Matikainen, P.T. Kovanen, and K.K. Eklund. 2010. Cholesterol crystals activate the NLRP3 inflammasome in human macrophages: a novel link between cholesterol metabolism and inflammation. *PLoS One*. 5:e11765.

Ray, K., B. Marteyn, P.J. Sansonetti, and C.M. Tang. 2009. Life on the inside: the intracellular lifestyle of cytosolic bacteria. *Nat Rev Microbiol*. 7:333-340.

Reis e Sousa, C., and R.N. Germain. 1995. Major histocompatibility complex class I presentation of peptides derived from soluble exogenous antigen by a subset of cells engaged in phagocytosis. *J Exp Med*. 182:841-851.

Reitman, M.L., and S. Kornfeld. 1981. UDP-N-acetylglucosamine:glycoprotein N-acetylglucosamine-1-phosphotransferase. Proposed enzyme for the phosphorylation of the high mannose oligosaccharide units of lysosomal enzymes. *J Biol Chem*. 256:4275-4281.

Roberts, L.R., H. Kurosawa, S.F. Bronk, P.J. Fesmier, L.B. Agellon, W.Y. Leung, F. Mao, and G.J. Gores. 1997. Cathepsin B contributes to bile salt-induced apoptosis of rat hepatocytes. *Gastroenterology*. 113:1714-1726.

Rock, K.L., L. Rothstein, C. Fleischacker, and S. Gamble. 1992. Inhibition of class I and class II MHC-restricted antigen presentation by cytotoxic T lymphocytes specific for an exogenous antigen. *J Immunol*. 148:3028-3033.

Rock, K.L., L. Rothstein, S. Gamble, and C. Fleischacker. 1993. Characterization of antigen-presenting cells that present exogenous antigens in association with class I MHC molecules. *J Immunol*. 150:438-446.

Roussi, S., F. Gosse, D. Aoude-Werner, X. Zhang, E. Marchioni, P. Geoffroy, M. Miesch, and F. Raul. 2007. Mitochondrial perturbation, oxidative stress and lysosomal destabilization are involved in 7beta-hydroxysitosterol and 7beta-hydroxycholesterol triggered apoptosis in human colon cancer cells. *Apoptosis*. 12:87-96.

Rozenova, K.A., G.M. Deevska, A.A. Karakashian, and M.N. Nikolova-Karakashian. 2010. Studies on the role of acid sphingomyelinase and ceramide in the regulation of tumor necrosis factor alpha (TNFalpha)-converting enzyme activity and TNFalpha secretion in macrophages. *J Biol Chem*. 285:21103-21113.

Sandes, E., C. Lodillinsky, R. Cwirenbaum, C. Arguelles, A. Casabe, and A.M. Eijan. 2007. Cathepsin B is involved in the apoptosis intrinsic pathway induced by Bacillus Calmette-Guerin in transitional cancer cell lines. *Int J Mol Med*. 20:823-828.

Sanjuan, M.A., C.P. Dillon, S.W. Tait, S. Moshiach, F. Dorsey, S. Connell, M. Komatsu, K. Tanaka, J.L. Cleveland, S. Withoff, and D.R. Green. 2007. Toll-like receptor signalling in macrophages links the autophagy pathway to phagocytosis. *Nature*. 450:1253-1257.

Schnupf, P., and D.A. Portnoy. 2007. Listeriolysin O: a phagosome-specific lysin. *Microbes Infect*. 9:1176-1187.

Schroder, K., and J. Tschopp. 2010. The inflammasomes. *Cell*. 140:821-832.

Scott, C.C., R.J. Botelho, and S. Grinstein. 2003. Phagosome maturation: a few bugs in the system. *J Membr Biol*. 193:137-152.

Settembre, C., A. Fraldi, L. Jahreiss, C. Spampanato, C. Venturi, D. Medina, R. de Pablo, C. Tacchetti, D.C. Rubinsztein, and A. Ballabio. 2008. A block of autophagy in lysosomal storage disorders. *Hum Mol Genet*. 17:119-129.

Shaughnessy, L.M., A.D. Hoppe, K.A. Christensen, and J.A. Swanson. 2006. Membrane perforations inhibit lysosome fusion by altering pH and calcium in Listeria monocytogenes vacuoles. *Cell Microbiol*. 8:781-792.

Shaughnessy, L.M., and J.A. Swanson. 2007. The role of the activated macrophage in clearing Listeria monocytogenes infection. *Front Biosci*. 12:2683-2692.

Simonaro, C.M., M. D'Angelo, M.E. Haskins, and E.H. Schuchman. 2005. Joint and bone disease in mucopolysaccharidoses VI and VII: identification of new therapeutic targets and biomarkers using animal models. *Pediatr Res*. 57:701-707.

Stuehr, D.J., O.A. Fasehun, N.S. Kwon, S.S. Gross, J.A. Gonzalez, R. Levi, and C.F. Nathan. 1991. Inhibition of macrophage and endothelial cell nitric oxide synthase by diphenyleneiodonium and its analogs. *FASEB J*. 5:98-103.

Sutterwala, F.S., Y. Ogura, M. Szczepanik, M. Lara-Tejero, G.S. Lichtenberger, E.P. Grant, J. Bertin, A.J. Coyle, J.E. Galan, P.W. Askenase, and R.A. Flavell. 2006. Critical role for NALP3/CIAS1/Cryopyrin in innate and adaptive immunity through its regulation of caspase-1. *Immunity*. 24:317-327.

Swanson, J.A. 1989. Phorbol esters stimulate macropinocytosis and solute flow through macrophages. *J Cell Sci*. 94 (Pt 1):135-142.

Swanson, J.A. 2008. Shaping cups into phagosomes and macropinosomes. *Nat Rev Mol Cell Biol*. 9:639-649.

Teitelbaum, R., M. Cammer, M.L. Maitland, N.E. Freitag, J. Condeelis, and B.R. Bloom. 1999. Mycobacterial infection of macrophages results in membrane-permeable phagosomes. *Proc Natl Acad Sci U S A*. 96:15190-15195.

Terman, A., T. Kurz, B. Gustafsson, and U.T. Brunk. 2006. Lysosomal labilization. *IUBMB Life*. 58:531-539.

Thibodeau, M.S., C. Giardina, D.A. Knecht, J. Helble, and A.K. Hubbard. 2004. Silica-induced apoptosis in mouse alveolar macrophages is initiated by lysosomal enzyme activity. *Toxicol Sci*. 80:34-48.

Thiele, D.L., and P.E. Lipsky. 1985. Regulation of cellular function by products of lysosomal enzyme activity: elimination of human natural killer cells by a dipeptide methyl ester generated from L-leucine methyl ester by monocytes or polymorphonuclear leukocytes. *Proc Natl Acad Sci U S A*. 82:2468-2472.

Thiele, D.L., and P.E. Lipsky. 1990. Mechanism of L-leucyl-L-leucine methyl ester-mediated killing of cytotoxic lymphocytes: dependence on a lysosomal thiol

protease, dipeptidyl peptidase I, that is enriched in these cells. *Proc Natl Acad Sci U S A*. 87:83-87.

Thornberry, N.A., H.G. Bull, J.R. Calaycay, K.T. Chapman, A.D. Howard, M.J. Kostura, D.K. Miller, S.M. Molineaux, J.R. Weidner, J. Aunins, and et al. 1992. A novel heterodimeric cysteine protease is required for interleukin-1 beta processing in monocytes. *Nature*. 356:768-774.

Ting, J.P., S.B. Willingham, and D.T. Bergstralh. 2008. NLRs at the intersection of cell death and immunity. *Nat Rev Immunol*. 8:372-379.

Tooze, S.A., H.B. Jefferies, E. Kalie, A. Longatti, F.E. McAlpine, N.C. McKnight, A. Orsi, H.E. Polson, M. Razi, D.J. Robinson, and J.L. Webber. 2010. Trafficking and signaling in mammalian autophagy. *IUBMB Life*. 62:503-508.

Traber, M.G., and J. Atkinson. 2007. Vitamin E, antioxidant and nothing more. *Free Radic Biol Med*. 43:4-15.

Trost, M., L. English, S. Lemieux, M. Courcelles, M. Desjardins, and P. Thibault. 2009. The phagosomal proteome in interferon-gamma-activated macrophages. *Immunity*. 30:143-154.

Tsang, A.W., K. Oestergaard, J.T. Myers, and J.A. Swanson. 2000. Altered membrane trafficking in activated bone marrow-derived macrophages. *J Leukoc Biol*. 68:487-494.

Turk, B., and V. Turk. 2009. Lysosomes as "suicide bags" in cell death: myth or reality? *J Biol Chem*. 284:21783-21787.

van der Wel, N., D. Hava, D. Houben, D. Fluitsma, M. van Zon, J. Pierson, M. Brenner, and P.J. Peters. 2007. M. tuberculosis and M. leprae translocate from the phagolysosome to the cytosol in myeloid cells. *Cell*. 129:1287-1298.

Varki, A., and S. Kornfeld. 1981. Purification and characterization of rat liver alpha-N-acetylglucosaminyl phosphodiesterase. *J Biol Chem*. 256:9937-9943.

Vellodi, A. 2005. Lysosomal storage disorders. *Br J Haematol*. 128:413-431.

Verani, A., G. Gras, and G. Pancino. 2005. Macrophages and HIV-1: dangerous liaisons. *Mol Immunol*. 42:195-212.

Wadhwa, R., T. Sugihara, A. Yoshida, H. Nomura, R.R. Reddel, R. Simpson, H. Maruta, and S.C. Kaul. 2000. Selective toxicity of MKT-077 to cancer cells is mediated by its binding to the hsp70 family protein mot-2 and reactivation of p53 function. *Cancer Res*. 60:6818-6821.

Waheed, A., A. Hasilik, and K. von Figura. 1981. Processing of the phosphorylated recognition marker in lysosomal enzymes. Characterization and partial purification of a microsomal alpha-N-acetylglucosaminyl phosphodiesterase. *J Biol Chem*. 256:5717-5721.

Wang, X., and P.J. Quinn. 1999. Vitamin E and its function in membranes. *Prog Lipid Res*. 38:309-336.

Warren, S.E., D.P. Mao, A.E. Rodriguez, E.A. Miao, and A. Aderem. 2008. Multiple Nod-like receptors activate caspase 1 during Listeria monocytogenes infection. *J Immunol*. 180:7558-7564.

Way, S.S., L.J. Thompson, J.E. Lopes, A.M. Hajjar, T.R. Kollmann, N.E. Freitag, and C.B. Wilson. 2004. Characterization of flagellin expression and its role in Listeria monocytogenes infection and immunity. *Cell Microbiol*. 6:235-242.

Wenger, D.A., G. DeGala, C. Williams, H.A. Taylor, R.E. Stevenson, J.R. Pruitt, J. Miller, P.D. Garen, and J.D. Balentine. 1989. Clinical, pathological, and biochemical studies on an infantile case of sulfatide/GM1 activator protein deficiency. *Am J Med Genet*. 33:255-265.

Werneburg, N.W., M.E. Guicciardi, S.F. Bronk, and G.J. Gores. 2002. Tumor necrosis factor-alpha-associated lysosomal permeabilization is cathepsin B dependent. *Am J Physiol Gastrointest Liver Physiol*. 283:G947-956.

Werneburg, N.W., M.E. Guicciardi, S.F. Bronk, S.H. Kaufmann, and G.J. Gores. 2007. Tumor necrosis factor-related apoptosis-inducing ligand activates a lysosomal pathway of apoptosis that is regulated by Bcl-2 proteins. *J Biol Chem*. 282:28960-28970.

Wilson, H.M. 2010. Macrophages heterogeneity in atherosclerosis - implications for therapy. *J Cell Mol Med*. 14:2055-2065.

Wu, Y.P., and R.L. Proia. 2004. Deletion of macrophage-inflammatory protein 1 alpha retards neurodegeneration in Sandhoff disease mice. *Proc Natl Acad Sci U S A*. 101:8425-8430.

Xu, Y., C. Jagannath, X.D. Liu, A. Sharafkhaneh, K.E. Kolodziejska, and N.T. Eissa. 2007. Toll-like receptor 4 is a sensor for autophagy associated with innate immunity. *Immunity*. 27:135-144.

Yacoub, A., M.A. Park, P. Gupta, M. Rahmani, G. Zhang, H. Hamed, D. Hanna, D. Sarkar, I.V. Lebedeva, L. Emdad, M. Sauane, N. Vozhilla, S. Spiegel, C. Koumenis, M. Graf, D.T. Curiel, S. Grant, P.B. Fisher, and P. Dent. 2008. Caspase-, cathepsin-, and PERK-dependent regulation of MDA-7/IL-24-induced cell killing in primary human glioma cells. *Mol Cancer Ther*. 7:297-313.

Yu, Z., W. Li, and U.T. Brunk. 2003. 3-Aminopropanal is a lysosomotropic aldehyde that causes oxidative stress and apoptosis by rupturing lysosomes. *APMIS*. 111:643-652.

Yuan, X.M., W. Li, U.T. Brunk, H. Dalen, Y.H. Chang, and A. Sevanian. 2000. Lysosomal destabilization during macrophage damage induced by cholesterol oxidation products. *Free Radic Biol Med*. 28:208-218.

Yuan, X.M., W. Li, H. Dalen, J. Lotem, R. Kama, L. Sachs, and U.T. Brunk. 2002. Lysosomal destabilization in p53-induced apoptosis. *Proc Natl Acad Sci U S A*. 99:6286-6291.

Zaki, M.H., K.L. Boyd, P. Vogel, M.B. Kastan, M. Lamkanfi, and T.D. Kanneganti. 2010. The NLRP3 inflammasome protects against loss of epithelial integrity and mortality during experimental colitis. *Immunity*. 32:379-391.

Zang, Y., R.L. Beard, R.A. Chandraratna, and J.X. Kang. 2001. Evidence of a lysosomal pathway for apoptosis induced by the synthetic retinoid CD437 in human leukemia HL-60 cells. *Cell Death Differ*. 8:477-485.

Zdolsek, J.M., and I. Svensson. 1993. Effect of reactive oxygen species on lysosomal membrane integrity. A study on a lysosomal fraction. *Virchows Arch B Cell Pathol Incl Mol Pathol*. 64:401-406.

Zhao, M., J.W. Eaton, and U.T. Brunk. 2001. Bcl-2 phosphorylation is required for inhibition of oxidative stress-induced lysosomal leak and ensuing apoptosis. *FEBS Lett*. 509:405-412.